THE PENNSYLVANIA
STATE UNIVERSITY

IONOSPHERIC RESEARCH

Scientific Report 462

THE PHOTOLYSIS OF CHLORINE IN THE PRESENCE OF OZONE, NITRIC OXIDE AND NITROGEN DIOXIDE

by

Wanee Wongdontri Stuper

August, 1979

IONOSPHERE RESEARCH LABORATORY

University Park, Pennsylvania

REPORT DOCUMENTATION PAGE		READ INSTRUCTIONS BEFORE COMPLETING FORM
1. REPORT NUMBER 462	2. GOVT ACCESSION NO.	3 RECIPIENT'S CATALOG NUMBER
4. TITLE (and Subtitle) The Photolysis of Chlorine in the Presence of Ozone, Nitric Oxide and Nitrogen Dioxide		5. TYPE OF REPORT & PERIOD COVERED Scientific Report 462
		6. PERFORMING ORG. REPORT NUMBER PSU-IRL-SCI-462
7. AUTHOR(s) Wanee Wongdontri Stuper		8. CONTRACT OR GRANT NUMBER(s) NASA IRL MD 5947 39-009-003
9. PERFORMING ORGANIZATION NAME AND ADDRESS National Aeronautics and Space Administration Washington, D. C. 20546		10. PROGRAM ELEMENT, PROJECT, TASK AREA & WORK UNIT NUMBERS
11. CONTROLLING OFFICE NAME AND ADDRESS		12. REPORT DATE August, 1979
		13. NUMBER OF PAGES 177
14. MONITORING AGENCY NAME & ADDRESS(If different from Controlling Office)		15. SECURITY CLASS. (of this report) NONE
		15a. DECLASSIFICATION/DOWNGRADING SCHEDULE

16. DISTRIBUTION STATEMENT (of this Report)

Supporting Agencies

17. DISTRIBUTION STATEMENT (of the abstract entered in Block 20, If different from Report)

18. SUPPLEMENTARY NOTES

19. KEY WORDS (Continue on reverse side If necessary and Identify by block number)

Chemical Aeronomy

20. ABSTRACT (Continue on reverse side If necessary and Identify by block number)

The following three systems were investigated: the Cl_2-O_3 system, the Cl_2-O_2-NO system and the Cl_2-NO_2-M system. In the first system, the reaction between ClO and O_3, the reaction between $OClO$ and O_3, and the mechanism of the Cl_2-O_3 system were studied. In the second system, the reaction between $ClOO$ and NO was investigated. In the last system, the reaction between Cl and NO_2 was investigated as well as the kinetics of the chemiluminescence of the $Cl-NO_2-O_3$ reaction.

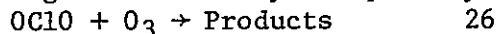In the first system, Cl_2 was photolyzed at 366 nm in the presence of O_3

DD FORM 1473 EDITION OF 1 NOV 65 IS OBSOLETE
1 JAN 73
S/N 0102-014-6601 |

within the temperature range 254-297°K. O_3 was removed with quantum yields of 5.8 ± 0.5, 4.0 ± 0.3, 2.9 ± 0.3 and 1.9 ± 0.2 at 297, 283, 273, and 252°K respectively, invariant to changes in the initial O_3 or Cl_2 concentration, the extent of conversion or the absorbed intensity, I_a. The addition of nitrogen had no effect on $-\Phi\{O_3\}$. The Cl_2 removal quantum yields were 0.11 ± 0.02 at 297°K for Cl_2 conversions of about 30%, much higher than expected from mass balance considerations based on the initial quantum yield of 0.089 ± 0.013 for OClO formation at 297°K. The final chlorine-containing product was Cl_2O_7. It was produced at least in part through the formation of OClO as an intermediate which was also observed with an initial quantum yield of $\Phi_i\{OClO\} = 2.5 \times 10^3$ exp$\{-(3025 \pm 625)/T\}$ independent of $[O_3]$ or I_a. The addition of nitrogen and oxygen had no effect on the values of $\Phi_i\{OClO\}$ and $-\Phi\{Cl_2\}$.

The results showed that OClO was formed by ClO radical combination as in reaction 23c.

$$2ClO \rightarrow ClOO + Cl \qquad 23a$$
$$\rightarrow Cl_2 + O_2 \qquad 23b$$
$$\rightarrow OClO + Cl \qquad 23c$$
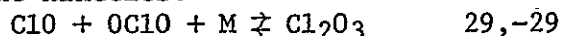
The relative importance of the channels for reaction 23 at 296°K are the following: $k_{23a}/k_{23} = 0.63$; $k_{23b}/k_{23} = 0.34$; $k_{23c}/k_{23} = 0.032$. Also, $k_{23c}/k_{23b} = 2.5 \times 10^3$ exp$[-(3025 \pm 625)/T]$.

The rate coefficient for the reaction of OClO with O_3 was studied by a direct mixing method and by the photolysis method.
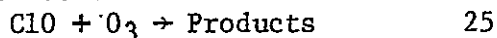
$$OClO + O_3 \rightarrow Products \qquad 26$$

The temperature dependence of k_{26} was studied in the temperature range 264-297°K. However, at temperatures below 297°K, the quilibrium reaction 29 complicated the kinetics.
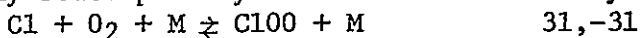
$$ClO + OClO + M \rightleftarrows Cl_2O_3 \qquad 29,-29$$

Thus the temperature dependence of k_{26} obtained from the photolysis method could only be evaluated from the steady state values of OClO. The recommended value for k_{26} is 2.3×10^{-12} exp$[-(4730 \pm 630)/T]$ cm^{3}sec^{-1}.

The upper limit for the rate coefficient of the reaction between ClO and O_3 was found to be less than 1×10^{-18} cm^{3}sec^{-1}.
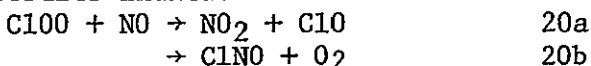
$$ClO + O_3 \rightarrow Products \qquad 25$$

The low values of k_{25} and k_{26} indicate that reaction 25 and 26 are probably not important in atmospheric chemistry.

In the second system, the reactions of ClOO with NO were studied by the photolysis of Cl_2 in the presence of NO and O_2 with or without added N_2 using steady state photolysis. ClOO is formed by the reversible reaction

$$Cl + O_2 + M \rightleftarrows ClOO + M \qquad 31,-31$$

The results indicate that ClOO reacts with NO via two channels:

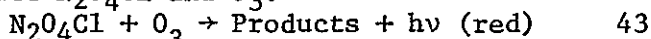$$ClOO + NO \rightarrow NO_2 + ClO \qquad 20a$$
$$\rightarrow ClNO + O_2 \qquad 20b$$

The ratio k_{20b}/k_{20a} was found to be 11.0 ± 2.2. The atmospherically important values $k_{20a} K_{31,-31} = (1.5 \pm 0.6) \times 10^{-32}$ cm^{6}sec^{-1} and $k_{20b} K_{31,-31} = (1.6 \pm 1.0) \times 10^{-31}$ cm^{6}sec^{-1} were evaluated at 298°K. From the results, it can be concluded that reactions 20a and 20b are probably not important in the stratosphere.
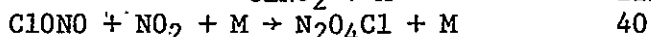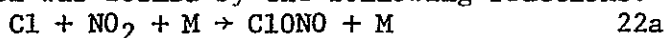
In the third system, Cl_2 was photolyzed at 366 nm and 219-273°K in the presence of NO_2 with added N_2 or O_2. The reaction mixture was bled continuously to a stream of ozonized oxygen from which chemiluminescence was observed during photolysis or shortly thereafter. The dark decay of the chemiluminescence was first order with a decay constant of 46.1 exp$[-(2000 \pm 300)/T]$ sec^{-1}. During the irradiation the initial relative quantum yield of the chemiluminescence, $\Phi_i^{rel}\{I\}$ was independent of the absorbed intensity, the total pressure, the Cl_2 pressure, and the diluent gas (N_2 or O_2). It increased with the NO_2

pressure at 273°K, but was independent of the NO_2 pressure at 238 or 219°K.

The observed chemiluminescence was due to the reaction between an intermediate N_2O_4Cl and O_3.

$$N_2O_4Cl + O_3 \rightarrow \text{Products} + h\nu \text{ (red)} \qquad 43$$

N_2O_4Cl was formed by the following reactions:

$$Cl + NO_2 + M \rightarrow ClONO + M \qquad 22a$$
$$\rightarrow ClNO_2 + M \qquad 22b$$
$$ClONO + NO_2 + M \rightarrow N_2O_4Cl + M \qquad 40$$

The formation of N_2O_4Cl required that the major product of reaction 22 was ClONO rather than $ClNO_2$. The upper limit for the rate coefficient of reaction 40 is 1×10^{-16} cm^{3}sec^{-1}. Therefore, reaction 40 is too slow to compete with the atmospheric photolysis of ClONO. Thus, reaction 40 is not important in atmospheric chemistry.

PSU-IRL-SCI-462
Classification Number: 1.9.2

Scientific Report 462

The Photolysis of Chlorine in the Presence
of Ozone, Nitric Oxide and Nitrogen Dioxide
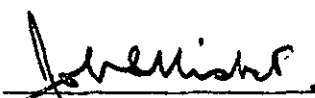

by

Wanee Wongdontri Stuper

August, 1979

Submitted by:

J. P. Heicklen, Professor
Chemistry

Approved by:

J. S. Nisbet, Director
Ionosphere Research Laboratory

Ionosphere Research Laboratory

The Pennsylvania State University

University Park, Pennsylvania 16802

ABSTRACT

The following three systems were investigated: the Cl_2-O_3 system, the Cl_2-O_2-NO system and the Cl_2-NO_2-M system. In the first system, the reaction between ClO and O_3, the reaction between OClO and O_3, and the mechanism of the Cl_2-O_3 system were studied. In the second system, the reaction between ClOO and NO was investigated. In the last system, the reaction between Cl and NO_2 was investigated as well as the kinetics of the chemiluminescence of the Cl-NO_2-O_3 reaction.

In the first system, Cl_2 was photolyzed at 366 nm in the presence of O_3 within the temperature range 254-297°K. O_3 was removed with quantum yields of 5.8 ± 0.5, 4.0 ± 0.3, 2.9 ± 0.3 and 1.9 ± 0.2 at 297, 283, 273, and 252°K respectively, invariant to changes in the initial O_3 or Cl_2 concentration, the extent of conversion or the absorbed intensity, I_a. The addition of nitrogen had no effect on $-\Phi\{O_3\}$. The Cl_2 removal quantum yields were 0.11 ± 0.02 at 297°K for Cl_2 conversions of about 30%, much higher than expected from mass balance considerations based on the initial quantum yield of 0.089 ± 0.013 for OClO formation at 297°K. The final chlorine-containing product was Cl_2O_7. It was produced at least in part through the formation of OClO as an intermediate which was also observed with an initial quantum yield of $\Phi_i\{OClO\} = 2.5 \times 10^3 \exp\{-(3025 \pm 625)/T\}$ independent of $[O_3]$ or I_a. The addition of nitrogen and oxygen had no effect on the values of $\Phi_i\{OClO\}$ and $-\Phi\{Cl_2\}$.

The results showed that OClO was formed by ClO radical combination as in reaction 23c.

$$2ClO \rightarrow ClOO + Cl \qquad 23a$$

$$\rightarrow Cl_2 + O_2 \qquad 23b$$

$$\rightarrow OClO + Cl \qquad 23c$$

The relative importance of the channels for reaction 23 at 296°K are the following: $k_{23a}/k_{23} = 0.63$; $k_{23b}/k_{23} = 0.34$; $k_{23c}/k_{23} = 0.032$. Also, $k_{23c}/k_{23b} = 2.5 \times 10^3 \exp[-(3025 \pm 625)/T]$.

The rate coefficient for the reaction of OClO with O_3 was studied by a direct mixing method and by the photolysis method.

$$OClO + O_3 \rightarrow Products \qquad 26$$

The temperature dependence of k_{26} was studied in the temperature range 264–297°K. However, at temperatures below 297°K, the equilibrium reaction 29 complicated the kinetics.
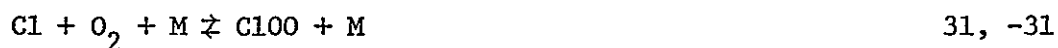
$$ClO + OClO + M \rightleftarrows Cl_2O_3 \qquad 29, -29$$

Thus the temperature dependence of k_{26} obtained from the photolysis method could only be evaluated from the steady state values of OClO. The recommended value for k_{26} is $2.3 \times 10^{-12} \exp[-(4730 \pm 630)/T]$ $cm^3 sec^{-1}$.

The upper limit for the rate coefficient of the reaction between ClO and O_3 was found to be less than 1×10^{-18} $cm^3 sec^{-1}$.

$$ClO + O_3 \rightarrow Products \qquad 25$$

The low values of k_{25} and k_{26} indicate that reaction 25 and 26 are probably not important in atmospheric chemistry.

In the second system, the reactions of ClOO with NO were studied by the photolysis of Cl_2 in the presence of NO and O_2 with or without added N_2 using steady state photolysis. ClOO is formed by the reversible reaction

$$Cl + O_2 + M \rightleftarrows ClOO + M \qquad\qquad 31, -31$$

The results indicate that ClOO reacts with NO via two channels:

$$ClOO + NO \rightarrow NO_2 + ClO \qquad\qquad 20a$$
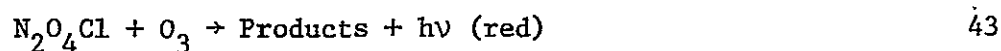
$$\rightarrow ClNO + O_2 \qquad\qquad 20b$$

The ratio k_{20b}/k_{20a} was found to be 11.0 ± 2.2. The atmospherically important values $k_{20a} K_{31,-31} = (1.5 \pm 0.6) \times 10^{-32}$ $cm^6 sec^{-1}$ and $k_{20b} K_{31,-31} = (1.6 \pm 1.0) \times 10^{-31}$ $cm^6 sec^{-1}$ were evaluated at 298°K. From the results, it can be concluded that reactions 20a and 20b are probably not important in the stratosphere.

In the third system, Cl_2 was photolyzed at 366 nm and 219-273°K in the presence of NO_2 with added N_2 or O_2. The reaction mixture was bled continuously to a stream of ozonized oxygen from which chemilum-- inescence was observed during photolysis or shortly thereafter. The dark decay of the chemiluminescence was first order with a decay constant of $46.1 \exp[-(2000 \pm 300)/T]$ sec^{-1}. During the irradiation the initial relative quantym yield of the chemiluminescence, $\Phi_i^{rel}\{I\}$ was independent of the absorbed intensity, the total pressure, the Cl_2 pressure, and the diluent gas (N_2 or O_2). It increased with

the NO_2 pressure at 273°K, but was independent of the NO_2 pressure at 238 or 219°K.

The observed chemiluminescence was due to the reaction between an intermediate N_2O_4Cl and O_3.

$$N_2O_4Cl + O_3 \rightarrow Products + h\nu \text{ (red)} \qquad\qquad 43$$

N_2O_4Cl was formed by the following reactions:

$$Cl + NO_2 + M \rightarrow ClONO + M \qquad\qquad 22a$$

$$\rightarrow ClNO_2 + M \qquad\qquad 22b$$

$$ClONO + NO_2 + M \rightarrow N_2O_4Cl + M \qquad\qquad 40$$

The formation of N_2O_4Cl required that the major product of reaction 22 was ClONO rather than $ClNO_2$. The upper limit for the rate coefficient of reaction 40 is 1×10^{-16} $cm^3 sec^{-1}$. Therefore, reaction 40 is too slow to compete with the atmospheric photolysis of ClONO. Thus, reaction 40 is not important in atmospheric chemistry.

TABLE OF CONTENTS

LIST OF TABLES

LIST OF FIGURES

ACKNOWLEDGMENTS

Chapter 1

INTRODUCTION

A.   The Role of Stratospheric Ozone

One of the most important goals in the study of upper atmospheric

chemistry is to be able to determine the effect of pollutants on

the ozone content. Ozone is one of the·most important constituents

of the earth's atmosphere because it absorbs solar radiation between

220 and 320 nm (1). It therefore provides a shield against the

harmful ultraviolet radiation for man (2) and at the same time is an

energy source for the stratosphere and mesosphere. The depletion

of the stratospheric ozone concentration may have both biological

(2,3) and climatological effects (4). Because of the thinner ozone

shield, more harmful ultraviolet radiation may reach the ground. This

could lead to an increase in the incidence of skin cancer. There are

quite a few catalytic cycles capable of influencing the stratospheric

ozone concentration. In this thesis, only chlorine, oxides of

chlorine, and oxides of nitrogen will be considered. The reactions

recently studied in this laboratory and their atmospheric implications

will also be discussed.

B.   The Role of ClO_x in the Atmosphere

Gas-phase chlorine forms a number of different species in the

atmosphere. The most common ones are HCl, Cl, ClO, OClO, ClOO, and

Cl_2. The sum of all of these species will be defined as ClO_x. The

sources of ClO_x are from both natural and anthropogenic origins. At

the ground level, the natural sources of HCl and Cl_2 are volcanic explosion (5,6) and sea salt spray (7,8). The anthropogenic sources are halogenated hydrocarbons used as solvents, herbicide sprays, aerosol propellants, and refrigerants. It is known that chlorine can cause plant damage. The chlorinated compounds are known to attack the liver (1) and some of them are also carcinogenic.

Recently Rowland and Molina (9-12) have pointed out the possibility that the commonly used chlorofluoromethanes might adversely affect the stratospheric ozone concentration. Two of the most important compounds are $CFCl_3$ and CF_2Cl_2, used primarily as aerosol propellants and refrigerants. Because of chemical inertness, their lifetimes in the troposphere (0-15 km) may be as long as 40-150 years (9). They seem to have no sinks in the troposphere. Their lifetimes are controlled by diffusion into the stratosphere (15-50 km) where they can be photodissociated by ultraviolet light (9). The photodissociation of chlorofluoromethanes releases chlorine atoms which can catalytically destroy stratospheric ozone. Wofsy et al. (13) predicted that the concentration of ozone could be reduced by an amount as large as 3% by 1980. This estimation was based on the 10% increasing rate of $CFCl_3$ and CF_2Cl_2 consumption per year.

It is worthwhile to note that the production of both $CFCl_3$ and CF_2Cl_2 were ceased at the beginning of this year (1979). According to Cicerone et al. (14), the effect of ClO_x on stratospheric ozone would still remain significant for several decades.

C. The Role of NO$_x$ in the Atmosphere

The common NO$_x$ constituents are NO, NO$_2$, NO$_3$, N$_2$O$_5$ and hydro-genated compounds such as HNO$_3$ and HNO$_2$. Of these oxides, only NO and NO$_2$ are important man-made pollutants (1). In the troposphere, the natural source of NO$_x$ is mainly biological activity in the earth's surface. The major man-made NO$_x$ sources are from motor vehicles and fuel combustion (1). It is known that oxides of nitrogen have harmful effects on materials, vegetation, and animal and human lives.

Nitrogen oxides are also one of the potential ozone destroyers through their catalytic cycle reactions with ozone and atomic oxygen. The important sources for stratospheric NO are the oxidation reaction between N$_2$O and O(^{1}D) (15-19), and the ionization and dissociation of N$_2$ following absorption of cosmic rays (20-22). Crutzen (23) and Johnston (24) have done extensive work on the NO$_x$ cycle. The ozone destruction efficiency of the NO$_x$ catalytic cycle is known to be less than that of the ClO$_x$ cycle. However, it is difficult to accurately predict the effect of the catalytic cycles in stratospheric ozone chemistry. This is because of the uncertainties in the actual concentration of the species involved, the possible heterogeneous reactions, and finally the possible interconnecting of the catalytic cycles.

D. Reactions of NO_x and ClO_x in the Stratosphere

The reactions in the stratosphere are mainly the reactions between the minor constituents and ozone. Ozone concentration reaches a maximum at the altitudes of 20-25 km. General reviews on the stratospheric ozone reactions were made by Crutzen (25) and Nicolet (26). Only the reactions of ozone with the NO_x and ClO_x cycles will be discussed here. Chapman (27) proposed that ozone is produced in the upper atmosphere by the reactions:

$$O_2 + h\nu \; (<240 \text{ nm}) \rightarrow 2O(^3P) \qquad\qquad 1$$

$$O(^3P) + O_2 + M \rightarrow O_3 + M \cdot \qquad\qquad 2$$
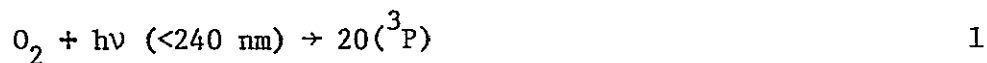
Ozone is destroyed by

$$O_3 + h\nu \; (<310 \text{ nm}) \rightarrow O_2 + O \qquad\qquad 3$$

$$O + O_3 \rightarrow 2O_2 \qquad\qquad 4$$

The electronic states of the products in O_3 photodissociation depend on the absorbed wavelength of the solar radiation. The more important ozone destroying reactions are those catalytic cycles involving NO_x (23,24) and ClO_x (9-12).

The NO_x cycle involves NO and NO_2 as catalysts for the combination of ozone and atomic oxygen through the following pair of reactions:

$$NO + O_3 \rightarrow NO_2 + O_2 \qquad\qquad 5$$

$$NO_2 + O(^3P) \rightarrow NO + O_2 \qquad\qquad 6$$

$$O_3 + O(^3P) \rightarrow 2O_2 \qquad\qquad\qquad \text{net reaction}$$

The rate coefficient for reaction 5 is $(2.34 \pm 0.23) \times 10^{-12}$ $\exp[-(1450 \pm 50)/T]$ $cm^3 sec^{-1}$ (28-32). At 298°K, the rate coefficient for reaction 6 is $(9.1 \pm 0.2) \times 10^{-12}$ $cm^3 sec^{-1}$ (33-35). The major sink for NO_x in the stratosphere appears to be the formation of HNO_3 via the following reaction:

$$NO_2 + OH + M \rightarrow HNO_3 + M$$
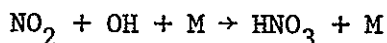
HNO_3 may photodissociate to give OH and NO_2 as major products. HNO_3 can be removed from the stratosphere by its downward transport into the troposphere where it will be rapidly removed by rain.

The problem with chlorine species begins after the chlorine containing compounds diffuse upward through the troposphere into the stratosphere. Chlorine atoms are released by the photodissociation of these chlorine containing compounds upon absorbing the ultraviolet radiation. The photodissociation occurs mainly at 175-220 nm. The solar radiation between 180 and 240 nm is weakly absorbed by O_2 and O_3 (1), and therefore it can penetrate all the way down to 20 km. The dominant photochemical processes are

$$CFCl_3 + h\nu \ (<226 \text{ nm}) \rightarrow CFCl_2 + Cl \qquad\qquad 8$$

$$CF_2Cl_2 + h\nu \ (<215 \text{ nm}) \rightarrow CF_2Cl + Cl \qquad\qquad 9$$
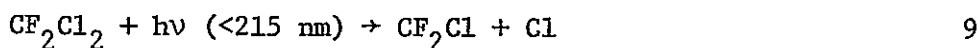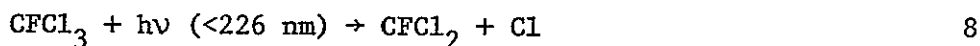
The quantum yields of both reactions 8 and 9 are unity as reported by Marsh and Heicklen (36), Jayanty et al. (37), and Milstein and Rowland (38).

When a chlorine atom is generated it reacts immediately with stratospheric ozone as in the following sets of reactions (9,29,39,40).

$$Cl + O_3 \rightarrow ClO + O_2 \qquad\qquad 10$$

$$ClO + O(^3P) \rightarrow Cl + O_2 \qquad\qquad 11$$

$$O_3 + O(^3P) \rightarrow 2O_2 \qquad\qquad \text{net reaction}$$

The rate coefficients for reactions 10 and 11 at 298°K are 1.2×10^{-11} $cm^3 sec^{-1}$ (41) and 5.3×10^{-11} $cm^3 sec^{-1}$ (42) respectively. The result of reaction 10 is the production of chlorine monoxide, ClO, which in turn reacts readily with oxygen atoms in reaction 11 to regenerate the chain carrier. The net result of this cycle is that Cl and ClO catalyze the combination of ozone and atomic oxygen.

The chain is interrupted by reactions which convert Cl to HCl (9-12). For example:

$$Cl + CH_4 \rightarrow HCl + CH_3 \qquad\qquad 12$$

$$Cl + H_2 \rightarrow HCl + H \qquad\qquad 13$$

$$Cl + HO_2 \rightarrow HCl + O_2 \qquad\qquad 14$$

$$Cl + H_2O_2 \rightarrow HCl + HO_2 \qquad\qquad 15$$

Chlorine atoms are removed from the chain reaction until HCl reacts with OH or $O(^1D)$ atoms to release Cl once again. The chain is terminated when the long-lived species such as HCl reach the troposphere by downward diffusion. They are presumably removed from the atmosphere by rain in a relatively short time.

There are several other reactions affecting chlorine species

such as the presence of NO and NO_2 below 35 km (39). At this

altitude NO and NO_2 compete effectively with oxygen atoms for ClO

as in reaction 16 and 17 below.

$$ClO + NO \rightarrow Cl + NO_2 \qquad\qquad 16$$

$$ClO + NO_2 + M \rightarrow ClONO_2 + M \qquad\qquad 17$$

The rate coefficients of reactions 16 and 17 at 298°K are

respectively 1.8×10^{-11} $cm^3 sec^{-1}$ (43,44) and 1.5×10^{-31} $cm^6 sec^{-1}$

for $M = N_2$ (45,46).

To estimate the importance of reaction 16, the three catalytic

cycles which are the pure ClO_x cycle, the pure NO_x cycle, and the

mixed ClO_x-NO_x cycle, must be considered. The pure ClO_x cycle

consists of reactions 10 and 11, and the pure NO_x cycle consists

of reactions 5 and 6 as mentioned previously. The mixed ClO_x-NO_x

cycle actually consists of two cycles, cycle A where there is no net

change in the odd oxygen $[O_3, O(^3P)]$, and cycle B where two odd

oxygen are destroyed. Cycles A and B consist of the following set

reactions:

Cycle A:

$$Cl + O_3 \rightarrow ClO + O_2 \qquad\qquad 10$$

$$ClO + NO \rightarrow Cl + NO_2 \qquad\qquad 16$$

$$\underline{NO_2 + h\nu \rightarrow NO + O} \qquad\qquad 18$$

$$O_3 + h\nu \rightarrow O + O_2 \qquad\qquad \text{net reaction}$$

Cycle B:

$$Cl + O_3 \rightarrow ClO + O_2 \qquad\qquad 10$$

$$ClO + NO \rightarrow Cl + NO_2 \qquad\qquad 16$$

$$\underline{NO_2 + O(^3P) \rightarrow NO + O_2} \qquad\qquad 6$$

$$O_3 + O(^3P) \rightarrow 2O_2 \qquad\qquad \text{net reaction}$$
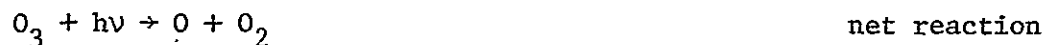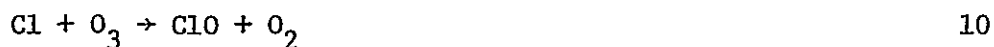
The significance of reaction 16 is that it converts NO to NO_2.

Reaction 16 also connects the ClO_x cycle to the NO_x cycle.

Above 35 km, the rate of reaction 11 is expected to be higher

than the rate of reaction 16. Hence the pure ClO_x cycle is expected

to be more effective than the mixed ClO_x-NO_x cycle. At lower altitudes

(<35 km), the rate of reaction 16 is faster than that of reaction 11

due to the low concentration of oxygen atoms. Hence the contribution

to ozone loss by the pure ClO_x cycle decreases because of the existence

of the mixed ClO_x-NO_x cycle.

Reaction 17 is a termination reaction for both the ClO_x and NO_x

cycles. Birks et al. (46) and Rowland et al. (47) found that $ClONO_2$

is quite stable in the gas phase and is unreactive towards NO, NO_2

or HCl. The reaction of $ClONO_2$ with O_3 is an order of magnitude

slower than the photolysis rate of $ClONO_2$ (46). The average

photolysis time for $ClONO_2$ is about 4.5 hours (47). The products of

the photolysis are not known. However, the products are assumed to

be ClO and NO_2 for modeling calculations. The presence of $ClONO_2$

in the stratosphere reduces the concentration of ClO and at the same

time ties up NO_2 into an inactive form until it photodissociates.

Since $ClONO_2$ is only significant in the lower stratosphere (15-35 km), it is expected to affect the NO_x cycle more than the ClO_x cycle. This is because the former cycle occurs mainly in the lower stratosphere, whereas the latter cycle occurs mainly in the upper stratosphere.

Another species which became of interest recently is chlorine nitrite, ClONO. Jesson et al. (48) suggested that ClONO might be important in the atmosphere. ClONO may be formed in the stratosphere by the following reaction:

$$ClO + NO + M \rightarrow ClONO + M \qquad\qquad 19$$

The third order rate of reaction 19 is quite slow because of the low total pressure, M, in the stratosphere. Therefore, there is not likely to be any significant amount of ClONO produced in the stratosphere. Molina and Molina (49) recently obtained the absorption cross section of ClONO. They concluded that ClONO would be readily photodissociated and would not be important in the atmosphere.

The chemistry of ClO_x strongly depends on the concentrations of other species such as NO_x and HO_x. It is clear that in order to accurately predict the effectiveness of the ClO_x and NO_x catalytic cycles on the stratospheric ozone, more quantitative determinations of stratospheric trace gases are needed. There is also a critical need for the rate coefficients of the reactions interconnecting the catalytic cycles as well as the understanding of the reactions of higher chlorine oxides.

E. This Work

The three systems studied here were:

1. Cl_2-O_3 system

2. Cl_2-O_2-NO system

3. Cl_2-NO_2-M system, where M is N_2 or O_2.

The main purposes for studying the first system were to investigate the mechanism of this system, to estimate the rate coefficients of the reaction between ClO and O_3 as well as the reaction between OClO and O_3. In the second system, the purpose was to obtain the rate coefficient of the reaction between ClOO and NO and also estimate its possible importance in the atmosphere. The purpose for investigating the third system was to study the chemiluminescent reaction of Cl atoms with NO_2 and O_3 and the mechanism of the reaction of Cl atoms with NO_2. The details of previous works done in each reaction will be discussed individually in the following sections.

E.1. The Cl_2-O_3 System

An understanding of the Cl_2 photocatalytic decomposition of ozone is of relevance to the understanding of the atmospheric ClO_x cycle. This system was extensively investigated 30 to 40 years ago (50-59). However, the details of the mechanism remain obscure. Davidson and Williams (60) have recently studied the Cl_2-O_3 system by measuring the stable products. The only product observed was Cl_2O_7. However, it seems that a satisfactory explanation for the

formation of Cl_2O_7 has not been reached. It is apparent that more work should be done to clarify the mechanism of this system.

E.2. The Reactions of ClO with O_3

Even if the reaction of ClO with O_3 is relatively slow, it is of potential importance in determining the effect of the ClO_x on stratospheric ozone. Very little information is available concerning this reaction. There were two independent studies by Clyne et al. (61) and Birks et al. (46), both using a discharge flow system with mass spectrometric detection of ClO. Clyne et al. have obtained an upper limit for the rate coefficient of 5×10^{-15} cm^3sec^{-1} and Birks et al. have found the value of 5×10^{-14} cm^3sec^{-1}. Lin et al. (62), using a steady state photolysis study of the Cl_2-O_3 system, reported the upper limit to be 1×10^{-18} cm^3sec^{-1}. This work intends to resolve this discrepancy.

E.3. The Reaction of OClO with O_3

The kinetics of the reaction of OClO with O_3 had never been studied directly before our work was initiated. It is unlikely that this reaction would be of much importance in the atmosphere. This is because OClO would probably be readily photodissociated. Nevertheless it seemed appropriate to obtain the rate coefficient of this reaction. The rate of the reaction between OClO and O_3 can then be compared with the photodissociation rate of OClO.

E.4. The Reactions of ClOO with NO

The assumption that reactions of ClOO radicals with other atmospheric constituents are unimportant is probably correct for most of the middle and upper stratosphere. The reasons for the low densities of ClOO radicals at that altitude are the relatively high temperature and low O_2 densities. However, in the lower stratosphere at altitudes between 15 and 20 km, significant concentrations of ClOO may be present. The ClOO radicals may participate in the reactions with other atmospheric constituents if the rate coefficieints are large enough.

ClOO radicals may react with nitric oxide, NO. This is possible because the concentration of NO is quite significant. The reaction between ClOO and NO has not been considered or studied previously.

$$ClOO + NO \rightarrow ClO + NO_2 \qquad\qquad 20a$$

$$\rightarrow ClNO + O_2 \qquad\qquad 20b$$

We estimate that this reaction could compete with reaction 10 if the rate coefficient, k_{20}, is 1×10^{-11} $cm^3 sec^{-1}$.

$$Cl + O_3 \rightarrow ClO + O_2 \qquad\qquad 10$$

Also reaction 20 can compete with reaction 21 if k_{20} is 1×10^{-12} $cm^3 sec^{-1}$.

$$HO_2 + NO \rightarrow HO + NO_2 \qquad\qquad 21$$

.Thus a measurement of the rate coefficient for reaction 20 seems

important.

E.5. The Mechanism of $Cl-NO_2-M$ Reactions and the Kinetic

Study of the Chemiluminescence in the $Cl-NO_2-O_3$ System

Chlorine atoms are known to add readily to NO_2. It was

commonly assumed that the only product of the reaction is nitryl

chloride, $ClNO_2$ (63,64). However there is another possible channel

for this reaction, that is, the production of. chlorine nitrite,

ClONO.

$$Cl + NO_2 + M \rightarrow ClNO_2 + M \qquad \qquad \qquad 22a$$

$$\rightarrow ClONO + M \qquad \qquad \qquad 22b$$

ClONO is known to be a rather unstable compound. It rapidly

undergoes isomerization to form the more stable $ClNO_2$ via hetero-

geneous processes (49). Niki et al. (65), using a Fourier transform

spectrometric method, recently observed that both $ClNO_2$ and ClONO

were the products in the photolysis of Cl_2-NO_2 mixtures. The

observed yield of ClONO was $\geq 80\%$. They suggested that Cl adds to

the O atom rather than the N atom of the NO_2 molecule.

Jesson et al. (48) suggested that ClONO might be important in

the chemistry of stratospheric chlorine. Molina and Molina (49)

recently obtained its ultraviolet absorption cross section. They

concluded that its lifetime against photodissociation in the

atmosphere is two to three minutes. Thus it is unlikely that ClONO

would play any significant role in the stratosphere. It is never-
theless important that the mechanism of the $Cl-NO_2$ reaction be
reinvestigated.

A strong emission in the red was observed when the photolyzed
mixtures of Cl_2-NO_2-M were mixed with a stream of ozonized oxygen.
Presumably an unstable intermediate, which was formed from the
reaction of Cl with NO_2, reacts with O_3 in the chemiluminescent
reaction. It was of interest to investigate this chemiluminescent
reaction in the $Cl-NO_2-O_3$ system.

Chapter 2

THE Cl_2-O_3 SYSTEM: THE REACTIONS OF ClO AND OClO WITH O_3 .

A. <u>Experimental</u>

A.1. <u>Materials and Their Purification</u>

All gases except OClO, azomethane, and O_3 were supplied by

Matheson Gas Products. The Cl_2 (Matheson high purity research

grade, 99.96% purity) was first degassed at -196°C and then

purified by distillation from -130°C to -160°C. · At -196°C, the

color of the purified solid was yellow with no trace of white

color. Several experiments were run in which prior to distillation,

Cl_2 was slowly passed through a glass column packed with KOH

pellets. This was to insure that the Cl_2 was free from any HCl

impurities. The KOH treatment was stopped after it was found that

the experimental results were not influenced by this procedure.

The purified Cl_2 was stored in the dark at room temperature. ·

Chlorine dioxide, OClO, was prepared from a procedure by King

and Partington (66) with some slight modifications. Purified Cl_2

was slowly passed over a U-shape Pyrex tube, packed with glass

beads and dry $AgClO_3$ (K and K Laboratories). The U-tube was submerged

at a bath kept at 80 ± 10°C. The product was condensed in another

U-tube at -196°C and the noncondensable product (O_2) was discarded.

OClO was separated from the excess Cl_2 by distillation from -130°C

to -160°C and then further purified by distillation from -60°C to

-196°C. OClO is a red-orange liquid at -23°C and a canary yellow

solid at -196°C. OClO was stored in the dark at liquid N_2

temperature.

Ozone was prepared from oxygen by the following method. A

Tesla coil was used to subject low pressure oxygen (≤ 12 Torr) to

an electrical discharge. The ozone produced was collected in a

U-tube trap maintained at -196°C. The noncondensable gas was

discarded. The ozone was purified by distillation from -186°C

to -196°C. It was stored in the dark at liquid N_2 temperature.

Azomethane, $CH_3N_2CH_3$, was prepared from a procedure described

by Renaud and Leitch (67) with some modifications. Ten grams of

sym-dimethylhydrazine dihydrochloride (Aldrich Chemical Company)

were dissolved in 30 cm^3 of water made basic with 2 g NaOH. The

mixture was then added dropwise while stirring to 100 cm^3 of water

containing 30 g of HgO (yellow form). N_2 gas was bubbled through

this mixture while the reaction was carried out. Water was removed

from the evolved gases by passing them through a $CaCl_2$ trap. The

azomethane was collected in a liquid N_2 trap and was purified by

distillation from -90°C to -130°C. It was stored in the dark at

room temperature.

For the distillations, only the middle fraction of the gases

was collected. The first and last fractions were discarded. The

chlorine dioxide, ozone and azomethane were degassed at -196°C

immediately before use.

The O_2 and N_2 were Matheson C.P. grade and were used without

further purification. It was observed by Jayanty (68) that the

experimental results were not influenced by whether the O_2 (≥ 500 Torr) was passed through a liquid N_2 trap to remove any condensable gases. This was also the case for high pressure N_2 (≥ 500 Torr) under our experimental conditions.

A.2. The Vacuum Line

All experiments were carried out in a conventional mercury-free high vacuum line utilizing Teflon stopcocks fitted with Viton "O" rings. A pressure of less than 1 mTorr was achieved by pumping continuously through a Welch Duo Seal Model 1402 mechanic pump in conjunction with an oil diffusion pump. Pressure was measured by a Veeco thermocouple gauge Model TG-7 with a vacuum gauge tube Model DV-1M and an alphatron vacuum gauge (NRC 820). Pressures below 30 Torr were measured by a silicone oil manometer (704 Dow Corning Oil). Pressures less than 0.8 Torr were obtained by expansion. High pressures (>30 Torr) were measured by an alphatron vacuum gauge calibrated with an oil manometer. A diagram of the vacuum line is given in Figure 1.

A.3. Reaction Vessels and Radiation Source

The reaction vessel was a cylindrical quartz cell 10 cm long and 5 cm in diameter. This cell was enclosed in a Styrofoam box which served as an insulator for low-temperature experiments. The Styrofoam box and the detection system were enclosed in a dark metal box. This box was used to prevent room light from interfering with the measurements. The Styrofoam box contained three evacuated double

Figure 1. Vacuum Line for the Cl_2-O_3 System

4 OR 10 mm TEFLON STOPCOCK

STORAGE BULB

4-WAY GROUND-GLASS STOPCOCK

ACE GLASS GAS INLET WITH A 4 mm TEFLON STOPCOCK

TO VEECO THERMOCOUPLE GAUGE

TO ALPHATRON GAUGE

TO GAS CHROMATOGRAPH

He FLOW

GAS CHROMATOGRAPH SAMPLE SPIRAL TRAP

SPIRAL TRAP

TO REACTION CELL

TO OIL MANO-METER

LIQUID N₂ TRAP

OIL DIFFUSION PUMP

TO MECHANICAL PUMP

19
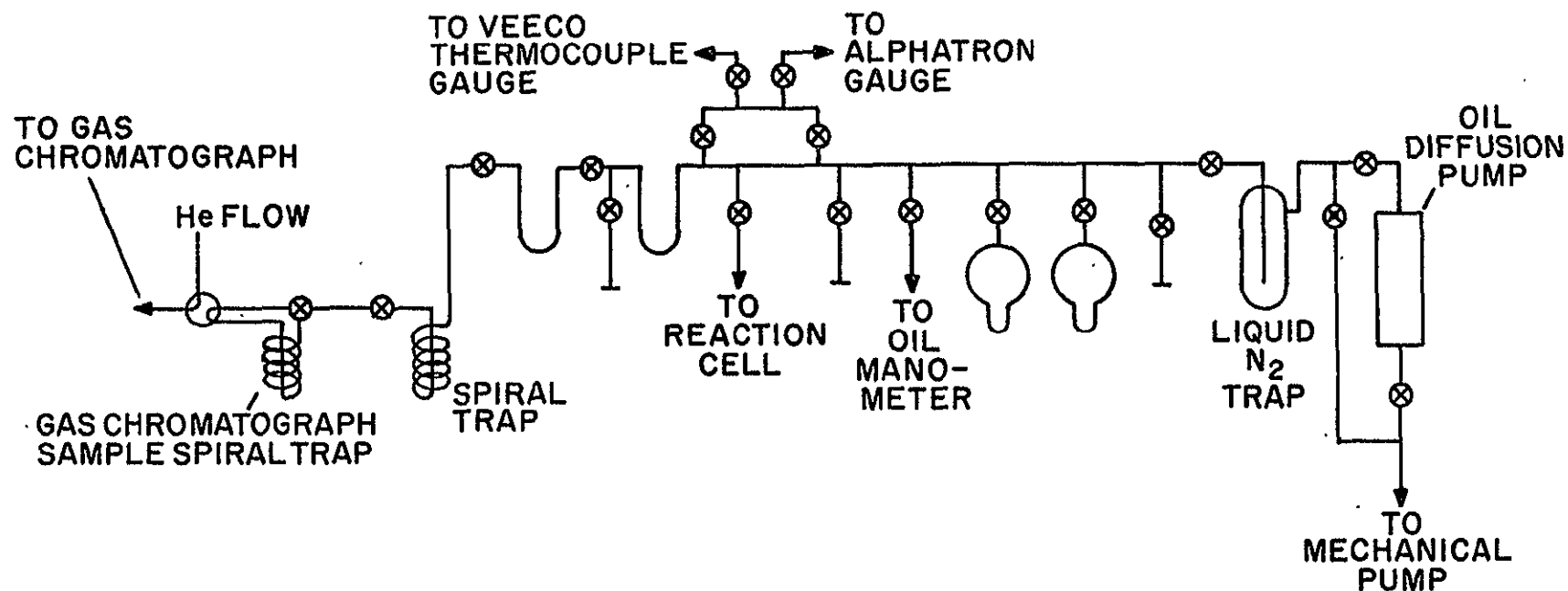
wall quartz windows. The window perpendicular to and centered along the reaction vessel allowed passage of the photolysis beam. The other two windows centered on the ends of the reaction cell served as access for the analysis beam and detection system. An evacuated double wall quartz window was actually a cylindrical Pyrex cell 5 cm long and 5 cm in diameter with a quartz window on each end of the cylindrical Pyrex cell. This cell was evacuated before being used to prevent condensation at low temperature. A diagram of this arrangement is given in Figure 2.

The temperature inside the Styrofoam box was lowered by passing nitrogen gas through a copper coil immersed in liquid nitrogen and flushing this cold gas through the box. The temperature was measured with two iron – constantan thermocouples attached to the reaction vessel. The positions of the thermocouples were carefully chosen to avoid being directly cooled by the blowing of the cold nitrogen gas or directly heated by the photolysis beam. . The thermocouple potential was measured with a precision potentiometer made by the Rubicon Company of Philadelphia, Pennsylvania. The temperature was manually controlled by changing the flow rate of the nitrogen.

The photolysis source was a high pressure Hanovia Hg arc lamp, 200 watts (Type 202-1003). The 366 nm line was obtained by passing the beam through a Corning filter (CS 7-37) prior to entering the reaction cell. A diagram of the reaction cell and the radiation system is shown in Figure 2.

Figure 2. Reaction Cell and Radiation Source for the Cl_2-O_3 System

TO VACUUM LINE

⊗ 4 mm TEFLON
STOPCOCK

F

F

E

D

ANALYSIS BEAM

TO DETECTION SYSTEM

D

D

K

PHOTOLYSIS BEAM

C

G   H

I

L

B

J

A
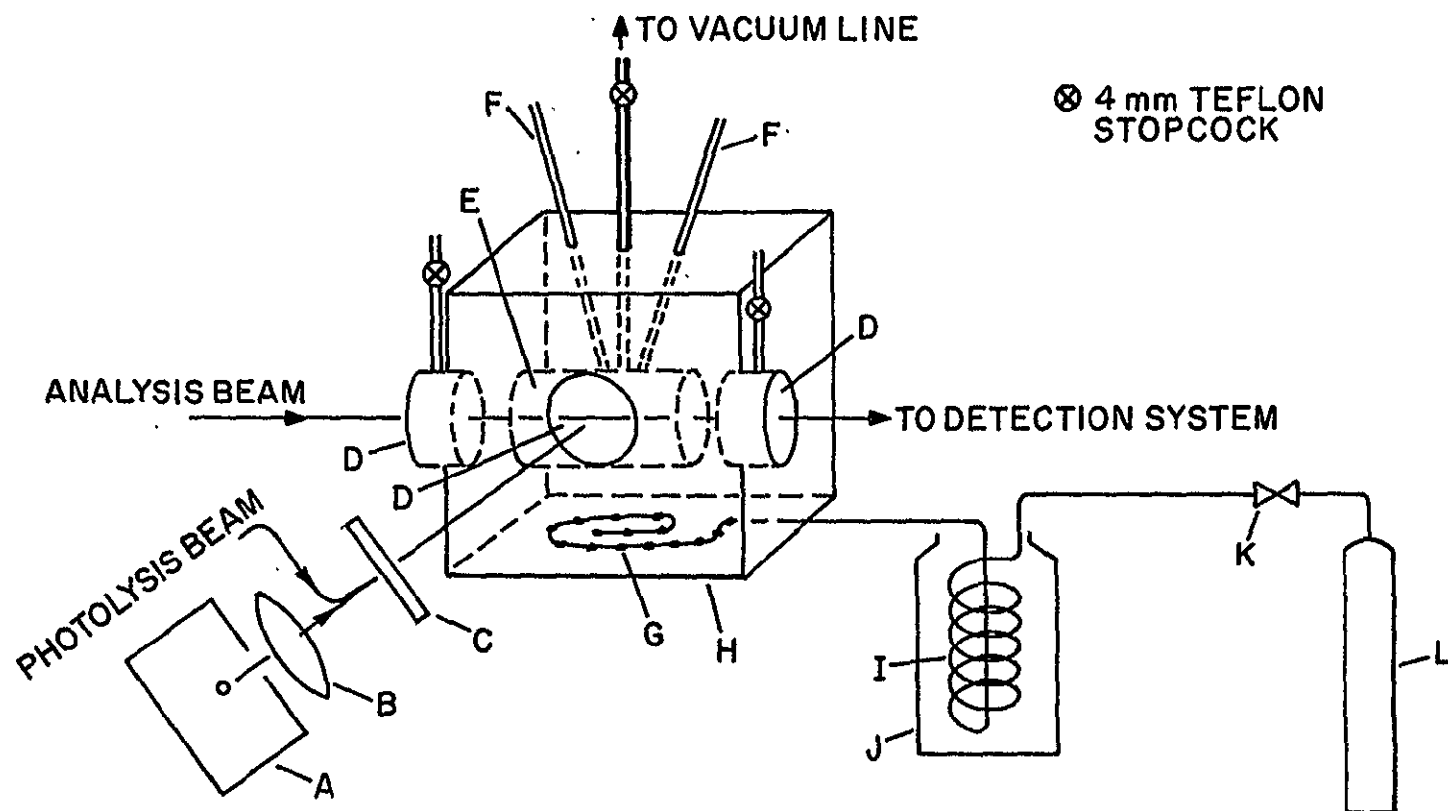
A   HANOVIA MERCURY ARC LAMP
B   QUARTZ LENS
C   CORNING GLASS FILTER
D   EVACUATED DOUBLE WALL
      QUARTZ WINDOWS
E   QUARTZ REACTION CELL
F   THERMOCOUPLES

G   COPPER TUBE WITH EXIT HOLES
H   STYROFOAM BOX
I   COPPER COIL
J   LIQUID NITROGEN DEWAR
K   NEEDLE VALVE
L   NITROGEN COMPRESSED GAS
      CYLINDER

22

A.4. Product Analysis System

The absorption of the reaction mixture was monitored at 400 nm as a function of irradiation time using the dual beam spectrophotometer. The 400 nm line was obtained by passing the radiation from a 300-watt tungsten lamp through a Corning filter (CS 7-59). Before entering the reaction cell the analysis beam was modulated using a PAR model 125 chopper. The chopper consisted of a chopping wheel with 16 slots and 16 mirrors. This provided a modulating frequency of 667 Hz. When the analysis beam impinged upon a slot, the beam was allowed to pass through the reaction vessel and was focused on a RCA 935 phototube. When the beam impinged upon a mirror, it was reflected and focused on to the second RCA 935 phototube without passing through the reaction vessel. Hence the outputs from the two phototubes were 90° out of phase. The outputs were then electronically added and introduced to a lock-in amplifier (PAR model 121).

Before photolysis, the positions of the two phototubes were adjusted so that both tubes received equal amounts of light from the analysis lamp. The signal from the phototubes, before entering the lock-in amplifier could be finely tuned by using a phase/amplitude adjustor. The circuit for the phase/amplitude adjustor is shown in Appendix I. The square wave, 667 Hz, from the chopper served as a reference signal to the lock-in amplifier. Any input signals other than 667 Hz were eliminated by the lock-in amplifier. The change in absorption caused by either the intermediate species or the products initiated by the photolysis unbalances the outputs of the

two phototubes. The unbalanced signal would be registered by the
lock-in amplifier and recorded as a function of time by a strip
chart recorder. The arrangement of the analysis system is shown
in Figure 3. A schematic diagram for the circuit of the analysis
system is given in Figure 4.

A.5. Procedure

Using the dual beam spectrometer the reaction mixture absorption
was monitored at 400 nm as a function of irradiation time. Initially
the absorption increased linearly, then leveled off and finally
reached a steady state (corresponding to several mTorr of OClO). The
steady state value slowly increased with continued irradiation until
near the end of the reaction, i.e., when nearly all the O_3 was
consumed, the absorption then increased to a sharp maximum and
finally declined to zero upon continued irradiation. The change in
the absorption profile of OClO with the irradiation time is shown
in Figure 5. The absorption spectrum of the photolysis mixture at
this maximum absorption was studied by Jayanty (68). The mixture was
condensed in a liquid N_2 trap and the residual Cl_2 was removed from
the mixture by distillation at $-130°C$. The greenish-yellow product
remaining after distillation was identified to be OClO by its
absorption spectrum.

The initial rates of OClO formation and its steady state
concentration were determined from the initial increase in absorption
and the initial steady state value, respectively. In order to obtain
absolute OClO concentrations, the effective absorption cross section

Figure 3. Schematic Diagram of the Dual Beam Spectrophotometer
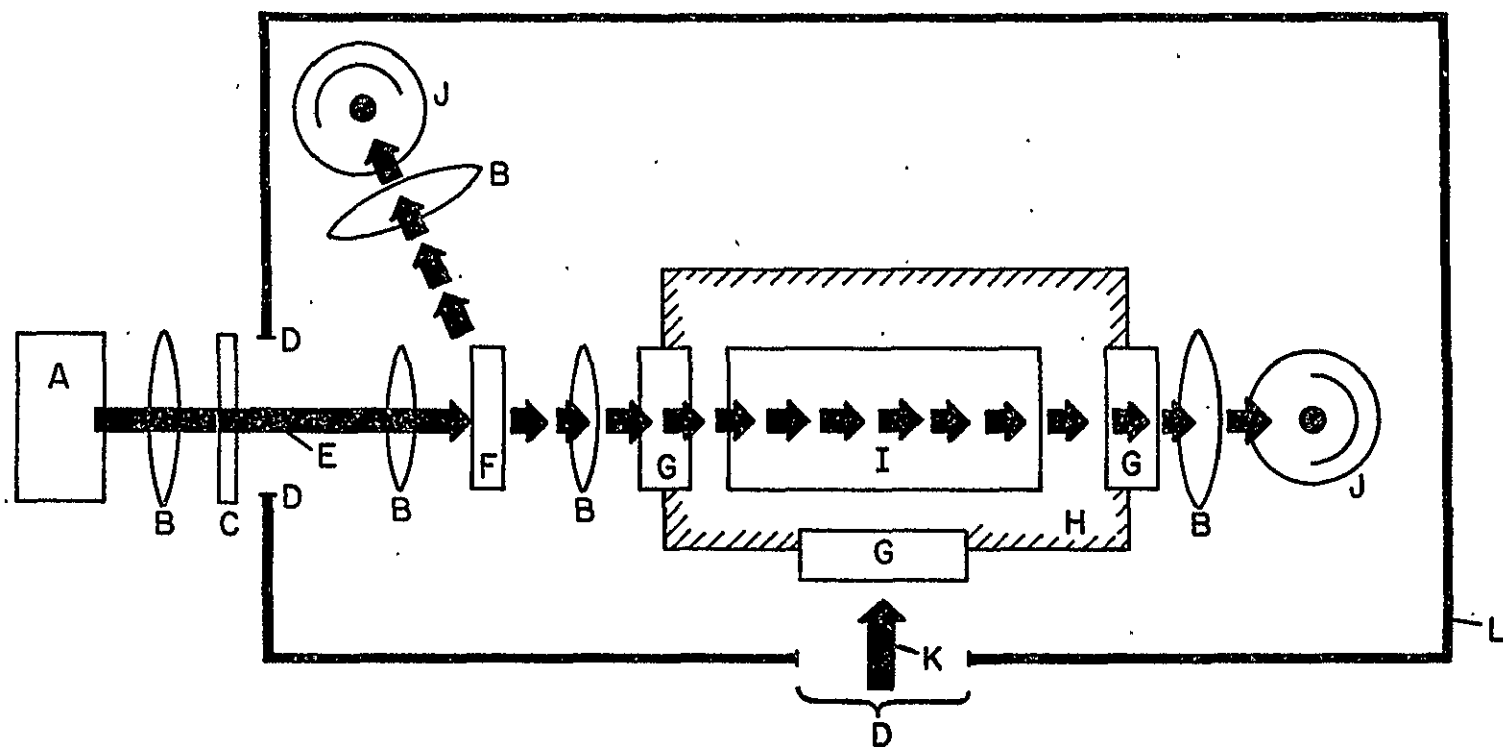
A   LIGHT SOURCE
B   QUARTZ LENS
C   CORNING GLASS FILTER
D   SLITS
E   ANALYSIS BEAM
F   LIGHT CHOPPER

G   EVACULATED DOUBLE WALL QUARTZ WINDOWS
H   STYROFOAM BOX
I   QUARTZ REACTION CELL
J   RCA 935 PHOTOTUBES
K   PHOTOLYSIS BEAM
L   DARK METAL BOX

26
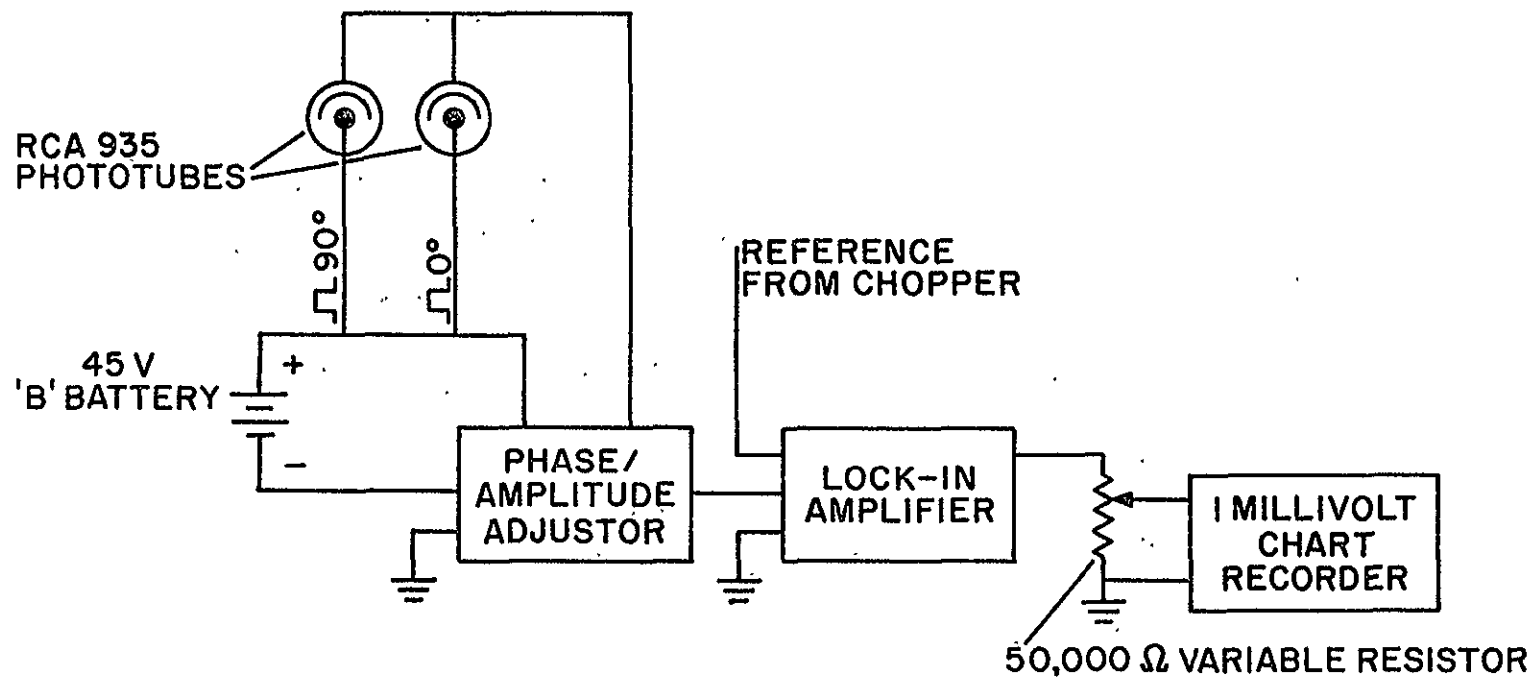
Figure 4. Detector Circuit of the Dual Beam Spectrophotometer
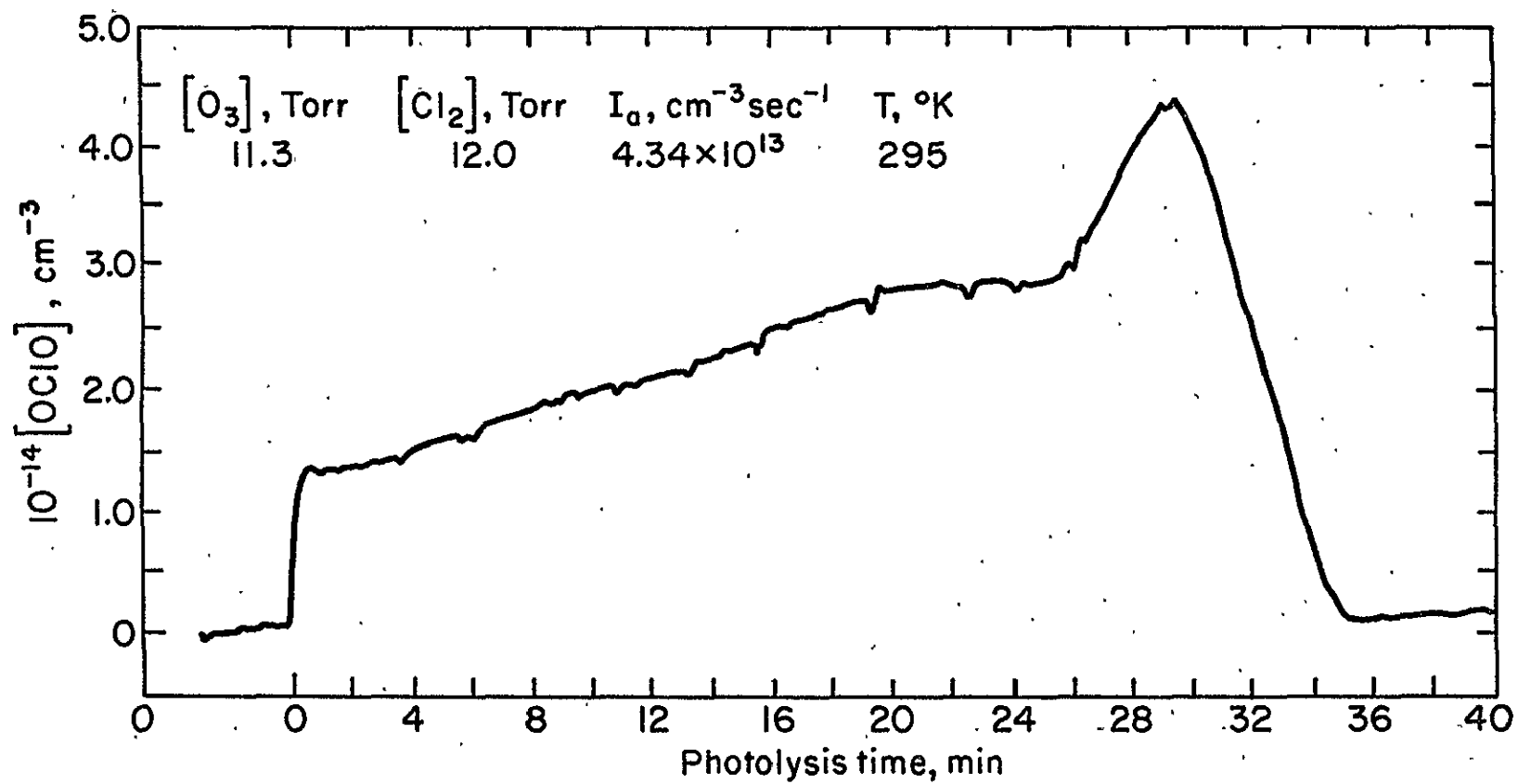
Figure 5. OClO Absorption Profile as a Function of Irradiation Time

was determined under identical conditions for the lamp-filter combination described in Section A.4. A known amount of OClO was introduced into the reaction cell and the percentage of the analysis light transmitted through the reaction cell was obtained. The absorption cross section of the OClO was calculated from Beer's law. The results of these measurements are listed in Table 1.

The rate of the reaction of OClO with O_3 was determined by two methods. In the first method mixtures of Cl_2 and O_3 were photolysed until some OClO (usually the steady state value) was produced. The light was then turned off and the OClO decay monitored as a function of time. This method could be used only at room temperature, because at lower temperatures Cl_2O_3 complicated the kinetics.

In the second method, OClO and excess O_3 were mixed directly in the quartz cell. The OClO decay was monitored as a function of reaction time. With this direct technique, experiments were possible at low temperatures because Cl_2O_3 formation could not occur. In order to obtain the "minimum" rate of the reaction at lower temperatures, it was necessary to warm the cell to room temperature and pump on it for some time. Additionally, it was necessary to periodically clean it with a HNO_3 solution. If this procedure was not followed, the rate of the reaction for subsequent runs was always higher.

Chlorine removal rates were determined in the photolysis experiments by measuring the chlorine concentration at 366 nm with the dual beam spectrophotometer. To provide the 366 nm analysis

Table 1

The Extinction Coefficient of OClO at 400 nm and 297°K

[OClO], Torr	% Transmittance	$10^{18}\sigma$ cm^2
1.21	65.5	1.17
1.32	63.6	1.14
1.33	63.3	1.15
1.36	62.5	1.15
1.56	58.9	1.16

beam, a low-pressure Hg lamp (Phillips 93109 E) was used with a Corning filter (CS 7-37). This lamp was used because of its stable beam and also because Cl_2 has a maximum absorption cross section at 366 nm. In order to observe a 30% change in the Cl_2 pressure, approximately one hour of irradiation was required. Because of instrument baseline drift over the long irradiation times, the change in Cl_2 concentration was determined by observing the change in the signal level during the short pump out time of the cell. It was possible that some OClO which was the intermediate of the Cl_2-O_3 photolysis system, might interfere. To prevent this, O_3 was present in excess for each run. Thus any OClO present was readily converted to higher chlorine oxides. To check this, several experiments were run in which excess O_3 was added after the end of the experiment. The mixture was allowed to stand for some time to allow complete reaction of any OClO which might be present. These experiments indicated that no interference from OClO was detected.

The ozone removal rates were determined by photolyzing the Cl_2-O_3 mixtures at 366 nm. The change in the O_3 concentration with irradiation time was followed by 260 nm. The 260 nm analysis light was obtained by passing the radiation from a Phillips Hg resonance lamp (93109 E) through a Cl_2 gas filter cell and a Corning filter (CS 7-54).

The O_2 production rates were measured by photolyzing of O_3 and Cl_2 in a 200 cm^3 quartz cell. The O_2 produced was measured by condensing the reaction mixture in a trap at -196°C and measuring the pressure of the non-condensable O_2 with an oil manometer.

The O_2 was then removed by pumping on the reaction·mixture at $-196°C$. The ·reaction mixture was warmed to $-189°C$, and the residual O_3 was then measured with an oil manometer. Calibration for expansion was done with comparable known pressures of O_2.

The possibility that other chlorine oxides might interfere with · the absorption measurements in our system were considered as follows: Cl_2O_7 is completely transparent at wavelengths higher than 320 nm · as reported by Goodeve et al. (69) and Lin (70). ClO_3, as reported by Goodeve et al. (71); absorbed in the ultraviolet and had a threshold at about 350 nm. Calculations using the maximum expected ClO_3 concentration, and the known absorption cross section showed that ClO_3 would not contribute significantly to the absorption in the region 350 nm to 420 nm. As reported by Rigaud et al. (72), the absorption cross section for ClO is very low at wavelengths higher than 300 nm. Its absorption cross section is about two orders of magnitude smaller than those of OClO at 400 nm. Therefore, ClO would not contribute significantly to the absorption measurements in the system. Thus, it appears that other chlorine· oxides would not interfere with the OClO measurements.

A.6. Actinometry

The absorbed light intensity was determined for each temperature by photolysis of an optically equivalent amount of azomethane. N_2 has been shown to be a primary product of the photolysis at 366 nm. The quantum yield of this reaction is unity and is independent of pressure, temperature, light intensity, or photolysis time (73-75).

The amount of N_2 produced was measured by a thermistor gas chromatograph. The column was a 10 ft. long, 1/4 inch O.D. copper tube packed with 80/100 mesh 5A molecular sieves. The column was kept at room temperature. Helium was used as a carrier gas. Prior to entering the column, the carrier gas was passed through Drierite and Ascarite to remove water and CO_2. The flow rate was 1.0 cm^3/sec. A Gowmac model 10-777 stainless steel block thermistor detector was used. The detector was kept at 0°C and operated at 15 milliamps. The gas chromatograph was calibrated using standard N_2 samples. The retention time for N_2 was approximately nine minutes. A schematic diagram of the gas chromatograph is shown in Figure 6.

B. Results

B.1. OClO Formation Quantum Yield

The photolysis of Cl_2-O_3 mixtures at 366 nm led to the removal of O_3 and Cl_2. As found by Jayanty et al. (76), O_2 and Cl_2O_7 are the final products of the photolysis and OClO is produced as an intermediate. Typical OClO growth profiles during irradiation and the decay profiles when the irradiation light is turned off are shown in Figure 7. Initially, the OClO concentration grows linearly and then levels off to a steady state value. When the light is turned off and O_3 is still present in excess, the OClO decays exponentially. As seen in Figure 7, at 295°K the OClO decays immediately in the dark. However, at lower temperatures there is a clear induction period before the OClO decays.
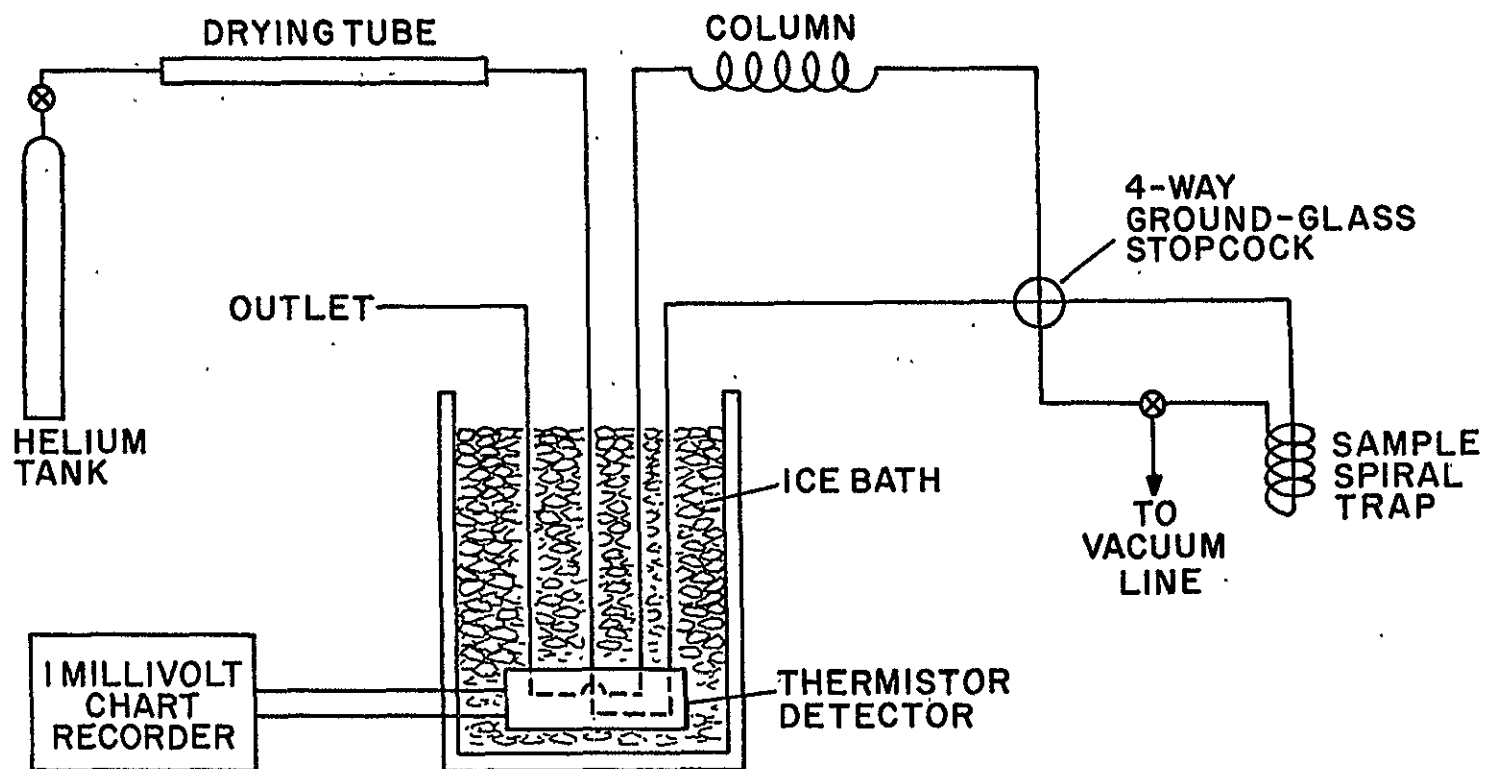
Figure 6. Diagram of the Gowmac Thermistor Gas Chromatograph

Figure 7. OClO profiles in the Photolysis of Cl_2-O_3 Mixtures.
The points are experimental values and the solid
curves are computer simulations using the following
rate coefficients for calculation:

T, °K	275.5	295
k_{10} ($cm^3 sec^{-1}$)	1.06×10^{-11}	1.13×10^{-11}
k_{23b} ($cm^3 sec^{-1}$)	2.09×10^{-14}	1.42×10^{-14}
k_{23c} ($cm^3 sec^{-1}$)	1.19×10^{-15}	1.40×10^{-15}
k_{23} ($cm^3 sec^{-1}$)	4.4×10^{-14}	4.4×10^{-14}
k_{26} ($cm^3 sec^{-1}$)	8.0×10^{-20}	2.65×10^{-19}
$k_{29}[M]$ ($cm^3 sec^{-1}$)	1.0×10^{-15}	---
$k_{-29}[M]$ (sec^{-1})	0.25	---
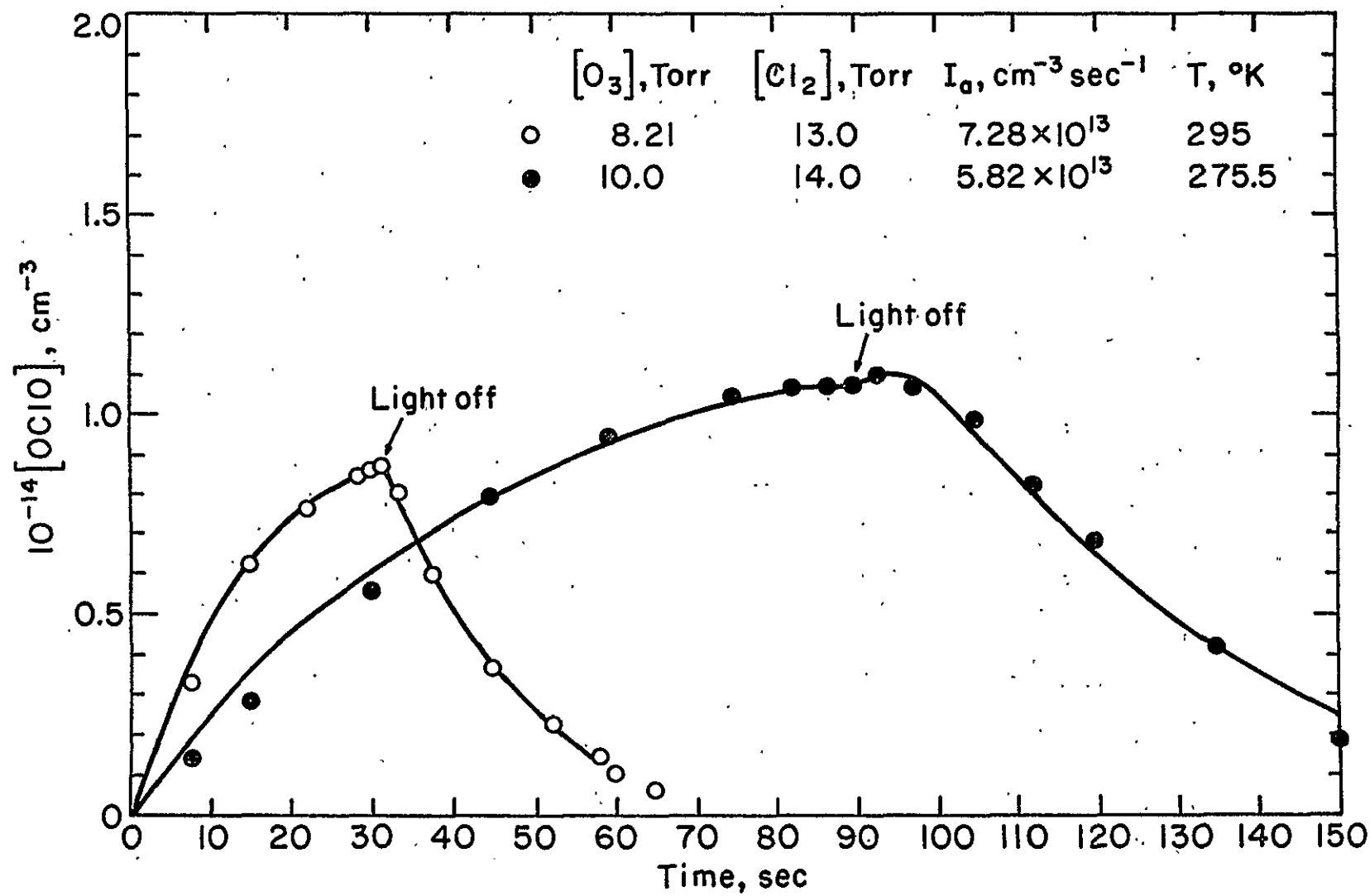
The quantum yield for OClO formation was obtained from the initial OClO growth rate as determined from the initial slope of the absorption profiles. The results at $297 \pm 3°K$ are given in Table 2. The reactant pressures were varied as follows: O_3 was varied from 3.4 to 12.5 Torr and Cl_2 was varied from 7.8 to 13.5 Torr. The absorbed light intensity, I_a, was changed by varying the chlorine pressure. Pressure and temperature effects were also studied, and the results are presented in Tables 3 and 4. It is apparent from Tables 2 and 3 that the OClO formation quantum yield, $\Phi_i\{OClO\}$, is invariant to I_a, O_3 and the presence or the absence of O_2 and N_2. From Table 4, it is clear that $\Phi_i\{OClO\}$ decreases with decreasing temperature. The results are also presented in Figures 8 and 9.

An Arrhenius plot of $\Phi_i\{OClO\}$ obtained from the initial rates is presented in Figure 10. The plot is reasonably linear and leads to the following Arrhenius expression: $\Phi_i\{OClO\} = 2.5 \times 10^3$ $\exp[-(3025 \pm 625)/T]$. At 297°K and 275°K the addition of up to 600 Torr N_2 or O_2 reduced $\Phi_i\{OClO\}$ slightly. The average value of $\Phi_i\{OClO\}$ as a function of temperature is given in Table 5.

B.2. Chlorine Removal Quantum Yield

The chlorine removal quantum yield, $-\Phi\{Cl_2\}$, was measured at 297°K under the following conditions: $[O_3] = 15.4 \pm 1.6$ Torr, $[Cl_2] = 1.16 \pm 0.16$ Torr, and $I_a = (2.82 \pm 0.44) \times 10^{13}$ $cm^{-3}sec^{-1}$. The measurements were made after 30% of the Cl_2 was consumed. For these conditions, $-\Phi\{Cl_2\} = 0.11 \pm 0.02$. The result is independent

Table 2

Photolysis of Cl_2-O_3 Mixtures at 366 nm and $297 \pm 3°K$

$[O_3]$, Torr	$[Cl_2]$, Torr	Temp, °C	$10^{-13} I_a$, $cm^{-3}sec^{-1}$	$\Phi\{OClO\}$[a]	$\Phi_i\{OClO\}$[b]	$[OClO]_{ss}$, mTorr	$10^{19} k_{26}$,[c] cm^3sec^{-1}	$10^{19} k_{26}$,[c] cm^3sec^{-1}
3.42	7.78	24.0	4.34	0.076	0.061	3.38	2.61	2.68
3.40	6.87	25.0	3.84	0.14	0.12	4.45	2.24	3.34
3.81	12.9	23.7	7.19	0.079	0.085	5.55	2.81	2.52
4.08	12.8	22.0	7.12	0.083	0.087	5.69	2.22	2.39
5.91	13.4	27.0	7.47	0.13	0.12	3.61	2.28	4.17
5.95	13.4	23.1	7.47	0.11	0.13	3.30	2.82	3.93
6.38	13.1	23.0	7.30	0.085	0.095	3.67	2.93	2.49
7.90	13.0	23.4	7.28	0.12	0.14	2.71	3.14	3.84
7.94	14.3	22.4	7.99	0.087	0.095	2.78	2.62	2.96
8.01	13.6	26.9	7.58	0.10	0.13	2.80	3.49	3.17
8.21	13.0	22.0	7.28	0.083	0.090	2.66	2.60	2.60
8.91	13.2	22.0	7.39	0.079	0.085	2.35	2.62	2.62
9.57	13.4	27.0	7.47	0.10	0.14	2.54	3.76	2.89
10.3	14.0	21.7	7.84	0.092	0.13	2.73	3.44	2.43
11.3	14.2	21.2	7.91	0.080	0.081	1.78	2.44	2.96
11.4	13.0	23.5	7.28	0.075	0.098	2.10	2.80	2.14

Table 2. (continued)

[a]From initial rate of formation.

[b]From equation XVII.

[c]From decay curve.

[d]From the steady state value of OClO, equation XVIII.

Table 3

Photolysis of Cl_2–O_3 Mixtures at 366 nm and $297 \pm 3°K$ in the Presence of O_2 or N_2

$[O_3]$, Torr	$[Cl_2]$, Torr	$[O_2]$, Torr	$[N_2]$, Torr	Temp, °C	$10^{-13} I_a$, $cm^{-3} sec^{-1}$	$\Phi_i\{OClO\}$[a]	$\Phi_i\{OClO\}$[b]	$[OClO]_{ss}$, mTorr	$10^{19} k_{26}$,[c] $cm^3 sec^{-1}$	$10^{19} k_{26}$,[d] $cm^3 sec^{-1}$
4.66	16.8	----	382	23.0	9.38	0.067	0.057	4.48	3.04	2.83
5.48	13.7	625	----	27.1	7.67	0.070	0.075	2.43	3.35	3.78
5.95	14.1	590	----	27.0	7.08	0.090	0.086	4.43	3.80	2.59
5.97	14.0	640	----	27.0	7.81	0.074	0.083	3.90	3.72	2.40
6.87	13.8	----	629	27.2	7.71	0.070	0.13	2.23	3.35	3.40
7.08	13.9	629	----	27.0	7.76	0.074	0.072	3.33	2.93	2.35
7.93	13.0	589	----	26.7	7.45	0.068	0.11	2.39	3.66	2.54
9.41	13.2	577	----	27.1	7.39	0.063	0.16	1.76	3.48	2.64
9.61	14.9	625	----	27.0	8.32	0.075	0.079	2.61	3.03	2.40
10.5	15.2	----	614	27.2	8.49	0.072	0.069	2.37	3.37	2.36
10.7	16.1	584	----	27.0	9.01	0.067	0.069	2.32	3.77	2.35
12.5	13.5	----	450	23.8	7.55	0.092	0.080	1.29	3.53	4.06

[a] From initial rate of formation.

[b] From equation XVII.

[c] From decay curve.

[d] From the steady state value of OClO, equation XVIII.

Table 4

Photolysis of Cl_2-O_3 Mixtures at 366 nm

and at Low Temperature

$[O_3]$, Torr	$[Cl_2]$, Torr	Temp, °C	$10^{-13} I_a$, $cm^{-3} sec^{-1}$	$\Phi_i\{OClO\}^a$	$[OClO]_{ss}$, mTorr	$10^{19} k_{26}^d$, $cm^3 sec^{-1}$
$T = 283 \pm 1°K$
3.91	10.1	10.2	4.56	0.053	4.23	1.25
6.54	13.5	10.2	6.09	0.059	5.59	0.84
9.14	13.0	10.3	5.86	0.077	3.98	0.98
9.45	12.8	10.0	5.77	0.071	3.71	1.00
11.3	13.5	10.5	6.09	0.057	2.56	1.03
$T = 275.5 \pm 1°K$
3.62	13.5	3.3	5.50	0.042	6.63	0.78
4.08[b]	13.0	2.1	5.29	0.042	4.98	0.87
4.90[b]	13.7	1.0	5.57	0.036	4.88	0.67
5.41	15.3	2.0	6.24	0.043	5.92	0.67
5.84	14.4	1.4	5.86	0.048	4.69	0.84
5.94	13.7	2.2	5.58	0.049	5.45	0.69
7.55	12.8	2.2	5.21	0.045	3.98	0.64
7.62[c]	12.9	0.0	5.25	0.040	3.34	0.66
8.56[b]	14.7	0.7	5.98	0.030	3.70	0.45
8.89	13.5	2.5	5.50	0.041	3.64	0.57
9.26	12.8	2.5	5.21	0.036	3.18	0.52
10.0	14.3	2.3	5.82	0.044	2.90	0.72
11.2	13.4	2.3	5.46	0.033	2.32	0.57
11.4	15.1	0.0	6.14	0.033	2.97	0.48
11.6[c]	15.7	0.0	6.40	0.024	2.09	0.51
11.7[b]	14.2	0.0	5.76	0.034	2.32	0.58
11.9[c]	11.6	0.0	4.74	0.037	2.82	0.42
$T = 263.6 \pm 1°K$
3.93	13.5	−9.2	5.82	0.022	7.29	0.33
4.01	13.1	−9.2	5.65	0.027	8.70	0.33
7.20	12.6	−9.1	5.44	0.027	4.93	0.31
9.96	13.0	−9.7	5.61	0.022	2.81	0.34
11.1	12.8	−9.7	5.52	0.027	2.98	0.34

[a]From initial rate of formation.

[b]With 600-660 Torr O_2 also present.

Table 4. (continued)

[c]With 450-640 Torr N_2 also present.

[d]From the steady state value of OClO, equation XVIII.

Figure 8. Plots of $\Phi_i\{OClO\}$ vs. I_a at $297 \pm 3°K$. $\odot$, with N_2 present; ■, with O_2 also present; x, without O_2 or N_2 present.

Figure 9. Plots of $\Phi_1\{OClO\}$ vs. $[O_3]$. At $297 \pm 3°K$: ☉, with N_2 present; ■, with O_2 also present; x, without O_2 or N_2 present. At $275 \pm 1°K$: ▲, with N_2 also present; ▲, with O_2 also present; △, without O_2 or N_2 present.
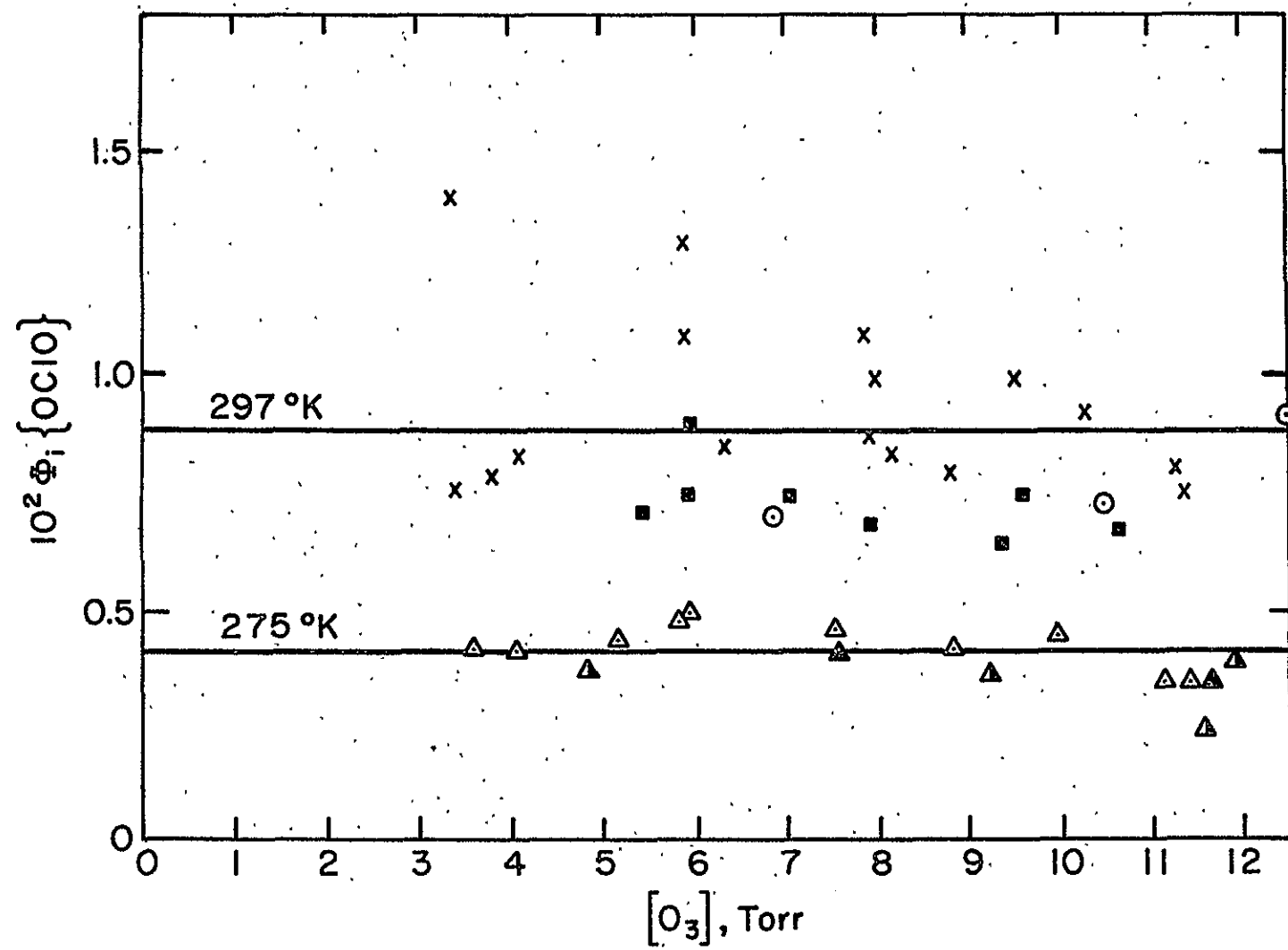
Figure 10. Arrhenius Plot of $\Phi_i\{OClO\}$ for the Photolysis of Cl_2-O_3 Mixtures

Table 5

Average Value of $\Phi_i\{OClO\}$
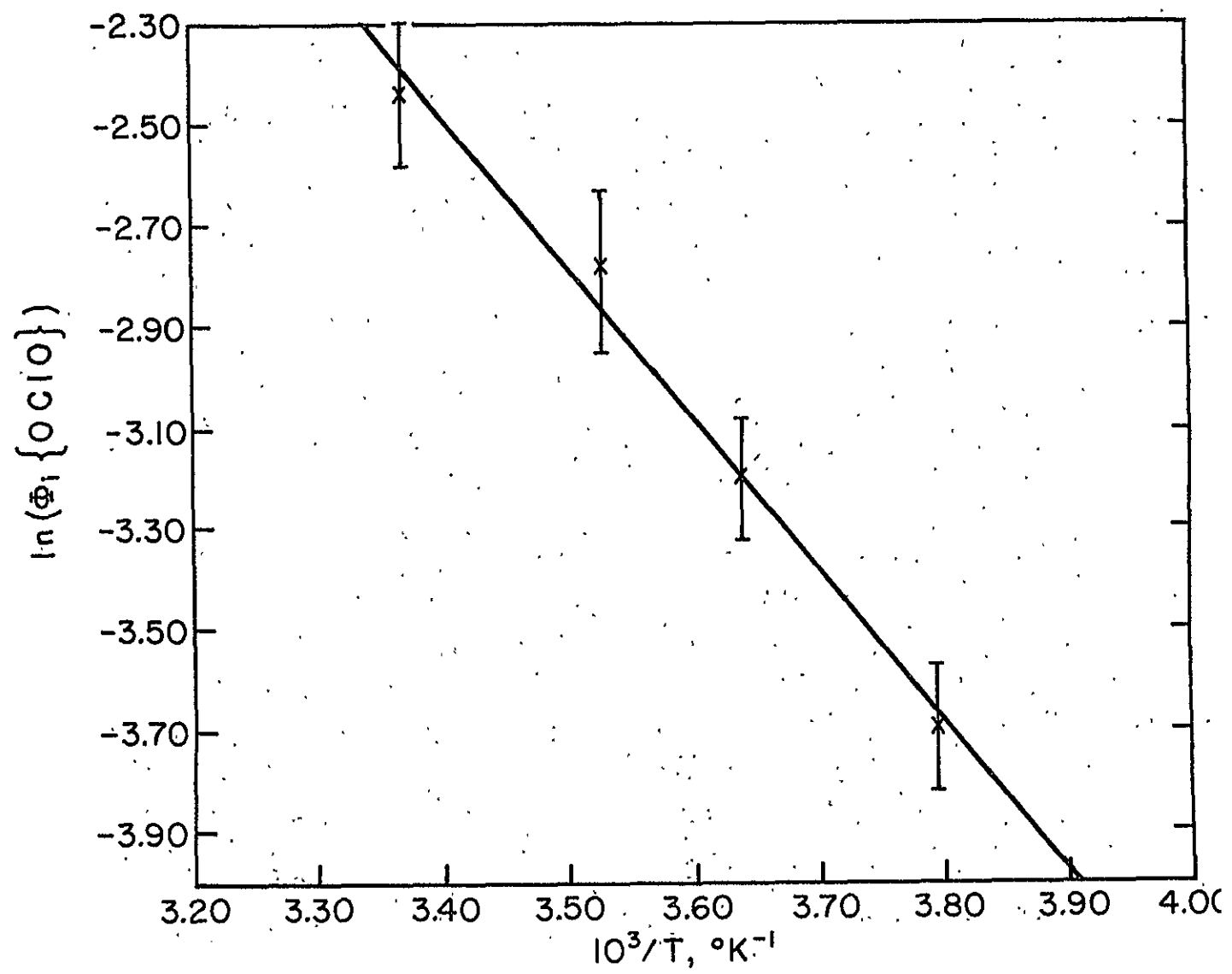
Temp, K	$\Phi_i\{OClO\}^a$	$\Phi_i\{OClO\}^b$
297	0.089 ± 0.013	0.100 ± 0.030
297	$0.075 \pm 0.011*$	
297	$0.073 \pm 0.008**$	
283	0.063 ± 0.010	
275.5	0.041 ± 0.005	
275.5	$0.034 \pm 0.009*$	
275.5	$0.033 \pm 0.003**$	
263.6	0.025 ± 0.03	

[a]From initial rate of formation.

[b]From equation XVII.

*450-640 Torr N_2 also present.

**600-660 Torr O_2 also present.

of the absence or presence of 650 Torr of N_2 or O_2. The results
are presented in Table 6.

B.3. Ozone Removal Quantum Yield

Jayanty and associates (76) used both infrared and ultraviolet
absorption spectroscopy to study the O_3 removal quantum yield at
297 $\pm$ 3°K. Our results using ultraviolet spectroscopy were consistent
with those obtained by Jayanty. Many experiments were done at
lower temperatures, covering O_3 pressures from 0.098 Torr to
0.499 Torr and I_a values from 2.1 x 10^{13} to 8.3 x 10^{13} $cm^{-3}sec^{-1}$.
To satisfy the pseudo-first order condition, Cl_2 was always present
in excess. The results are given in Table 7. Typical decay plots of
of O_3 with time at various temperatures are shown in Figure 11. The
constant rate of O_3 removal indicates the decay rate is zero order in
O_3 pressure. However, at high percentages of conversion (>90%), the
rate slows indicating the possibility of competitive process for
chlorine atoms.

The values of $-\Phi\{O_3\}$ at 297°K are 5.9 $\pm$ 0.4 and decrease with
decreasing temperature. The results at room temperature agree
qualitatively with those of Jayanty and associates (76), Norrish and
Neville (59) and Lin et al. (62). The value of $-\Phi\{O_3\}$ is invariant to
changes in either $[O_3]$ or the I_a. The addition of O_2 reduced the value
of $-\Phi\{O_3\}$ (76). It was also found by Jayanty and associates (76) that
addition of up to 680 Torr of N_2 had no effect on $-\Phi\{O_3\}$.

B.4. O_2 Formation Quantum Yield

The O_2 formation quantum yield was obtained from the ratio of
O_2 produced to O_3 lost. This ratio was measured at 296 $\pm$ 1°K for

Table 6

Chlorine Removal Quantum Yield at 30% Conversion in

the Photolysis of Cl_2-O_3 Mixtures at 366 nm and 296°K

$[O_3]_0$, Torr	$[Cl_2]_0$, Torr	$10^{-13} I_a$, $cm^{-3} sec^{-1}$	$-\Phi\{Cl_2\}$
13.8*	1.32	3.26	0.12
15.0**	1.28	3.16	0.11
15.0	1.17	2.88	0.13
15.5**	1.24	3.06	0.11
16.7	1.28	3.16	0.09
17.1	1.01	2.49	0.09

*With 650 Torr N_2 also present.

**With 650 Torr O_2 also present.

Table 7

Ozone Removal Quantum Yield in the Photolysis

of Cl_2-O_3 Mixtures at 366 nm

| $[O_3]_0$, Torr	$[Cl_2]$, Torr	$10^{-13} I_a$, $cm^{-3} sec^{-1}$	$-\Phi\{O_3\}$
Experiments at 297 $\pm$ 3°K			
0.048	0.86	3.2	5.5
0.112	3.31	1.2	5.6
0.482	11.1	4.1	6.2
0.534	10.3	3.8	6.2
Experiments at 283 $\pm$ 1°K			
0.098	11.5	4.9	3.7
0.099	11.1	4.7	3.4
0.106	11.6	4.9	3.8
0.114	11.1	4.7	3.8
0.146	4.90	2.1	4.2
0.147	11.1	4.7	4.1
0.162	17.9	8.3	3.6
0.174	10.5	4.5	3.9
0.185	10.8	4.6	3.9
0.244	11.8	5.0	4.2
0.306	11.3	4.8	4.2
0.340	6.07	2.6	4.5
0.369	21.2	9.0	3.8
0.449	11.1	4.7	4.7
Experiments at 273 $\pm$ 1°K			
0.113	11.1	5.7	2.4
0.124	3.93	2.0	2.7

Table 7. (continued)

$[O_3]_0$, Torr	$[Cl_2]$, Torr	$10^{-13}\ I_a$, $cm^{-3}sec^{-1}$	$-\Phi\{O_3\}$
0.149	20.0	11.3	2.6
0.154	18.2	9.3	2.6
0.180	11.1	5.7	2.7
0.193	5.14	2.6	3.3
0.220	11.1	5.7	2.9
0.363	8.64	4.4	2.7
0.429	20.9	10.7	3.2
0.449	6.00	3.1	3.0
0.494	10.7	5.5	3.4
0.537	11.1	5.7	3.2
0.547	11.1	5.7	2.9
Experiments at 252 ± 1°K			
0.131	10.6	9.2	1.9
0.155	10.7	9.3	1.7
0.188	11.4	9.9	1.9
0.395	10.7	9.3	1.9
0.413	3.97	3.4	1.1
0.427	10.7	9.3	1.8
0.465	14.4	15.1	2.2

Figure 11. Plots of $[O_3]$ vs. Photolysis Time.
The reaction conditions are as
follows:

	$[O_3]$, Torr	$[Cl_2]$, Torr	T, °K
x	0.482	11.1	296
■	0.449	11.1	283
⊗	0.494	10.7	273
⊙	0.437	10.7	252
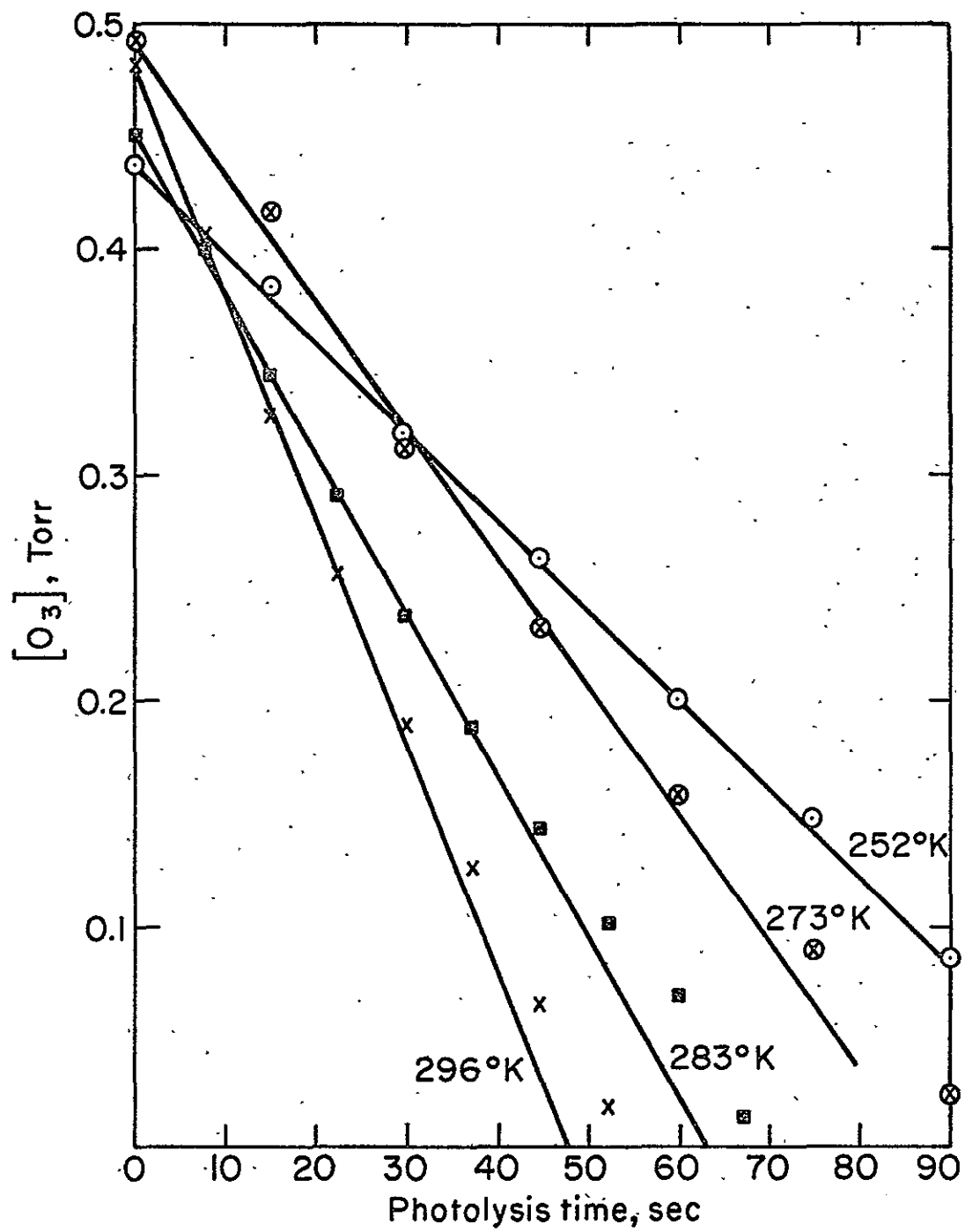
O_3 conversions ranging from 18% to 100%. The initial O_3 pressures

range from 5.76 to 12.7 Torr and the initial Cl_2 pressure from 6.85

to 25.9 Torr. The results are presented in Table 8. The ratio of

O_2 formed to O_3 consumed was about 1.5 as expected for a catalyzed

decomposition of O_3. From the known value of $-\Phi\{O_3\}$, the average

value of $\Phi\{O_2\}$ at 296°K is 8.6 $\pm$ 0.3 in the absence of added O_2 or

N_2. The uncertainties due to pressure measurement by the expansion

method are less than 2%.

B.5. Kinetics of the OClO + O_3 Reaction

The rate of the reaction of OClO with O_3 was determined in two

ways. In the first method, mixtures of Cl_2-O_3 were photolyzed until

the steady state value of OClO produced. When the radiation was

terminated OClO decayed as shown in Figure 7. Presumably the decay

is due to the reaction with O_3.
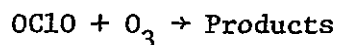
$$OClO + O_3 \rightarrow Products \qquad\qquad 26$$

Typical first order plots of OClO decay in the dark at 297°K are

shown in Figures 12, 13, and 14 for $[O_3]$, pressure, and temperature

variations respectively. Since the amount of O_3 change during the

reaction was negligible, the values of k_{26} were obtained by dividing

the slope obtained from the first order plot with the initial O_3

pressure. Figures 12 and 13 showed the deviation from linearity after

80% of OClO was consumed. This deviation might be due to the additional

loss of OClO through other processes.

From Figure 14, it is apparent that the plot is linear only at

297°K. Below this temperature, there is a significantly increasing

deviation from linearity with decreasing temperature. The decay data

Figure 12. First Order Plots of OClO Decay in the Dark after
the Photolysis of Cl_2-O_3 Mixtures at $297 \pm 3°K$
and at Different O_3 Pressures. The reaction
conditions are as follows.

	$[O_3]$, Torr	Cl_2, Torr
▦	11.40	13.0
⊙	8.91	13.2
●	5.95	13.4
x	4.08	12.8

Table 8

O_2 Formation in the Chlorine-Photosensitized

Decomposition of O_3 at 366.0 nm and $296 \pm 1°K$

$[O_3]$, Torr	$[Cl_2]$, Torr	$10^{-13} I_a$, $cm^{-3}sec^{-1}$	$\Delta[O_2]/\Delta[O_3]$	% Conversion of O_3
5.76	19.9	4.47	1.53	100
7.55	25.9	5.83	1.46	100
8.05	22.6	5.09	1.55	100[a]
8.56	7.39	1.66	1.49	100[a]
10.9	11.5	2.59	1.55	100[a]
11.4	6.85	1.54	1.46	100[a]
11.6	10.0	2.25	1.46	100[a]
11.6	11.1	2.50	1.39	86
12.7	20.3	4.57	1.44	81
12.7	20.3	4.57	1.45	78

[a]Photolysis time is twice that calculated to be necessary for 100% conversion of O_3.
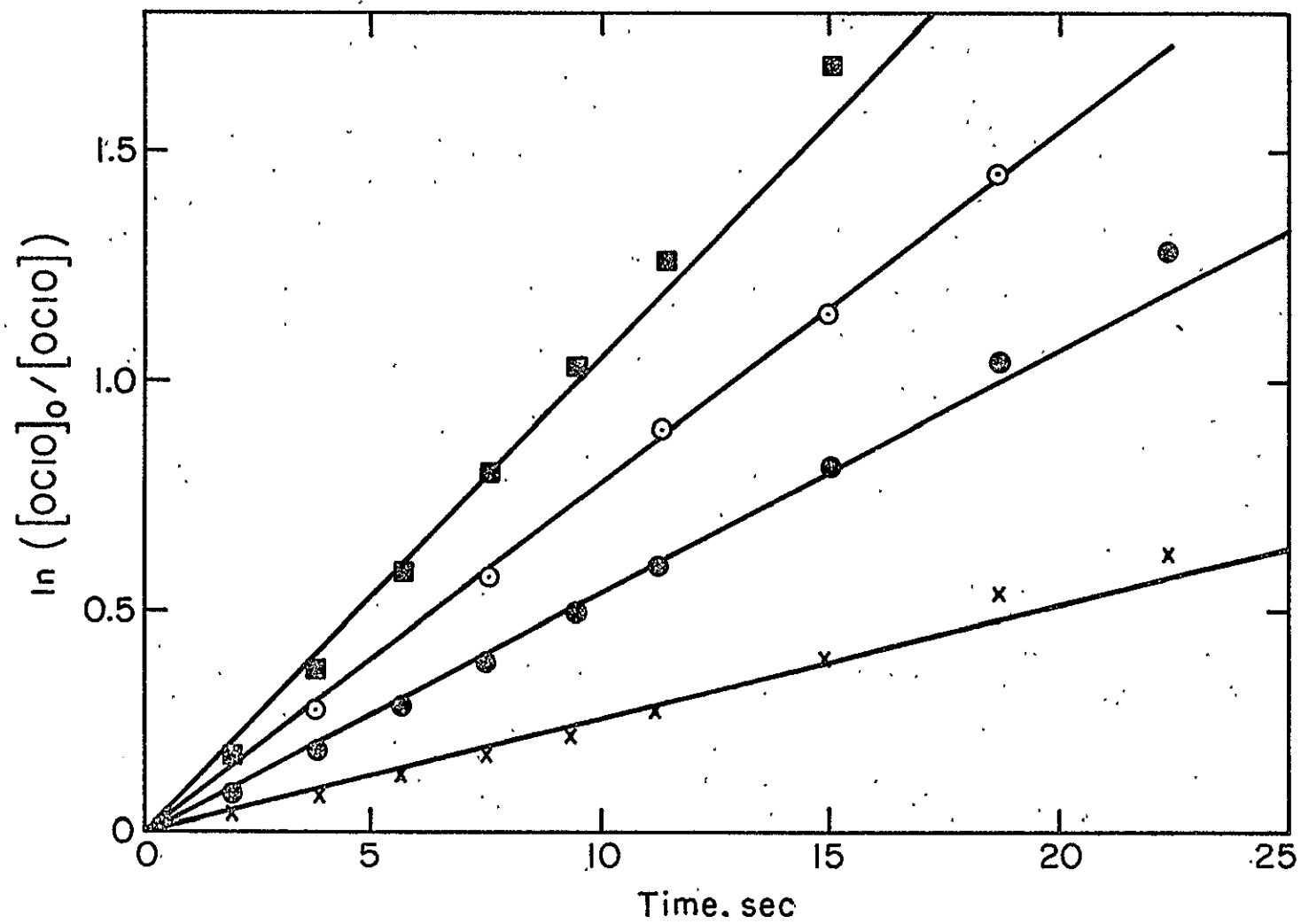
Figure 13. First Order Plots of OClO Decay in the Dark after the Photolysis of Cl_2-O_3 Mixtures at 297 $\pm$ 3°K and in the Presence of O_2 or N_2. The reaction conditions are as follows.

	$[O_3]$, Torr	$[Cl_2]$, Torr	$[O_2]$, Torr	$[N_2]$, Torr
■	6.38	13.1	----	----
⊙	6.87	13.8	----	629
x	7.08	13.9	629	----
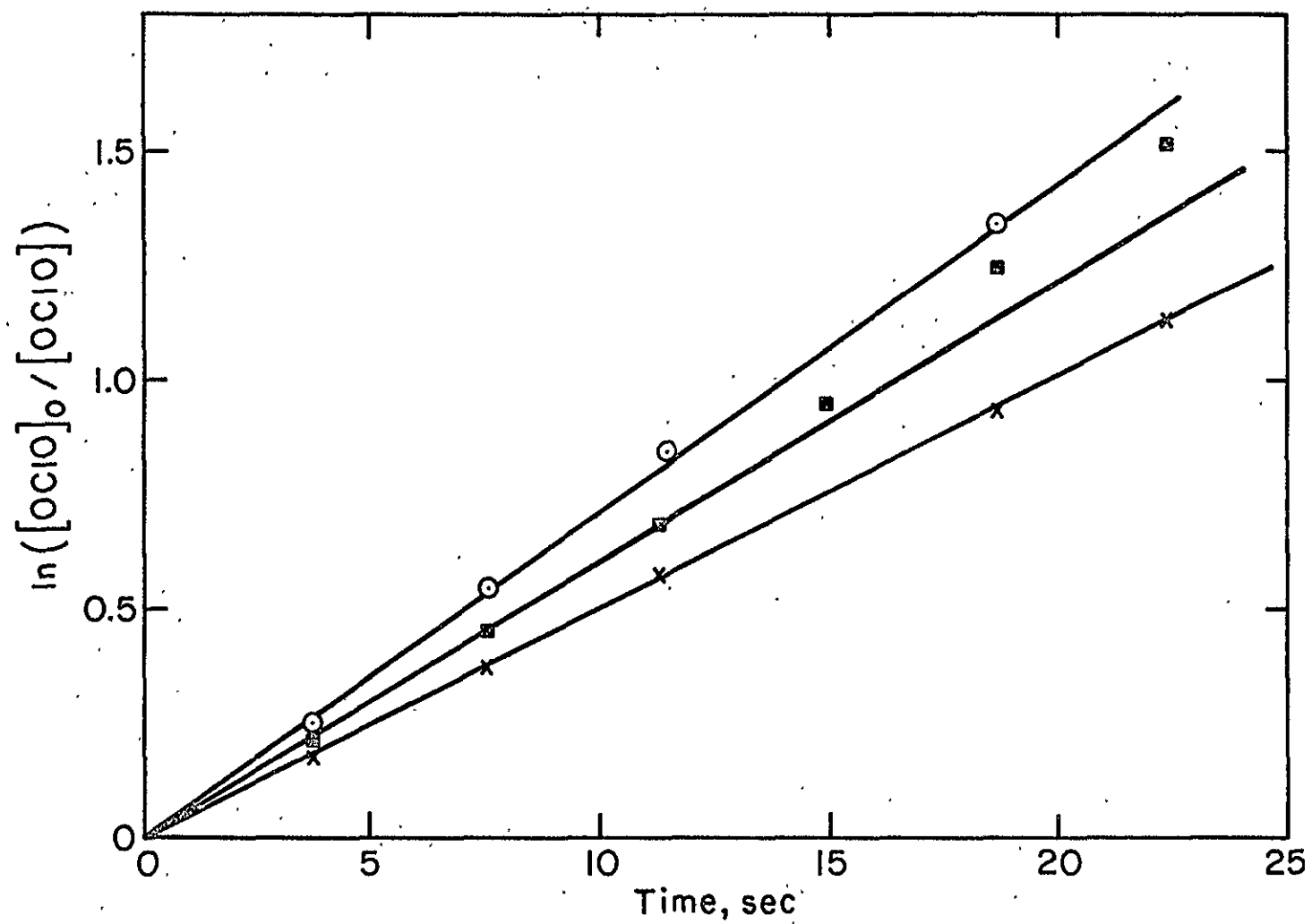
Figure 14. First Order Plots of OClO Decay in the Dark after the Photolysis of Cl_2-O_3 Mixtures at Various Temperatures. The reaction conditions are as follows.

	$[O_3]$, Torr	$[Cl_2]$, Torr	T, °K
x	8.91	13.2	296.1
■	9.45	12.8	283.1
●	9.46	12.8	275.5
○	7.26	12.6	264.0
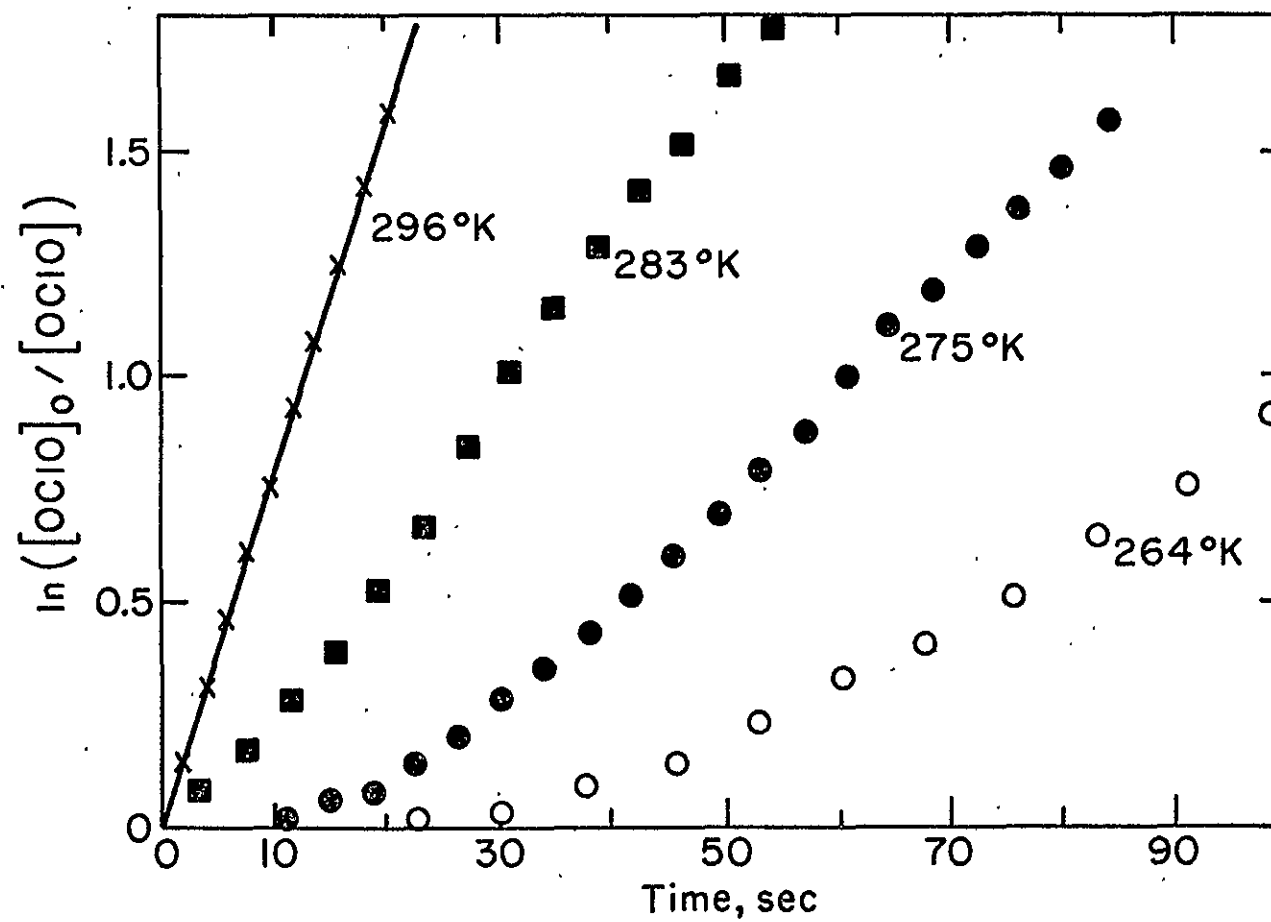
at 297°K are given in Tables 2 and 3. The average value of k_{26}

at 297°K is $(3.02 \pm 0.49) \times 10^{-19}$ $cm^3 sec^{-1}$ independent of I_a, $[O_3]$

and the presence or absence of N_2 and O_2. All of the values of

k_{26} obtained from the decay curves are summarized in Figure 15.

The data at lower temperatures cannot be summarized in this form.

The values of k_{26} were also computed from the steady state

expression for OClO during irradiation. The results are presented

in Tables 2, 3, and 4.

In the second method, the pure OClO was used to study the

kinetics of OClO + O_3 reaction. The OClO was directly mixed with

excess O_3 in the reaction cell. Excess O_3 was used to satisfy the

pseudo-first order condition. The loss of OClO was followed at

400 nm. The OClO decay was observed to be first order in OClO in

the presence of O_3. Typical first order plots of OClO decay at

four temperatures for the same O_3 are shown in Figure 16.

The rate coefficient k_{26} obtained from the plots are presented

in Table 9. The value of k_{26} is independent of the O_3 pressure;

thus the reaction is first order in O_3. An Arrhenius plot of k_{26} is

shown in Figure 17. The best straight line through the three data

points gives an Arrhenius expression of $k_{26} = 6.1 \times 10^{-13}$

$exp[-4308/T]$ $cm^3 sec^{-1}$. Also shown in Figure 17 are the data points

obtained from the steady-state of OClO in the photolysis of Cl_2-O_3

mixtures. The Arrhenius expression which best fits these data is

1.9×10^{-11} $exp[-(5360)/T]$ $cm^3 sec^{-1}$. The average of the two Arrhenius

expressions is 2.3×10^{-12} $exp[-(4730 \pm 630)/T]$ $cm^3 sec^{-1}$, and is the

recommended value.

Figure 15.   Plots of k_{26} (Obtained from the OClO Decay Curve after the Photolysis of Cl_2-O_3 Mixtures) vs. [O_3] at $297 \pm 3°K$.   ⊙, with N_2 also present; ■, with O_2 also present; x, without O_2 or N_2 present.
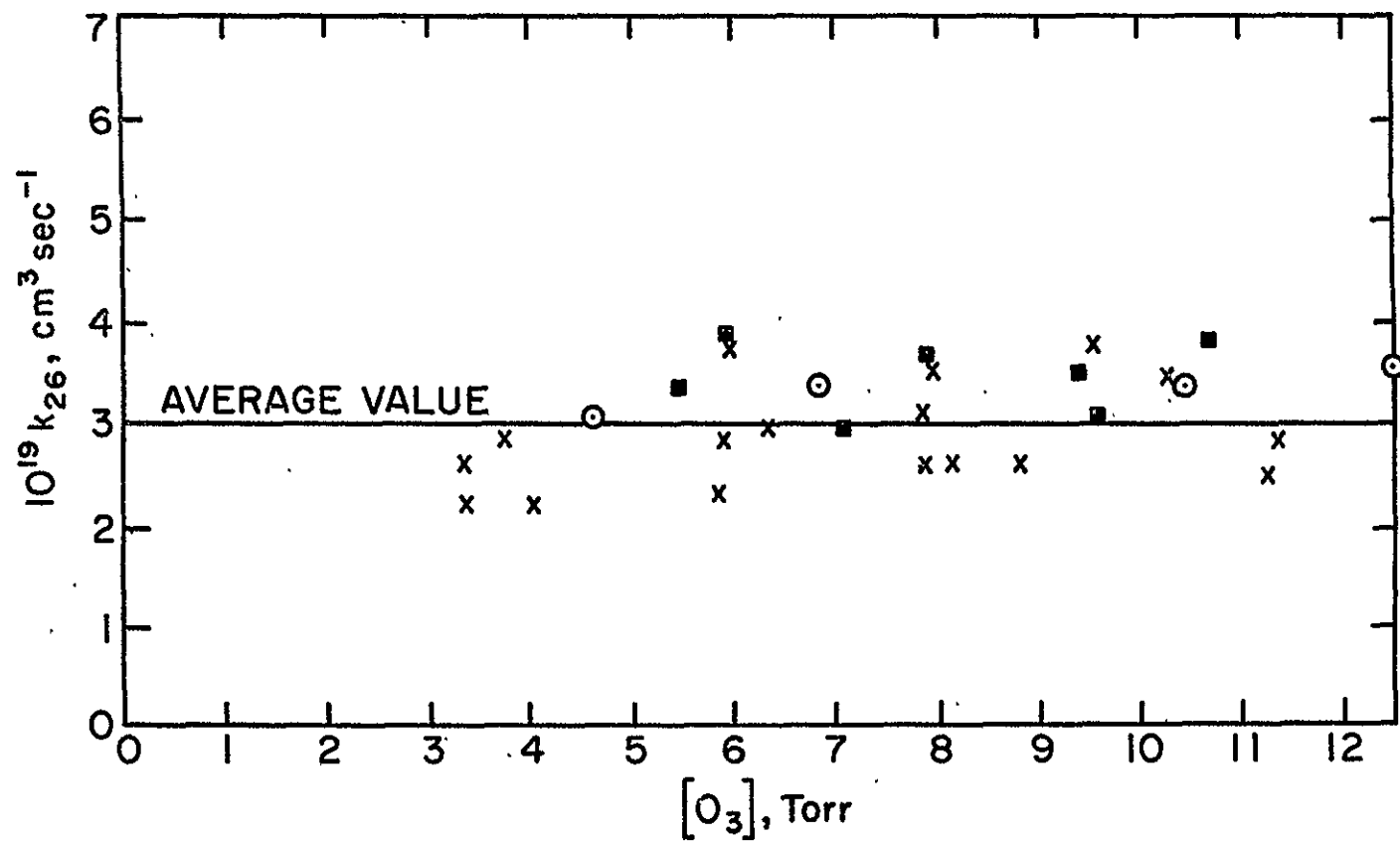
Figure 16. First Order Plots of OClO Decay in the Presence of
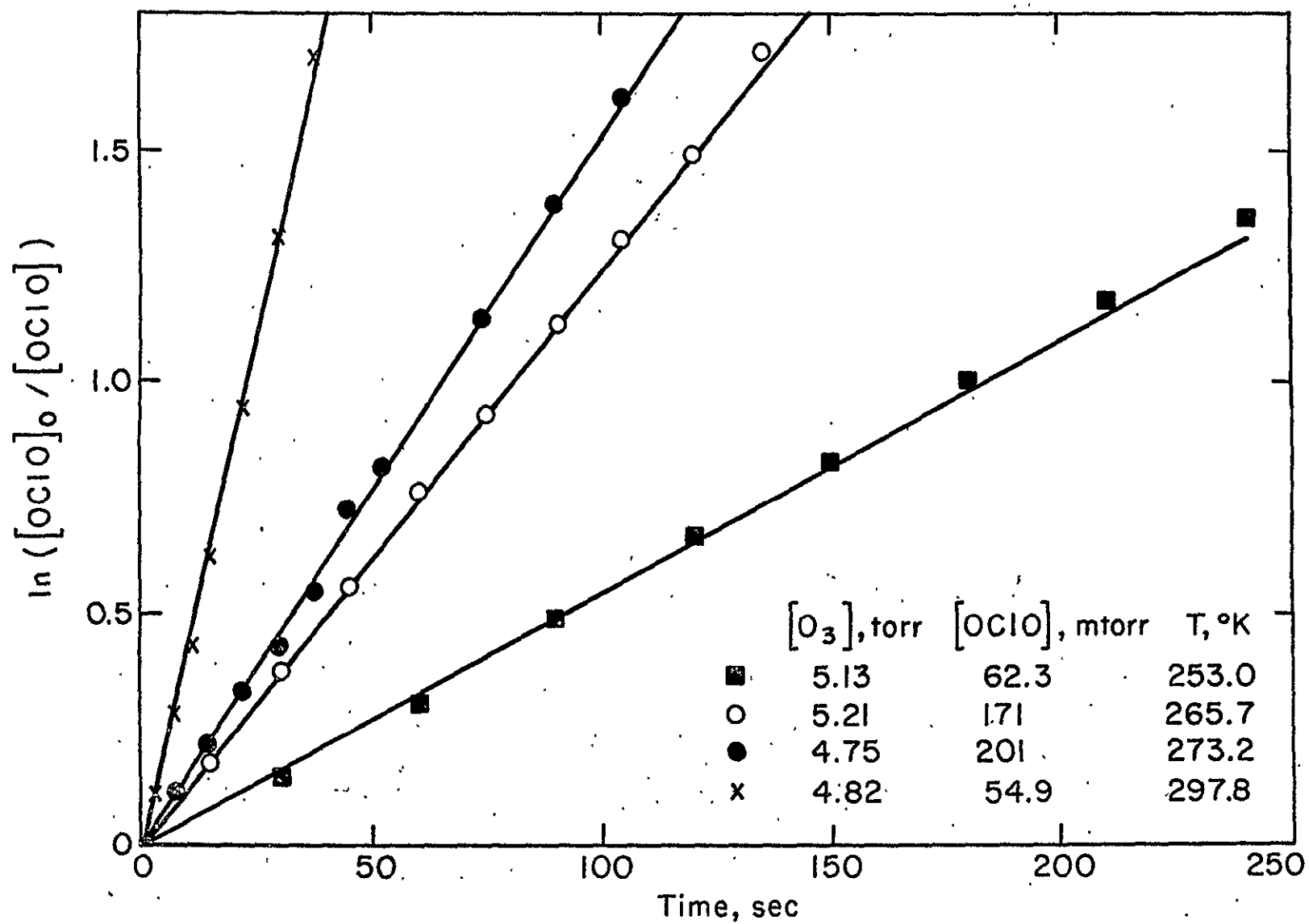Excess O_3 (Direct Reaction of OClO with O_3)

Table 9

Reactions of OClO with O_3

$[O_3]$, Torr	$[OClO]$, mTorr	Temp, °K	$10^{19} k_{26}$, $cm^3 sec^{-1}$
		Temperature = 296.3 ± 1.7°K	
4.82	54.9	297.7	2.67
4.90	37.3	297.7	2.69
5.45	59.7	297.6	3.02
5.91	43.5	297.4	2.98
5.99	38.2	297.6	2.82
7.39*	40.2	295.0	3.36
7.43*	42.2	293.4	3.12
8.36	42.8	293.2	3.44
8.40	35.0	295.0	3.39
8.71	44.1	296.5	3.48
11.1	65.9	297.7	3.06
17.5	53.1	297.4	3.24
19.2	31.1	295.1	2.79
		Temperature = 273.4 ± 1.0°K	
2.84	161.0	273.5	0.73
4.47	88.4	275.5	0.89
4.75	201.0	273.0	0.92
5.41	75.1	274.5	0.73
5.52	40.9	273.0	0.62
6.02	34.9	273.0	0.73
8.48	50.3	274.0	0.92
8.79	43.5	273.5	0.74
8.87	48.3	273.0	0.93
9.49	43.5	273.3	0.94
9.49	43.5	273.1	0.87
11.2	41.5	273.0	0.92

Table 9. ·(continued)

$[O_3]$, Torr	$[OClO]$, mTorr	Temp, °K	$10^{19} k_{26}$, $cm^3 sec^{-1}$
23.8	44.2	272.8	0.94
29.0	· 41.5	273.0	0.88
Temperature $= 262.0 \pm 1.0$°K			
2.53	131.3	262.0	0.48
4.40	49.05	263.0 .	0.48
4.59	153.7	262.0	0.41
6.42	58.75	261.4	0.46
7.70	131.3	261.7	0.45

*With 100 Torr N_2 also present.
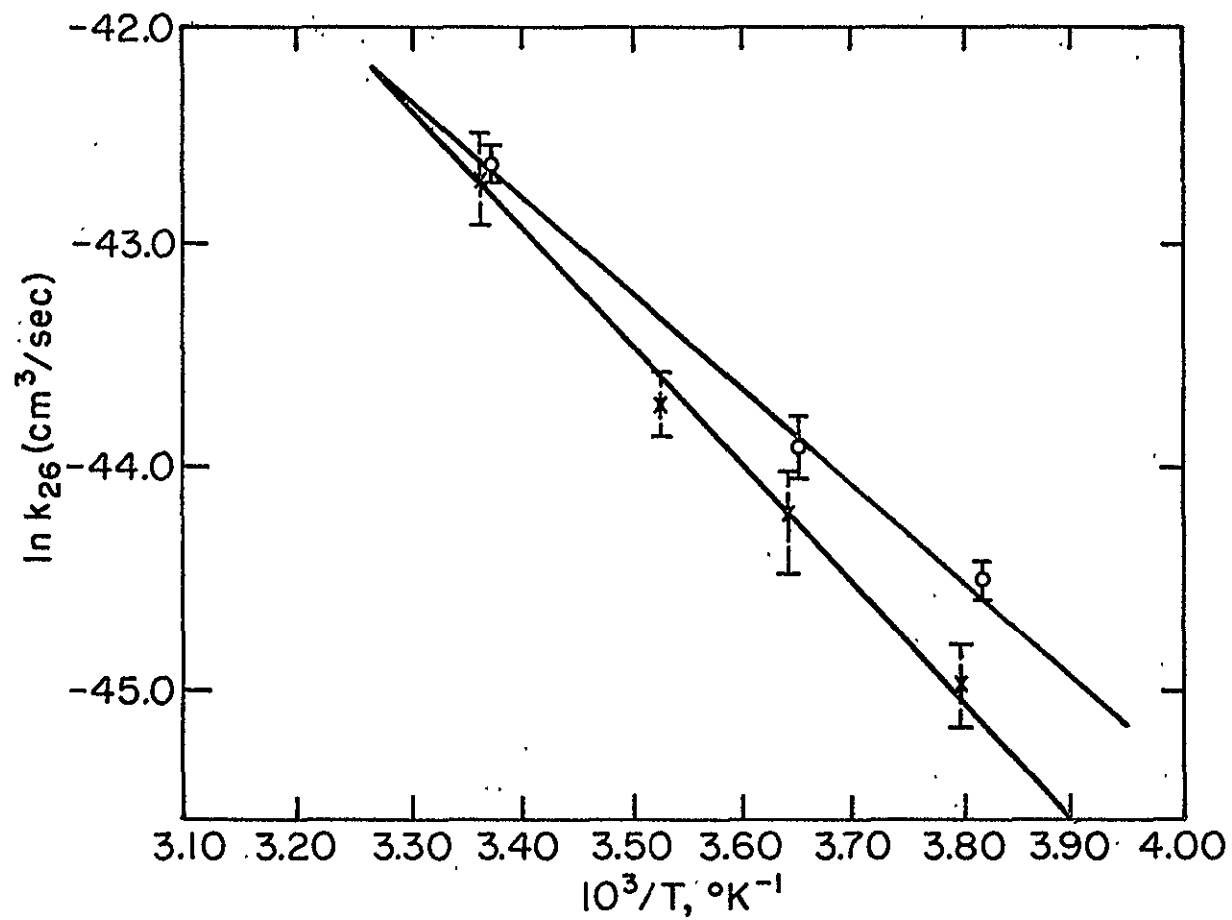
Figure 17. Arrhenius Plots of k_{26}. $\bigcirc$, values from the direct $OClO-O_3$ reaction; x, values from the steady state $OClO$ values.

At room temperature both determinations give essentially the same value for k_{26} [(3.08 $\pm$ 0.25) x 10^{-19} $cm^3 sec^{-1}$ from direct mixing and (2.88 $\pm$ 0.59) x 10^{-19} $cm^3 sec^{-1}$ from the steady-state value of OClO in the Cl_2-O_3 photolysis]. Furthermore, the value obtained in the dark decay of OClO after photolysis of Cl_2-O_3 mixtures is (3.02 $\pm$ 0.49) x 10^{-19} $cm^3 sec^{-1}$ in excellent agreement with the other two values. Lin et al. (62) have made two independent determinations of k_{26} at room temperature, both of which give 3.0 x 10^{-19} $cm^3 sec^{-1}$ in excellent agreement with our three determinations. The value for k_{26} = (1.20 $\pm$ 0.15) x 10^{-19} $cm^3 sec^{-1}$ obtained by Birks et al. (46) at 298°K appears to be too low.

C. Discussion

The major conclusions that can be drawn from the Cl_2-O_3 system are:

1. The photolysis of Cl_2-O_3 mixtures at 366 nm leads to the removal of O_3 and Cl_2 and to the production of O_2 and Cl_2O_7 as final products. OClO is produced as an intermediate.

2. The reaction of OClO and O_3 is first order in both OClO and O_3. The value of the rate coefficient for this reaction is indifferent to the presence or absence of O_2 and N_2 ($\geq$500 Torr).

3. The O_3 removal quantum yield is approximately 6 at 297°K and is invariant to changes in $[O_3]$ and I_a. As it was observed by Jayanty and associates (76), the addition of N_2 (680 Torr) has no effect on -$\Phi\{O_3\}$, however; the addition of O_2 reduced -$\Phi\{O_3\}$.

4. The chlorine removal quantum yield is very small (0.11 +
0.02) and is invariant to the presence or absence of O_2 and N_2.

5. The oxygen formation quantum yield is about one and one half
times the O_3 removal quantum yield.

6. $\Phi_i\{OClO\} = 2.5 \times 10^3 \exp[-(3025 \pm 625)/T]$. The OClO formation
quantum yield is invariant to changes in $[O_3]$, I_a and the presence or
absence of O_2 and N_2.

The fact that the values of $\Phi_i\{OClO\}$ and $-\Phi\{Cl_2\}$ are low, and
the fact that the ratio of O_2 produced to O_3 consumed is 1.5 indicates
that the photolysis of Cl_2-O_3 mixtures is primarily a photocatalytic
decomposition of O_3. The mechanism of the photolysis can be discussed
in terms of a set of reactions which have been shown to be important.
At 366 nm only Cl_2 absorbs and it photodecomposes to give chlorine
atoms which can then react with O_3.

$$Cl_2 + h\nu \ (366 \ nm) \rightarrow 2Cl \qquad\qquad\qquad rate = I_a$$

$$Cl + O_3 \rightarrow ClO + O_2 \qquad\qquad\qquad\qquad 10$$

The rate constant for reaction 10 is $k_{10} = (2.7 \pm 1.2) \times 10^{-11}$
$\exp[-(257 \pm 106)/T] \ cm^3 sec^{-1}$ (77-82).

There are two extreme cases to be considered: case (a), the
ClO radicals produced in 10 do not react with O_3 under any conditions
and case (b), the ClO radicals always react with O_3. Thus for case (a)

$$2ClO \rightarrow Cl + ClOO \qquad\qquad\qquad\qquad 23a$$

$$\rightarrow Cl_2 + O_2 \qquad\qquad\qquad\qquad 23b$$

$$\rightarrow OClO + Cl \qquad\qquad\qquad\qquad 23c$$

$$ClOO + M \rightarrow Cl + O_2 + M \qquad\qquad 24$$

and for case (b)

$$ClO + O_3 \rightarrow OClO + O_2 \qquad\qquad 25a$$

$$\rightarrow Cl + 2O_2 \qquad\qquad 25b$$

In either case (a) or case (b), the subsequent reactions of OClO will be

$$OClO + O_3 \rightarrow sym\text{-}ClO_3 + O_2 \qquad\qquad 26$$

$$2ClO_3 + O_3 \rightarrow Cl_2O_7 + O_2 \qquad\qquad 27$$

since Cl_2O_7 is found to be a final product of the photolysis reaction and OClO is an intermediate (76). Reaction 26 might also give ClO + $2O_2$ as products, but the data of Birks et al. (46) is inconsistent with the occurrence of this channel. We ignore this channel since it does not significantly alter the kinetic analysis.

The ClOO radical is unstable and decomposes rapidly at room temperature via reaction 24 (61). Reaction 26 is known (53). Presumably the reaction leads to symmetrical ClO_3 initially, but an unsymmetrical form cannot be ruled out. The subsequent fate of ClO_3 is not entirely clear. Early workers observed both Cl_2O_6 and Cl_2O_7 as products of the Cl_2-photocatalytic decomposition of O_3 (83). The relative amounts of the oxides appeared to depend on experimental conditions. At higher temperatures (30°C), Cl_2O_7 is favored, whereas at lower temperatures, Cl_2O_6 could be observed (83). It seems likely that under conditions such that ClO_3 formation is rapid and the temperature

is low Cl_2O_6 condensation would be favored. This suggests that the reaction of ClO_3 with O_3 is slow and has an activation energy. However recently, Davidson and Williams (60) could detect only ClO_4^- after hydrolysis of the reaction products indicating that Cl_2O_7 was the only product even though they worked under conditions in which earlier workers detected Cl_2O_6 formation.

In the present work ClO_3 formation was not observed by spectroscopic methods because of the low concentration of ClO_3 ($[ClO_3] <$ 20 mtorr). However, the formation of Cl_2O_7 and the reaction of OClO with O_3 requires that ClO_3 must have been present as an intermediate.

Mechanisms (a) and (b) are mutually exclusive, because the data shows that $-\Phi\{O_3\}$ is invariant to $[O_3]$ and the absorbed light intensity, I_a. If both mechanisms were operating simultaneously, $-\Phi\{O_3\}$ would be dependent upon $[O_3]$, because reaction 25 involves O_3, but reaction 23 does not, $-\Phi\{O_3\}$ would also be dependent on I_a, because reaction 23 is bimolecular in radicals and reaction 25 is not. Therefore, our task is to decide whether mechanism (a) and (b) is operative.

First, let us consider that mechanism (b) is operating. This mechanism predicts that $-\Phi\{O_3\} = \Phi\{O_2\} = 7$, $\Phi\{OClO\} = 2$ and $-\Phi\{Cl_2\} = 1$. The measured $-\Phi\{O_3\}$ is nearly 7, but $\Phi\{O_2\}$ is 50% greater than $-\Phi\{O_3\}$. $\Phi_i\{OClO\} = 0.089 \pm 0.013$ and $-\Phi\{Cl_2\} = 0.11 \pm 0.02$ at 297°K; clearly mechanism (b) is not important and need not be considered any further.

Thus, mechanism (a) can be summarized as the following set of reactions:

$$\overset{.}{C}l_2 + h\nu \ (366 \ nm) \rightarrow 2Cl \qquad\qquad Rate = I_a$$

$$Cl + O_3 \rightarrow ClO + O_2 \qquad\qquad 10$$

$$2ClO \rightarrow Cl + ClOO \qquad\qquad 23a$$

$$\rightarrow Cl_2 + O_2 \qquad\qquad 23b$$

$$\rightarrow OClO + Cl \qquad\qquad 23c$$

$$ClOO + M \rightarrow Cl + O_2 + M \qquad\qquad 24$$

$$OClO + O_3 \rightarrow sym\text{-}ClO_3 + O_2 \qquad\qquad 26$$

$$2ClO_3 + O_3 \rightarrow Cl_2O_7 + O_2 \qquad\qquad 27$$
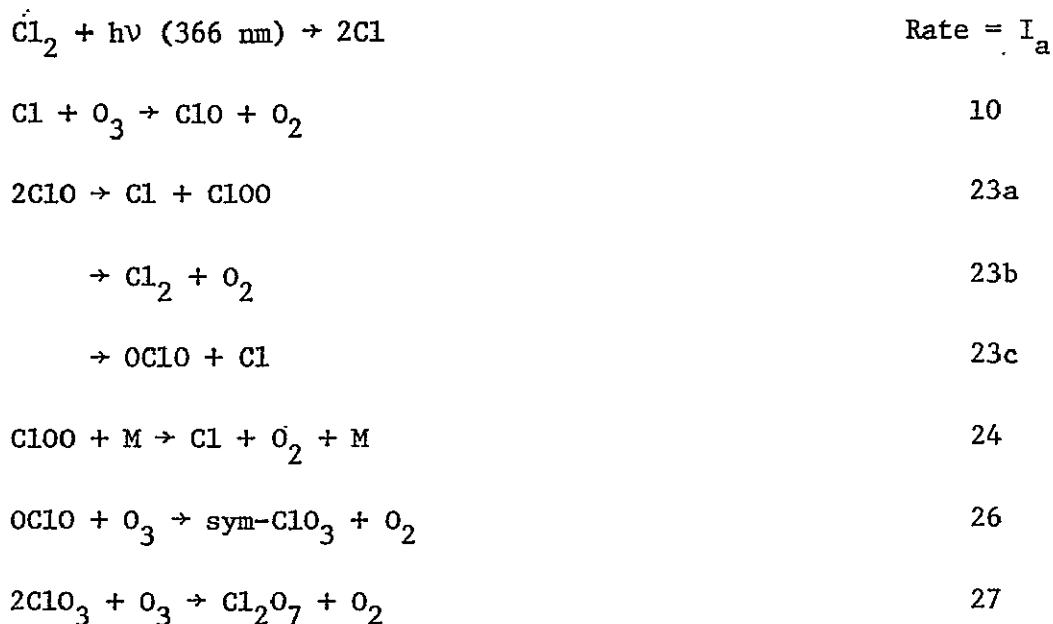
The values of the known rate coefficients for the reactions in mechanism (a) are summarized in Table 10.

An analysis of the above reactions leads to the following steady-state concentration expression for the radicals in the system.

$$[Cl]_{ss} = \frac{2I_a + 4I_a k_{23a} \cdot \beta + 2I_a \cdot \alpha}{k_{10}[O_3]} \qquad\qquad I$$

$$[ClO]_{ss} = (2I_a \cdot \beta)^{1/2} \qquad\qquad II$$

$$[OClO]_{ss} = \frac{2I_a \cdot \alpha}{k_{26}[O_3]} \qquad\qquad III$$

$$[ClO_3]_{ss} = \left(\frac{I_a \cdot \alpha}{k_{27}[O_3]} \right)^{1/2} \qquad\qquad IV$$

where $\alpha = k_{23c} \cdot \beta$

$$\beta = (k_{23c} + 2k_{23b})^{-1}$$

Table 10

The Rate Coefficients for the Reactions in the Photolysis of Cl_2-O_3 Mixtures

Rate Coefficient	$cm^3 sec^{-1}$	Temp, °K	Reference
k_{11}	$(2.7 \pm 1.2) \times 10^{-11} \exp[-(257 \pm 106)/T]$	205–298	77–82
k_{23}	2.3×10^{-14}	300.	90
k_{23}	4.4×10^{-14}	298	41
k_{23a}	$1.2 \times 10^{-12} \exp[(-1179)/T]$		90
k_{23c}	$2.1 \times 10^{-12} \exp[(-2201)/T]$		90
k_{24}	$1.14 \times 10^{-11} \exp[-(3370 \pm 350)/T]$		41
k_{25}	$\leq 1 \times 10^{-18}$		This lab
	$\leq 5 \times 10^{-15}$		61
	$\leq 5 \times 10^{-14}$		46
k_{26}	$2.3 \times 10^{-12} \exp[-(4730 \pm 630)/T]$		This lab
k_{29}	$1.7 \times 10^{-33(a)}$	275.5	This lab
	$1.15 \times 10^{-33(a)}$	264	This lab
k_{-29}	2.68×10^{-19}	275.5	This lab
	1.08×10^{-19}	264	This lab

[a]The unit for k_{29} is $cm^6 sec^{-1}$.

Mechanism (a) leads to the following rate laws.

$$\Phi_i\{OClO\} = \frac{2}{1 + 2k_{23b}/k_{23c}}$$ V

$$-\Phi\{O_3\} = \frac{4 + 3k_{23c}/k_{23}}{2k_{23b}/k_{23} + k_{23c}/k_{23}}$$ VI

$$-\Phi\{Cl_2\} = (1/2)\Phi_i\{OClO\}$$ VII

$$\Phi\{O_2\} = (3/2)[-\Phi\{O_3\}]$$ VIII

The mechanism predicts that $\Phi_i\{OClO\}$, $-\Phi\{O_3\}$ and $-\Phi\{Cl_2\}$ are invariant to $[O_3]$ and I_a, and $\Phi\{O_2\}$ is one and one half of $-\Phi\{O_3\}$. These predictions are completely consistent with the observed data. The fact that $-\Phi\{Cl_2\}$ does not equal one half of $\Phi_i\{OClO\}$ is discussed later. Equation V can be rearranged to give:

$$\Phi_i\{OClO\} = \frac{2k_{23c}}{k_{23c} + 2k_{23b}} \simeq \frac{k_{23c}}{k_{23b}}$$ IX

if $k_{23c} \ll 2k_{23b}$. $\Phi_i\{OClO\}$ was determined as a function of temperature (see Table 6 and Figure 10). Since $\Phi_i\{OClO\}$ is nearly k_{23c}/k_{23b}, the Arrhenius expression for k_{23c}/k_{23b} is the same as $\Phi_i\{OClO\}$.

$$\frac{k_{23c}}{k_{23b}} = 2.5 \times 10^3 \exp[-(3025 \pm 625)/T]$$ X

The ratio of the three channels of reaction can be computed from equations V and VI.

$$\frac{k_{23b}}{k_{23}} = \frac{1}{\Phi_i\{OClO\}} \cdot \frac{4}{2\gamma + [-\Phi\{O_3\}] - 3} \qquad \text{XI}$$

$$\frac{k_{23c}}{k_{23}} = \frac{4}{2\gamma + [-\Phi\{O_3\}] - 3} \qquad \text{XII}$$

$$\frac{k_{23a}}{k_{23}} = 1 - \frac{k_{23b}}{k_{23}} - \frac{k_{23c}}{k_{23}} \qquad \text{XIII}$$

$$\gamma = \frac{[-\Phi\{O_3\}]}{\Phi_i\{OClO\}}$$

where the measured value of $-\Phi\{O_3\} = 5.8$ and $\Phi_i\{OClO\} = 0.089$ at 273°K. The values computed from equations XI, XII, and XIII are the following: $k_{23a}/k_{23} = 0.63$, $k_{23b}/k_{23} = 0.34$ and $k_{23c}/k_{23} = 0.032$. Since $\Phi_i\{OClO\}$ and $-\Phi\{O_3\}$ are pressure invariant (76), these ratios are also invariant over the range of pressures employed in this study.

At low temperatures, equation XI can be rearranged to

$$\frac{k_{23}}{k_{23b}} \simeq \frac{1}{2}[-\Phi\{O_3\}] \qquad \text{XIV}$$

The ratio of k_{23}/k_{23b} is obtained from the study of the temperature dependence of $-\Phi\{O_3\}$. The values of k_{23}/k_{23b} calculated from equation XIV are 1.99 at 283°K, 1.45 at 273°K and 1.0 at 252°K. This implies that reaction 23 proceeds predominantly through channel 23b at low temperatures.

From the Arrhenius expression of k_{23c}/k_{23b} (equation X), the large value of the preexponential factor A_{23c}/A_{23b} suggests that the

reaction channel 23b and 23c proceed through very different transition
states. From the large value of A_{23c}, it is reasonable to assume
that the reaction 23c is an atom abstraction reaction with a linear
transition state. The lower value of A_{23b} suggests that reaction 23b
involves a tighter transition state than that to reaction 23c. It is
reasonable to assume that reaction 23b involves a four center
transition state.

The reactions of ClO with itself, reaction 23, have been studied
in some detail recently, but there is still controversy about the
relative importance of the three channels at higher pressure. Basco
and Dogra (84,85) have interpreted their flash photolysis data at
high pressures (about 75 Torr argon) in terms of reaction 23b
exclusively. Johnston et al. (86) working at low light intensities
found a pressure effect on ClO disproportionation and proposed the
reaction

$$2ClO + M \rightarrow Cl_2 + O_2 + M \qquad\qquad 28$$

In a more recent paper, Wu and Johnston (87) have confirmed the effect
of total pressure on their results, but now feel that the pressure
effect may actually be associated with other reactions in their
system or that at low light intensity the mechanism of ClO dispro-
portionation differs from that at higher light intensity.

At low pressures, Clyne and coworkers (61,88,89) have conclusively
shown that reaction 23a is dominant and in their most recent paper
(61) have shown that the distribution at low pressures is the
following: 23a (95%), 23c (5%). They have also done computer

modeling of the results of Basco and Dogra and find that their

results can be reinterpreted in terms of reaction 23a as the

dominant channel contrary to the interpretation of Basco and Dogra.

Recently Clyne and Watson (90) have reevaluated all the data

in terms only of reactions 23a and 23c and recommend the expressions

$$k_{23a} = 1.2 \times 10^{-12} \exp[-9.8 \text{ KJ/mole/RT}] \text{ cm}^3 \text{sec}^{-1}$$

$$k_{23c} = 2.1 \times 10^{-12} \exp[-18.3 \text{ KJ/mole/RT}] \text{ cm}^3 \text{sec}^{-1}$$

though the data do not exclude reaction 23b occurring to some extent

and k_{23a} may really represent $k_{23a} + k_{23b}$.

It is not clear how all these results can be brought into

harmony, however; it seems likely to us that reactions 23a and 23b

are important under all pressure conditions. The data of Clyne et al.

(61) are consistent with a contribution from both reactions 23a and

23b, and in fact in our system reaction 23b must be the major

termination step. It is possible that Cl atom formation in the

Basco and Dogra work may have been overlooked.

The upper limit for k_{25} may be computed by requiring that

reaction 25 be negligible compared to reaction 23. Then

$$k_{25} < \frac{k_{23}}{[O_3]} \cdot \left(\frac{I_a}{k_{23b}} \right)^{1/2} \qquad \text{XV}$$

where $k_{23} = 2.3 \times 10^{-14} \text{ cm}^3 \text{sec}^{-1}$ according to Clyne and Watson (90)

and $4.4 \times 10^{-14} \text{ cm}^3 \text{sec}^{-1}$ according to Watson (41). Even at our

highest value of $[O_3]/(I_a)^{1/2} = 1.6 \times 10^{11} \text{ (sec/cm}^3)^{1/2}$, there is

no variation of $\Phi_1\{OClO\}$. This means there is no contribution to

OClO due to reaction 25a and for this to be true k_{25} must be less than 1×10^{-18} $cm^3 sec^{-1}$. This upper limit of k_{25} is in good ·agreement with a conclusion reached by Lin et al. (62). The low · value of k_{25} is also consistent with the upper limit of about 5×10^{-15} $cm^3 sec^{-1}$ obtained by Clyne et al. (61) and 5×10^{-14} $cm^3 sec^{-1}$ obtained by Birks et al. (46). However, Clyne et al. using a discharge flow technique found that in the presence of O_3 more OClO was produced than could be explained by reaction 23c alone and considered it probable that their upper limit was the actual value for k_{25}.

The OClO profile at 298°K shown in Figure 7 may be analyzed quantitatively for self consistency over the entire region (light and dark) by integrating the differential equations for OClO formation and decay. The differential equation during irradiation is

$$\frac{d}{dt}[OClO] = \Phi_i\{OClO\} \; I_a - k_{26}[O_3][OClO] \qquad \text{XVI}$$

Integration gives

$$\cdot [OClO]_t = (\Phi_i\{OClO\} \; I_a/k_{26}[O_3])(1 - \exp\{-k_{26}[O_3]t\}) \qquad \text{XVII}$$

A plot of $[OClO]$ vs. $\exp\{-k_{26}[O_3]t\}$ should be linear with a slope and intercept of $\Phi_i\{OClO\}I_a/k_{26}[O_3]$. Figure 18 shows that the plots at $297 \pm 3°K$ are reasonably linear as required. Values of $\Phi_i\{OClO\}$ obtained from the slopes of these plots are presented in Tables 2, 3, and 5. They are in good agreement with the values obtained from the

Figure 18. Plots of [OClO] vs. $\exp(-k_{26}[O_3]t)$ for Selected Data at 297 $\pm$ 3°K
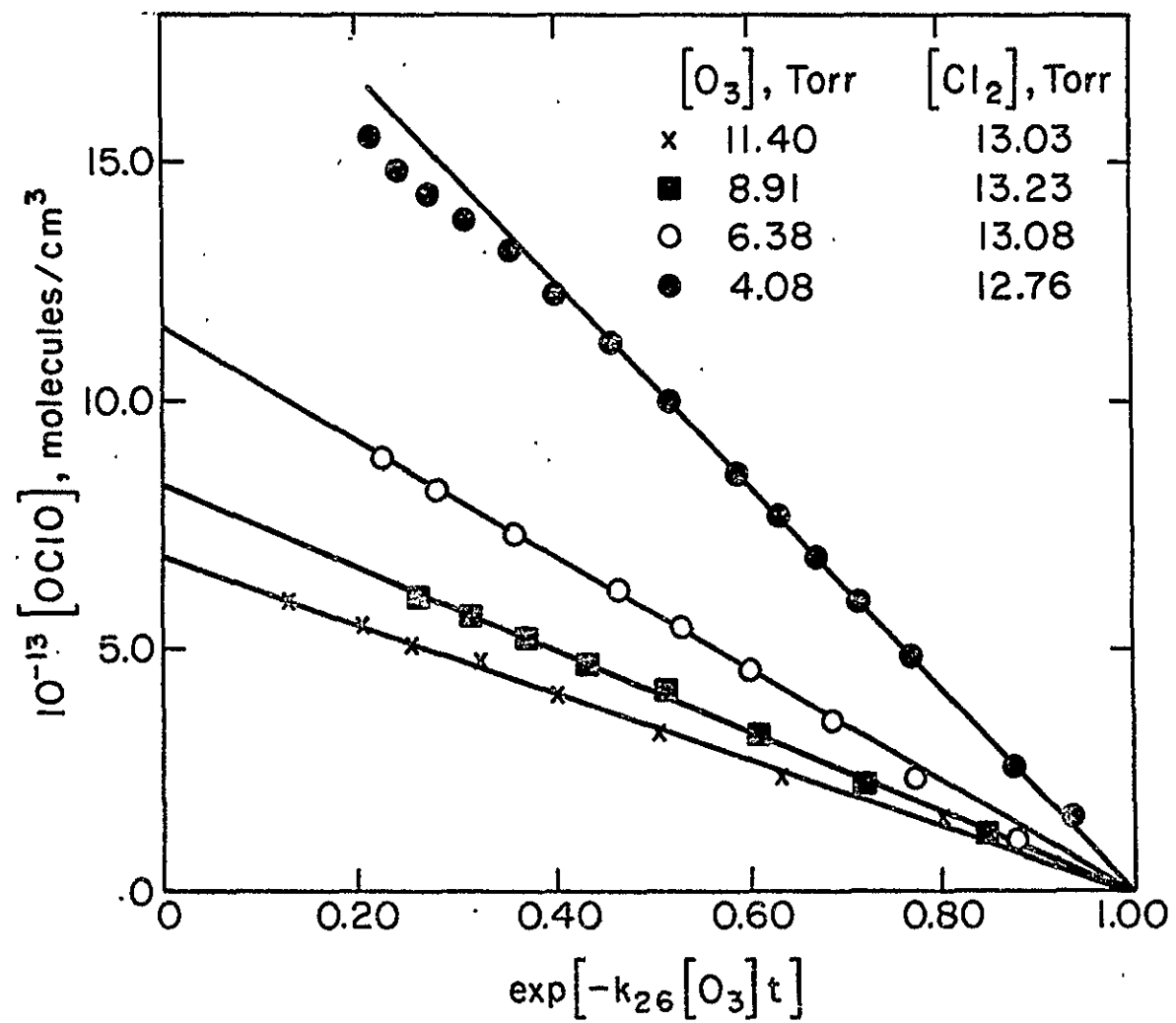
initial growth rates. At lower temperatures, plots of equation XVII are not linear.

Equation II, the steady state expression for OClO during irradiation, can be rearranged to:

$$[OClO]_{ss} = \frac{\Phi_i \{OClO\} I_a}{k_{26}[O_3]} \qquad\qquad XVIII$$

Values of k_{26} computed from equation XVIII using the observed values of $[OClO]_{ss}$ are also presented in Tables 2, 3, and 4. At 297°K these values are in good agreement with those obtained from the decay plots (see Figure 19).

At temperatures below 297°K the OClO decay profiles in the dark show an induction period (Figure 7) and the integrated growth curves (equation XVIII) are not linear indicating that the mechanism thus far outlined is not complete at lower temperatures. These observations can be interpreted in terms of the equilibrium

$$ClO + OClO + M \rightleftarrows Cl_2O_3 + M \qquad\qquad 29, -29$$

The Cl_2O_3 acts as a reservoir of OClO leading to the slow initial rate of OClO depletion upon the termination of light.

As a test of this hypothesis, profiles for OClO were calculated for all temperatures by numerically integrating the rate equations for ClO and Cl_2O_3. The only assumption made in this computation was that Cl has reached its steady state value. An adaptive pattern search routine (91) was used to calculate the rate coefficients for reaction 29 and -29. The details are given in Appendix II. This

C - 2

Figure 19. Plots of k_{26} vs. $[O_3]$ at $297 \pm 3°K$. x, values obtained
from the initial slope of the decay curves in the dark
after the photolysis; ☻, values obtained from the
steady state OClO values during the photolysis; ☉,
values obtained from the direct reaction of OClO with O_3.

algorithm varies the rate constants k_{29}, k_{-29}, k_{23c}, and k_{26} such that the mean square error between the calculated and the experimental values of OClO are minimized. The OClO growth is controlled initially by the parameter k_{23c}/k_{23b} and the decay is controlled by k_{26}. However, absolute values for k_{23b} and k_{23c} are needed for the computation. These were obtained from the values of $\Phi_i\{OClO\}$, $-\Phi\{O_3\}$ and the literature value for k_{23} (4.4×10^{-14} $cm^3 sec^{-1}$) (41).

In order to test the validity of this integration method, room temperature profiles for OClO were also fitted. For this case the values of k_{29} and k_{-29} used were zero. This is equivalent to having a complete Cl_2O_3 dissociation.

At 275°K and 264°K, $k_{29}[M]$ was varied from 1.00×10^{-11} to 1.00×10^{-16} $cm^3 sec^{-1}$ and $k_{-29}[M]$ from 10.00 to 0.01 sec^{-1}. The constant k_{23c} was allowed to vary within $\pm 20\%$ of the calculated value from $\Phi_i\{OClO\}$, $-\Phi\{O_3\}$ and k_{23}. The constant k_{26} was varied within the range of values obtained from the steady state of OClO and from the direct mixing experiments. Typical computer profiles, together with the experimental profiles are shown in Figure 7. The overall errors of the computed profiles were within $\pm 20\%$ of the experimental profiles. The average value of $k_{29}[M]$ is $(1.2 \pm 0.4) \times 10^{-15}$ $cm^3 sec^{-1}$ at 275.5°K, and $(5.5 \pm 1.5) \times 10^{-16}$ $cm^3 sec^{-1}$ at 264°K. The average value of $k_{-29}[M]$ is (0.19 ± 0.08) sec^{-1} at 275.5°K and (0.08 ± 0.03) sec^{-1} at 264°K. The results are the average of six runs at 275.5°K and four runs at 264°K. At both temperatures, the average pressures for the runs used to determine $k_{29}[M]$ and $k_{-29}[M]$ were 20.2 ± 3.2 Torr. When converted to third

and second order rate coefficients, we obtain k_{29} = 1.70 x 10^{-33} and

1.15 x 10^{-33} $cm^6 sec^{-1}$ at 275.5 and 264°K, respectively, and

k_{-29} = 2.68 x 10^{-19} and 1.08 x 10^{-19} $cm^3 sec^{-1}$ at 275.5 and 264°K

respectively.

We estimate that these values are accurate to within a factor

of two. Of course, at 296°K, Cl_2O_3 formation is not important

because of the rapid reverse reaction, and below 264°K the reactions

are too slow to obtain meaningful results. The values of k_{29} show

a slight positive activation energy, though this may just reflect

the error in the measurements. The rate coefficients for k_{-29} are

consistent with a bond dissociation enthalpy of about 12 kcal/mole

for Cl_2O_3.

So far a discussion of $-\Phi\{Cl_2\}$ was neglected in interpreting the

data. Mass balance considerations require that in the initial part

of the experiment $-\Phi\{Cl_2\}$ = $\Phi_i\{OClO\}/2$. In our experiments, $-\Phi\{Cl_2\}$

was measured, by necessity, for large conversions, and it was found

to be much greater than $\Phi_i\{OClO\}/2$. Possibly secondary reactions

may be involved in which the higher oxides of chlorine (ClO_3, ClO_4,

and possibly Cl_2O_5 or Cl_2O_6) react whether with Cl_2 or ClO to produce

Cl_2O_7. This may be a surface reaction. The details of such a

reaction cannot be determined from our data.

If the reaction removing additional Cl_2 does not involve $OClO$

as an intermediate, then the $OClO$ concentration is not affected by

it. However, if additional $OClO$ is produced, as seems likely, then

the steady state concentration of $OClO$ should show an accelerated

rise as the reaction proceeds toward completion. The steady state

value of OClO is inversely proportional to $[O_3]$ even if OClO is not an intermediate in the secondary reaction. We attempted to monitor [OClO] for long conversions, but the uncertainty in the measurements caused by instrument drift made it difficult to determine if [OClO] increased more than would be expected due to the depletion of O_3.

D. Atmospheric Implications

To estimate the importance of reaction 25 in the stratosphere, the reaction rate was compared with the following:

1. The photodissociation rate of ClO,

2. The rate that ClO reacts with other species present in the stratosphere such as $O(^3P)$ and NO.

The photodissociation rate, J, of any species can be calculated using the following equation,

$$J = \text{solar flux intensity x the absorption cross section}$$
$$\text{of that species} \qquad\qquad XIX$$

Thus for the ClO-O_3 system the ratio of the photolysis rate of ClO vs. the rate of reaction with O_3 is

$$\frac{\text{Photolysis Rate}}{R_{25}} = \frac{J\{ClO\}}{k_{25}[O_3]} \qquad\qquad XX$$

Assuming the solar flux intensity to be 1×10^{15} cm^{-2}sec^{-1} (1), the absorption cross section of ClO at 303.45 nm = 0.7×10^{-18} cm^2 (41) and $[O_3]$ at 20 km to be 4×10^{12} cm^{-3} (1), the result from equation XX shows that the photolysis process is at least 175 times faster than reaction 25.

The rate of reaction 25 was also compared with the rate of reactions 11 and 16.

$$ClO + O(^3P) \rightarrow Cl + NO_2 \qquad\qquad 11$$

$$ClO + NO \rightarrow Cl + NO \qquad\qquad 16$$

where $k_{11} = 5.3 \times 10^{-11}$ cm^3sec^{-1} at 298°K (42) and $k_{16} = 1.8 \times 10^{-11}$ cm^3sec^{-1} at 298°K (43,44). The reaction ratios for these equations are:

$$R_{11}/R_{25} = k_{11}[O]/k_{25}[O_3] \qquad\qquad XXI$$

$$R_{16}/R_{25} = k_{16}[NO]/k_{25}[O_3] \qquad\qquad XXII$$

The pertinent concentrations at 20 km were taken to be (1): $O(^3P) = 1 \times 10^6$ cm^{-3}, $O_3 = 4 \times 10^{12} cm^{-3}$, and $NO = 2 \times 10^8$ cm^{-3}. The results show that at 20 km reactions 11 and 16 are at least 13 and 900 times respectively more important than reaction 25.

The importance of reaction 26 in the stratosphere was evaluated in a similar manner. Using the absorption cross section for OClO at 351.2 nm, 1.1×10^{-17} cm^2 (41), the photolysis rate is approximately 1×10^4 times faster than reaction 26. It can be concluded that the values of the rate coefficients for reactions 25 and 26 are too low to make these reactions of any significance in the earth's atmosphere.

Chapter 3

THE Cl_2-O_2-NO SYSTEM: THE REACTION OF ClOO WITH NO

A. Experimental

A.1. Materials and Their Purification

All gases were supplied by Matheson gas products. The Cl_2 was

purified by distillation from -130°C to -160°C as described in

Chapter 2 Section A.1. NO was purified by distillation from -186°C

to -196°C and stored at room temperature.

Before use, N_2 was slowly plassed through two U-tube traps

maintained at -196°C. Chromatographic analysis of N_2 showed that less

than 2.5 ppm of CH_4 was present. There were no detectable levels of

other hydrocarbon impurities. The O_2 was freed of hydrocarbon

impurities by the following method: A mixture of approximately

2 Torr Cl_2, 20 mTorr NO and 750 Torr O_2 was photolyzed in a 5-liter

Pyrex bulb with a medium-pressure mercury arc lamp (Hanovia 404101).

After irradiation the mixture was purified by distillation from -186°C

to -196°C and stored. Chromatographic analysis of the purified

oxygen indicated less than 0.8 ppm CH_4 and less than 0.1 ppm C_2H_6.

There were no detectable levels of the heavier hydrocarbons.

The quantitative analysis of the hydrocarbon impurities present

in O_2 and N_2 was done using a gas chromatograph equipped with a

flame ionization detector. A four-foot seven mm O.D. glass column

packed with either 80/100 mesh Chromosorb 101 or 80/100 mesh 5A

molecular sieves was used for the analysis. The column was kept at

room temperature. Helium was used as a carrier gas with a flow rate of 72 cm^3/min. The retention times of methane and ethane, using the 80/100 mesh Chromosorb 101 column are approximately 0.5 and 2.0 min respectively. The retention time using the 5A molecular sieve glass column is approximately 0.4 min for CH_4. A schematic diagram of the flame ionization gas chromatograph is shown in Figure 20.

A.2. Vacuum Line

The vacuum line was divided into four parts. Two parts of the line were for Cl_2 and O_2/N_2 purification. These parts were always isolated from the whole system when they were not in use. This was done because the Cl_2-O_2-NO system was sensitive to residual surface as well as gaseous impurities. The other two parts of the vacuum line were for handling Cl_2 and NO. Two separate silicone oil manometers were used to measure Cl_2 and NO pressures. A 0-800 Torr Wallace and Tiernan vacuum gauge was added to the system to measure the absolute pressure of O_2 and N_2. A diagram of the vacuum line is given in Figure 21.

A.3. Reaction Vessel and Photolysis Source

The reaction cell was a 200 cm^3 cylindrical quartz cell, 10 cm long and 5 cm in diameter. It was enclosed in a Styrofoam box with an access for cold N_2 gas to pass through. The temperature of the reaction cell was measured using an iron-constantan thermocouple as described in Chapter 2, Section A.3.
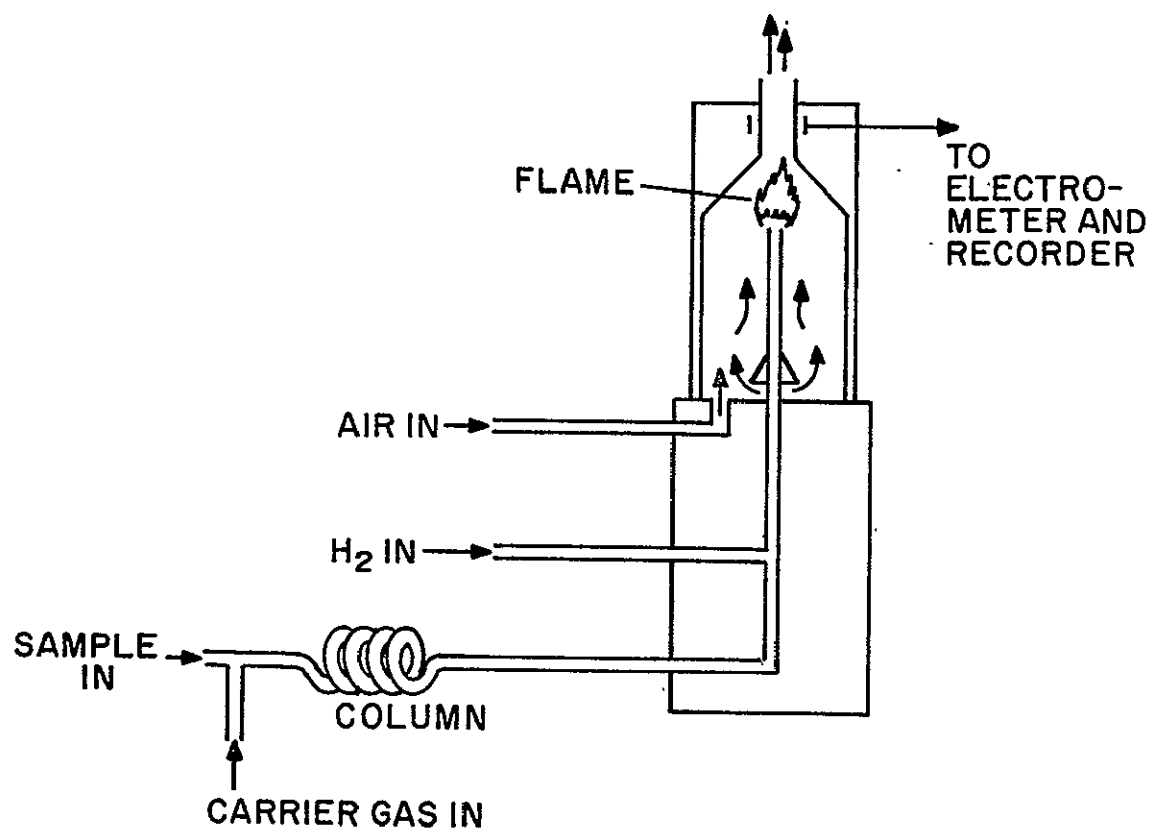
Figure 20.   Diagram of a Gas Chromatograph with Flame Ionization Detector

⊗ 4 OR 10 mm TEFLON STOPCOCK

◯ STORAGE BULB

⊗ GAS INLET

TO VEECO
THERMOCOUPLE
GAUGE

TO
ALPHATRON
GAUGE

TO
WALLACE-
TIERNAN
GAUGE

TO OIL
MANOMETER

TO
REACTION
CELL

LIQUID
N₂
TRAP

TO
OIL
MANO-
METER

SPIRAL
TRAP

OIL DIFFUSION PUMP

TO
CHEMILUMINESCENCE
CELL

LIQUID N₂ TRAP

TO
MECHANI-
CAL PUMP

TO
REACTION
CELL
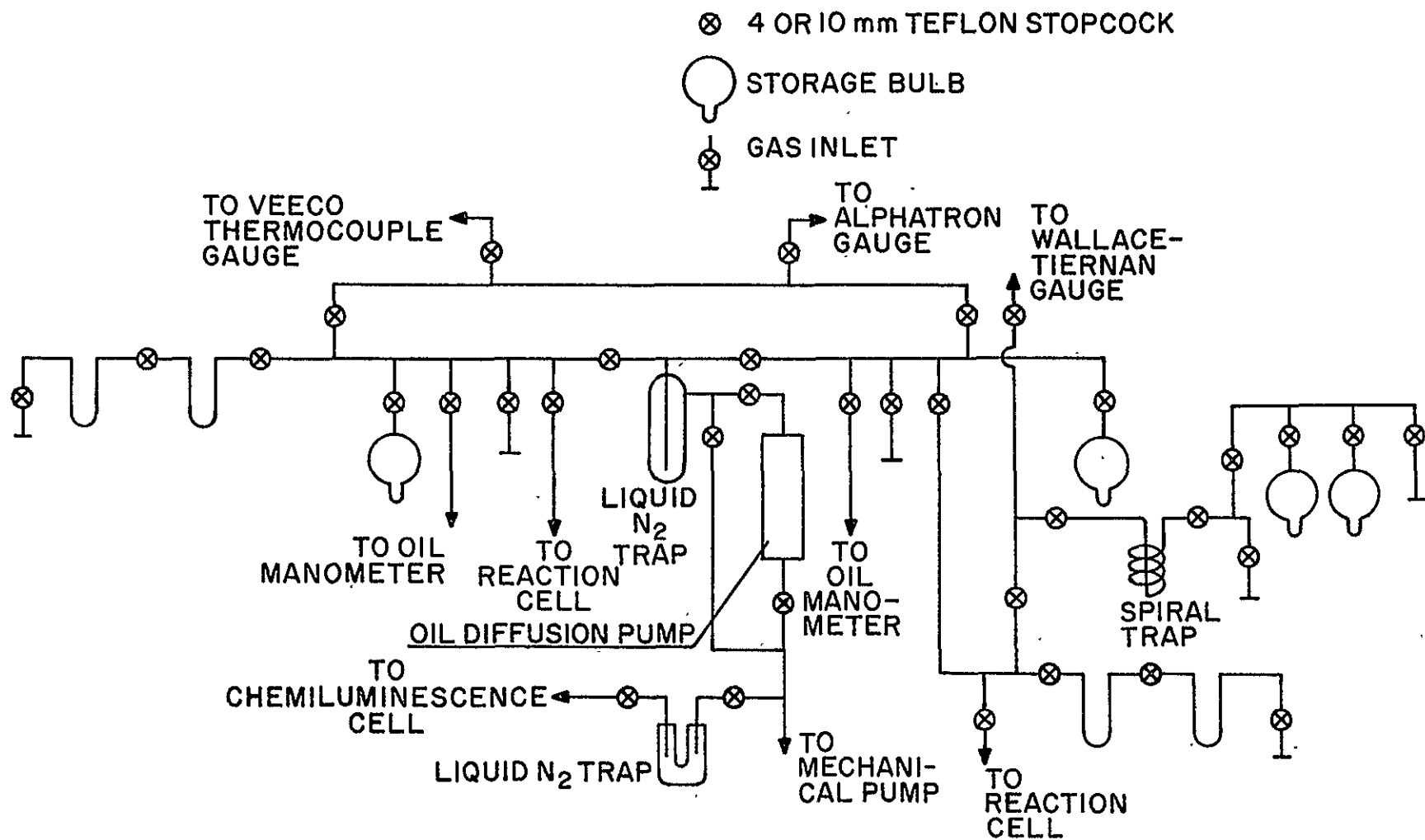
Figure 21.   Vacuum Line for the Cl_2-O_2-NO System

95

The photolysis source was a high pressure Hanovia Hg arc lamp, 200 watts (type 202-1003). The 366 nm line was isolated by passing the photolysis beam through a Corning filter (CS 7-37) before entering the reaction cell. A diagram of the reaction vessel is given in Figure 22.

A.4. The Analysis System

The chemiluminescence analysis system was similar to that described by Stedman et al. (92). It consisted of a 100 cm^3 cylindrical quartz cell with two inlets, one for the ozonized O_2 and the other for the reactants. The O_3 and the sample inlet tubes were concentrically arranged for efficient mixing. The ozonized O_2 was prepared by passing the stream of O_2 ($\sim$130 cc/min) through a high voltage discharge. The reactant mixture was leaked out of the reaction cell through a capillary tube and to the chemiluminescence cell either continuously or intermittently. The capillary was placed right in the center of the reaction cell as shown in Figure 22. The diameter of the capillary tube was chosen such that the pressure drop in the reaction vessel was approximately 1% per minute. The pressure in the chemiluminescence cell was kept between 1-3 Torr by continuously pumping with a Welch high velocity mechanical pump.

The red emission due to the chemiluminescent reaction between O_3 and NO was passed through a Corning cut off filter (CS 2-62) and was viewed with a photomultiplier (EMI 9785B). The chemiluminescence cell and the photomultiplier were kept in the dark at room
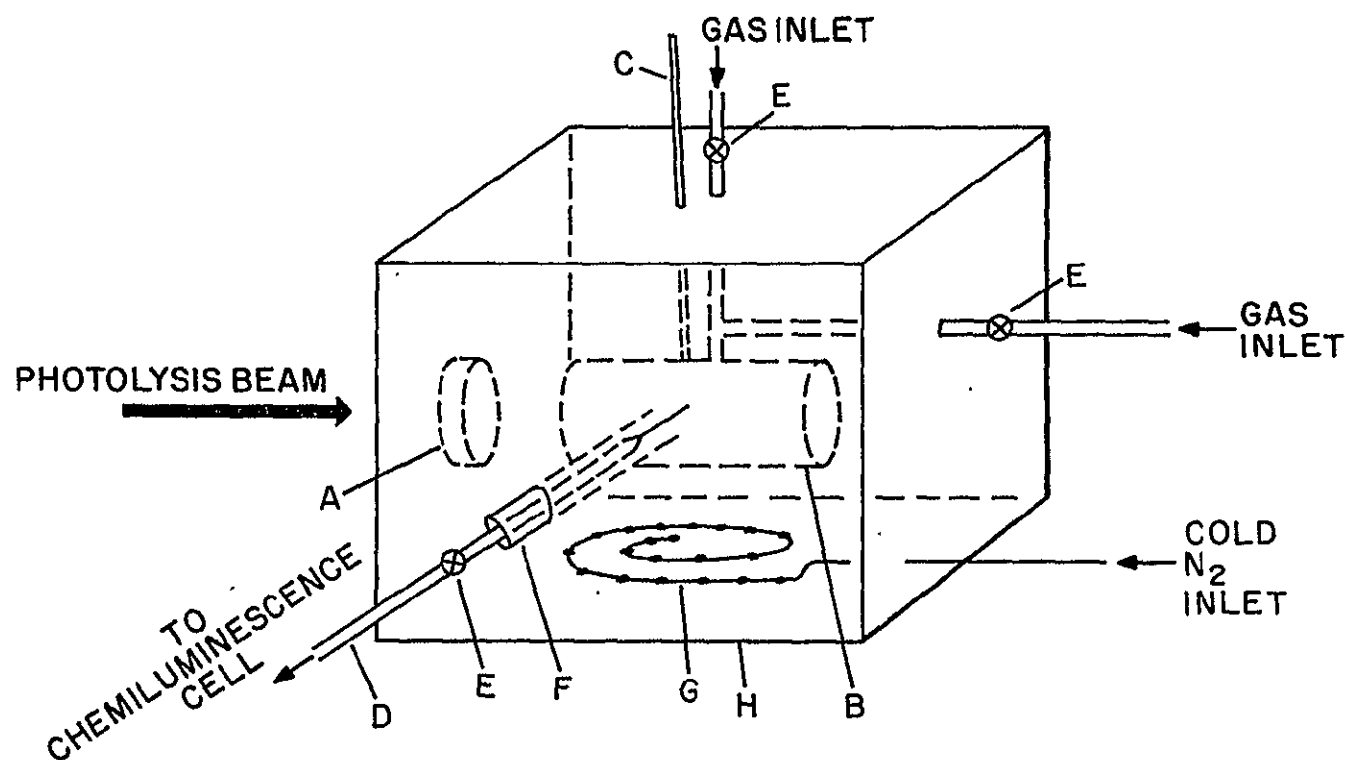
A   EVACUATED DOUBLE WALL QUARTZ WINDOW
B   QUARTZ REACTION CELL
C   THERMOCOUPLE
D   SAMPLING GLASS TUBE WITH CAPILLARY
    TIP PLACED INSIDE THE REACTION CELL

E   4 MM TEFLON STOPCOCK
F   ACE GLASS FITTING
G   COPPER TUBE WITH EXIT HOLES
H   STYROFOAM BOX

Figure 22.   Reaction Cell for the Cl_2-O_2-NO System

temperature. The photomultiplier was operated at a cathode to anode voltage of 1 KV. The photocurrent was amplified using a Kiethly electrometer 601 with a d.c. zero offset and displayed on a strip chart recorder. A schematic diagram of this system is shown in Figure 23.

A.5. Chemiluminescent Reaction

The reaction between NO and O_3 has been extensively investigated by Stedman et al. (92), Clough and Thrush (93), Fontijn et al. (94), and Clyne et al. (95). It is known that the reaction between NO and O_3 results in light emission. This chemiluminescence is due to the following reactions.

$$NO + O_3 \rightarrow NO_2^* + O_2 \qquad\qquad 5a$$

$$\rightarrow NO_2 \text{ (electronic ground state) } + O_2 \qquad\qquad 5b$$

$$NO_2^* \rightarrow NO_2 + h\nu \quad \text{(red)} \qquad\qquad 30$$
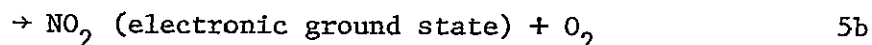
The relative intensity distribution of the emission spectrum (93) shows that no light is emitted below about 600 nm. The use of a 600 nm cut-off filter (CS 2-62) and the upper limit of our photomultiplier system (800 nm) limited our measurements to the region between 600 and 750 nm. The emission intensity is linearly proportional to [NO] and $[O_3]$. It is inversely proportional to the total pressure in the chemiluminescence cell (94). Since the stream of the ozonized oxygen and the pumping speed were kept constant, it was observed that the

SAMPLE

OZONISED OXYGEN

CORNING
GLASS FILTER

POWER SUPPLY
I KV

TO
LIQUID N$_2$
TRAP
AND
MECHANICAL
PUMP

CHEMILUMINESCENCE
CELL

PHOTOMULTIPLIER

ELECTROMETER

BUCKING CIRCUIT

$10^9 \Omega$
RESISTOR

45 V
BATTERY

47 KΩ

TO
RECORDING
SYSTEM

99
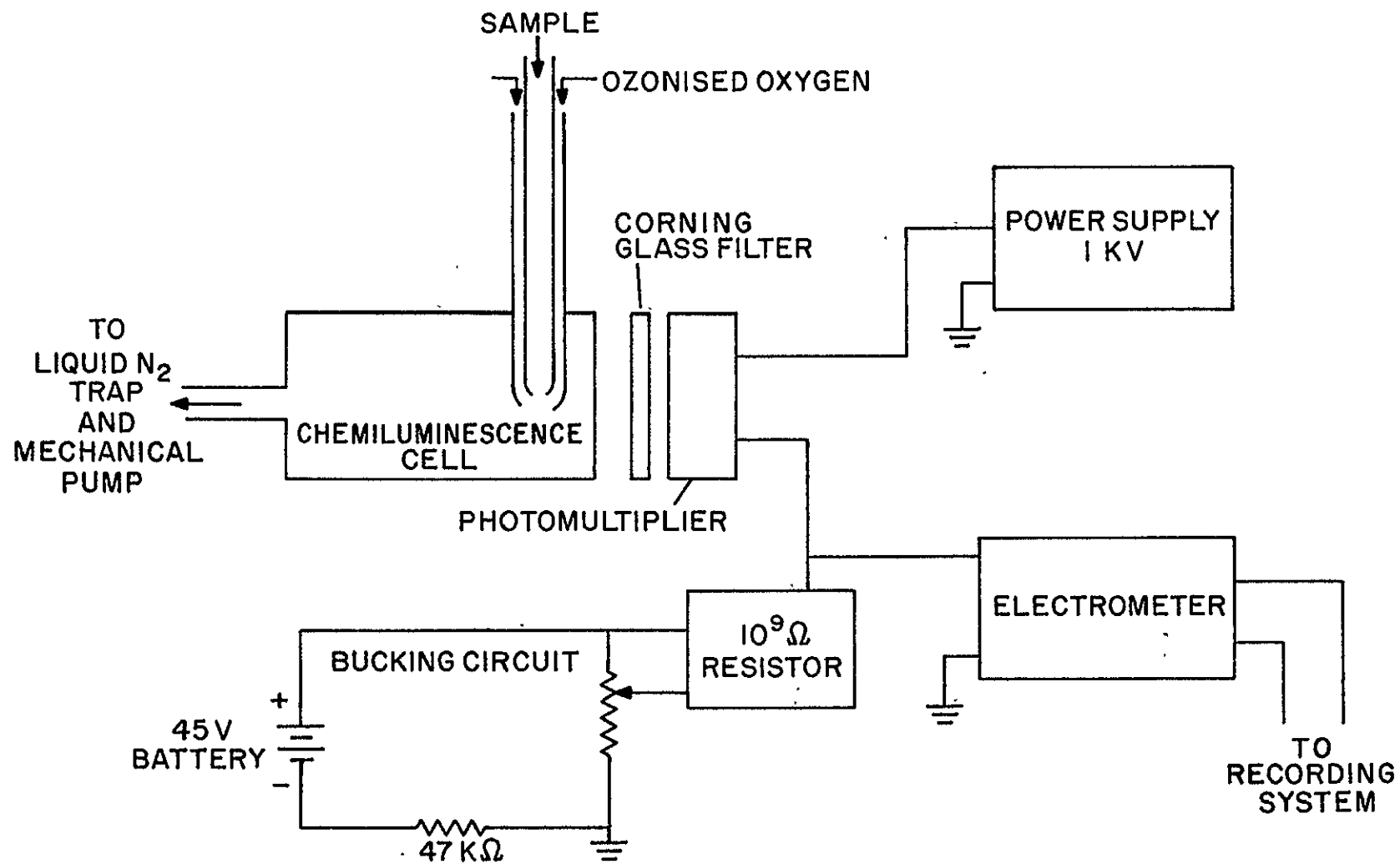
Figure 23.   Schematic Diagram of the Chemiluminescence Detection System

emission intensity was linearly proportional to [NO] throughout our experimental conditions.

A.6. Procedure

Mixtures of Cl_2, O_2, and NO with or without added N_2 were irradiated at 366 nm and 298°K. The photolysis leads to the removal of NO. The NO concentration was monitored continuously during the irradiation using the chemiluminescent reaction with O_3. The cell contents were bled into a chemiluminescence chamber through a sampling capillary tube attached to the reaction cell as shown in Figure 22. O_2 or N_2 served as a carrier gas. The reactant samples were then mixed with the ozonized oxygen. To obtain the absolute concentration of NO, the emission intensity of the chemiluminescent reaction was calibrated with known NO samples.

A.7. Actinometry

The absorbed light intensity, I_a, was determined by photolysis of optically equivalent amounts of azomethane in the presence of NO. At 366 nm, azomethane photodissociates to yield two methyl radicals (73,96) which in turn react with NO. The NO removal quantum yield for this system is 2.0. The NO concentration was monitored continuously using the chemiluminescent reaction with O_3.

B. Results

The photolysis of Cl_2 in the presence of O_2 at 366 nm and 298°K leads to the formation of ClOO radicals. The photolysis leads

to the removal of NO if there are small amounts present in the Cl_2-O_2 mixture. Initially the rate of NO removal is rapid, but it decreases as the reaction proceeds. A typical profile is shown in Figure 24.

Initial NO removal quantum yields, $-\Phi_i\{NO\}$, were evaluated from the initial slopes of the NO loss profiles. The initial rate of NO removal was corrected for the pressure drop in the reaction cell as well as for the electronic time constant of the measurement system. The pump out rate through the sampling capillary was 1.58×10^{-2} min^{-1}, leading to a correction of less than 10% for the initial rate. The measurement time constant ranged between 3 and 6 sec leading to a typical correction of 10-15%.

Experiments were done covering a wide range of experimental conditions: $[Cl_2]$ from 1.44 to 5.33 Torr, [NO] from 3.8 to 38.1 mTorr, $[O_2]$ from 222 to 642 Torr, $[N_2]$ from 278 to 609 Torr, and I_a from 0.65×10^{13} to 6.06×10^{13} $cm^{-3}sec^{-1}$. When NO is present at more than 36 mTorr, the reaction with Cl_2 in the dark becomes significant. To avoid any complications due to the dark reaction between Cl_2 and NO, the maximum NO used for the $-\Phi_i\{NO\}$ determinations was limited to 31.9 mTorr. The results for I_a, [NO], $[O_2]$, and $[N_2]$ variations are presented in Tables 11, 12, 13, and 14 respectively. The results are also shown in Figures 25, 26, and 27. It is apparent that the initial NO removal quantum yields are independent of I_a, [NO], and $[O_2]$. The average value of $-\Phi_i\{NO\}$ is 0.11 ± 0.02 at 298°K. However, if $[O_2]$ is reduced while the total pressure is maintained constant with added N_2, $-\Phi_i\{NO\}$ decreases.

Figure 24. NO Concentration Profile vs. Irradiation Time

$[Cl_2] = 2.84$ Torr

$[NO] = 19.3$ mTorr

$[O_2] = 54.8$ Torr

$I_a = 3.95 \times 10^{13}$ cm^{-3}sec^{-1}

103
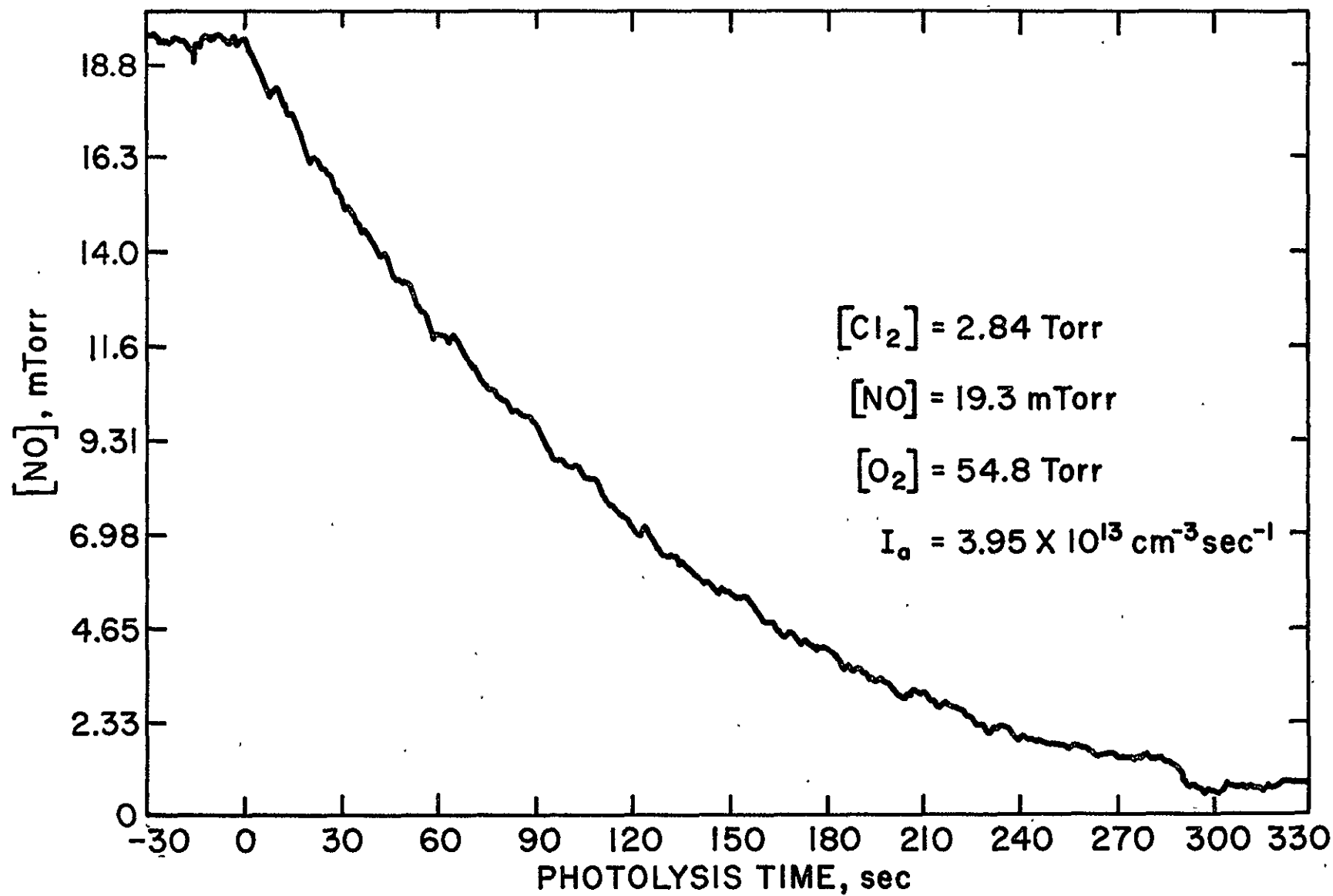
Table 11

NO Removal Quantum Yield in the Photolysis

of Cl_2-O_2-NO Mixtures at Various I_a Values

[Cl_2], Torr	[NO], mTorr	[O_2], Torr	$10^{-13} I_a$ $cm^{-3} sec^{-1}$	$-\Phi_i\{NO\}$
1.44	19.8	564	0.65	0.13
1.98	10.5	564	0.90	0.10
2.82	11.1	567	1.28	0.13
3.54	9.1	562	1.60	0.12
4.74	10.4	593	2.14	0.12
2.52	7.3	585	3.50	0.13
3.50	13.2	541	4.87	0.13
3.61	10.4	584	5.02	0.14
4.02	9.4	554	5.59	0.12
4.36	9.7	584	6.06	0.10

Table 12

NO Removal Quantum Yield in the Photolysis

of Cl_2-O_2-NO Mixtures at Various NO Pressures

$[Cl_2]$, Torr	$[NO]$, mTorr	$[O_2]$, Torr	$10^{-13}I_a$, $cm^{-3}sec^{-1}$	$-\Phi_i\{NO\}$
a) Experiments Done at Low I_a				
3.11	5.4	561	1.41	0.13
3.85	6.3	555	1.45	0.10
3.54	9.1	562	1.60	0.12
2.37	25.1	567	1.07	0.12
2.50	25.4	642	1.11	0.11
b) Experiments Done at High I_a				
3.07	3.8	566	4.27	0.12
2.46	5.6	579	3.42	0.11
2.94	6.2	586	4.08	0.12
3.70	6.9	530	5.15	0.11
2.50	9.7	581	3.52	0.11
2.45	10.8	545	3.41	0.11
2.78	11.1	588	3.87	0.11
2.37	16.9	564	3.29	0.10
2.68	18.0	559	3.73	0.08
2.53	18.6	583	3.52	0.08
2.84	19.3	548	3.95	0.11
2.92	20.2	538	4.05	0.09
2.10	28.2	507	2.92	0.10
2.14	29.1	591	2.97	0.09
2.49	31.9	585	3.46	0.11

Table 13

NO Removal Quantum Yield in the Photolysis

of Cl_2-O_2-NO Mixtures at Various O_2 Pressures

$[Cl_2]$, Torr	$[NO]$, mTorr	$[O_2]$, Torr	$10^{-13} I_a$ $cm^{-3} sec^{-1}$	$-\Phi_i\{NO\}$
3.85	25.2	222	1.46	0.10
3.97	26.4	240	1.78	0.13
4.28	13.6	273	1.94	0.10
4.08	38.1	287	1.85	0.12
4.16	12.3	316	1.88	0.11
5.33	13.5	422	2.41	0.13

Table 14

NO Removal Quantum Yield in the Photolysis

of Cl_2-NO Mixtures at Various O_2 and N_2 Pressures

$[N_2]/[O_2]$	$[Cl_2]$, Torr	$[NO]$, mTorr	$[O_2]$, Torr	$[N_2]$, Torr	$10^{-13}\ I_a$, $cm^{-3}sec^{-1}$	$-\Phi_i\{NO\}$
∞	3.35	18.6	----	609	1.51	0.015
∞[a]	1.05	18.6	----	525	1.46	0.033
7.06	3.66	16.0	72.8	514	1.66	0.043
6.52[a]	4.15	16.2	72.2	471	1.87	0.066
4.97[a]	4.05	16.4	88.3	439	1.83	0.071
4.02	3.73	19.5	117.0	470	1.69	0.059
3.36[a]	1.52	23.3	125.3	421	2.12	0.079
3.36	-1.59	24.5	126.9	426	2.21	0.068
2.00	3.42	16.9	218.0	437	1.55	0.071
1.85	4.16	25.2	250.0	462	1.88	0.065
0.98	2.22	24.4	282.8	278	3.08	0.077

[a]These data were obtained in a later set of measurements and $-\Phi_i\{NO\}$ values are systematically somewhat higher.
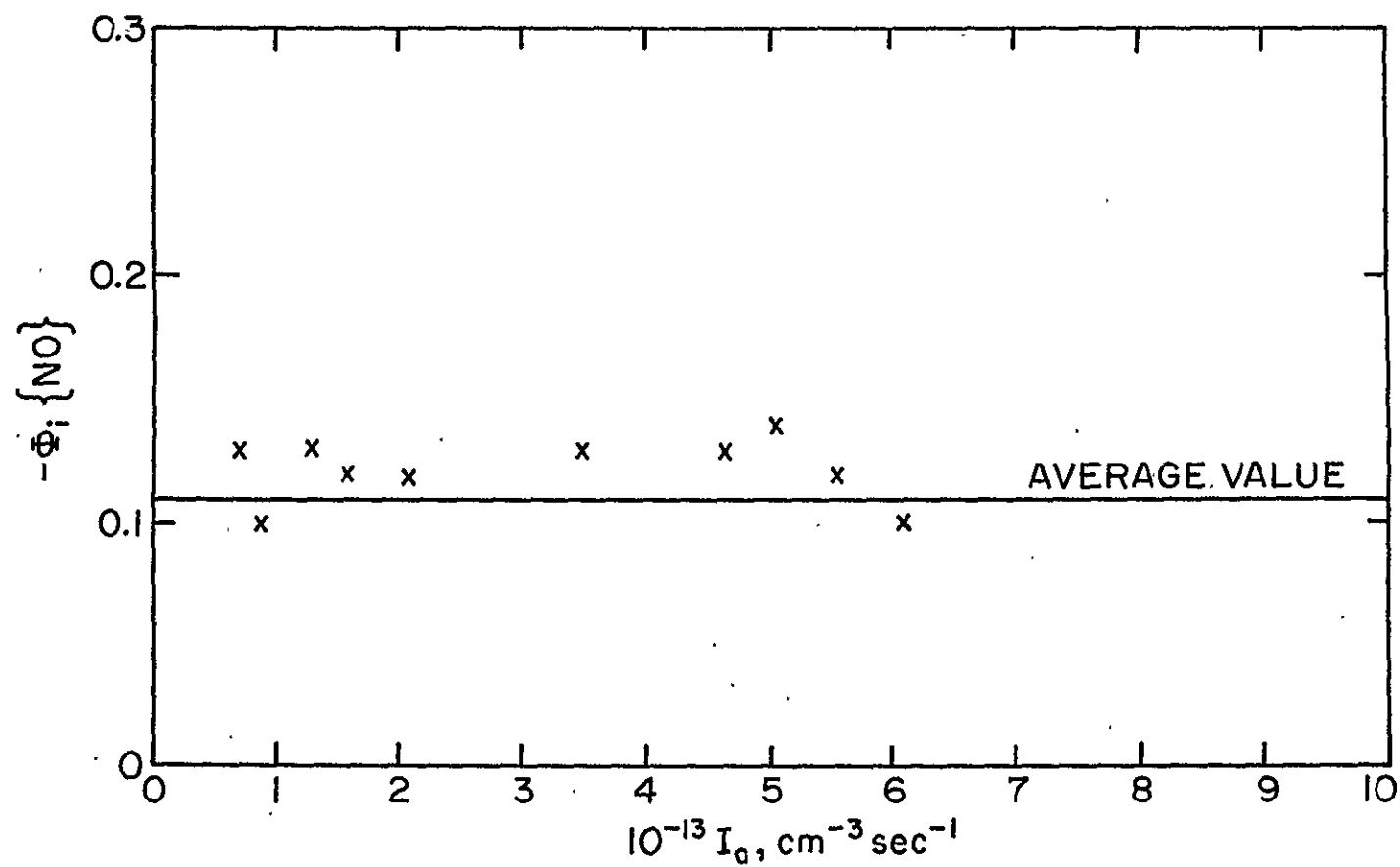
Figure 25. Plots of $-\Phi_i\{NO\}$ vs. I_a at 298°K
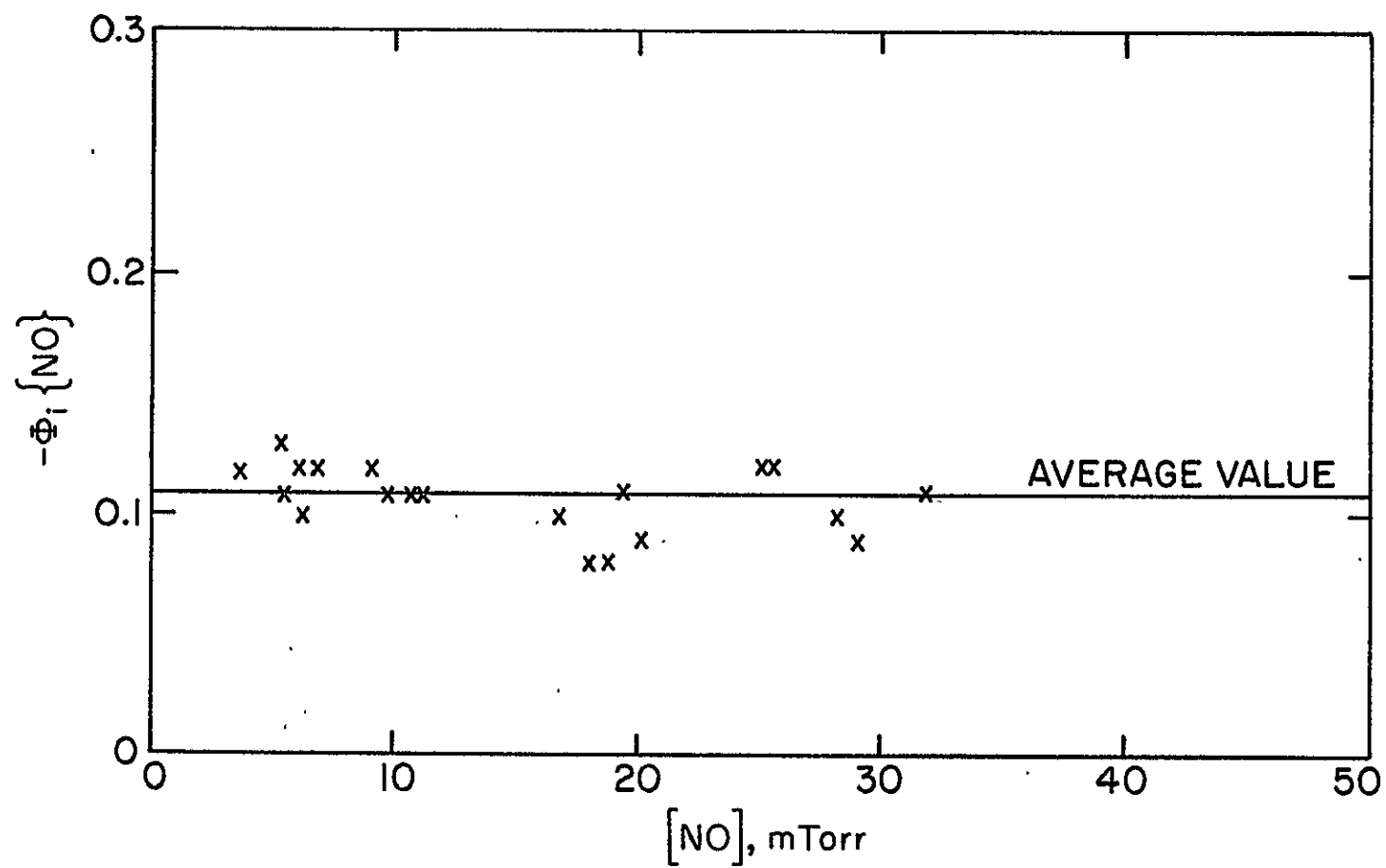
Figure 26. Plot of $-\Phi_i\{NO\}$ vs. [NO]
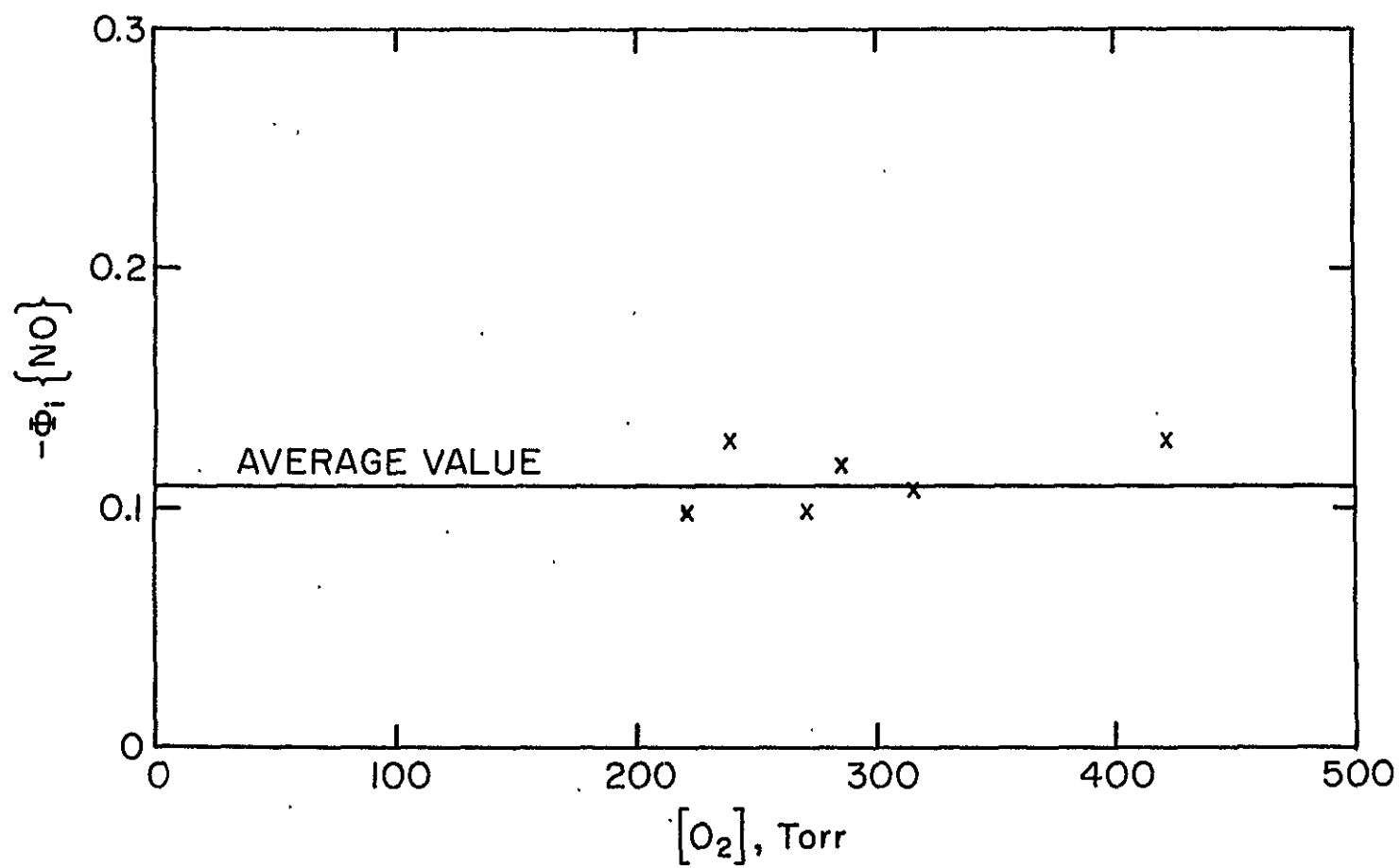
Figure 27. Plot of $-\Phi_i\{NO\}$ vs. $[O_2]$ at 298°K

This effect is shown in Table 14. Note that the limiting value of $-\Phi_i\{NO\}$ with no O_2 present is small but not zero. Table 14 also shows that $-\Phi_i\{NO\}$ is reduced if the total pressure is increased while maintaining a constant O_2 pressure.

C.   Discussion

On the basis of the experimental results, the following mechanism for the photolysis of chlorine in the presence of O_2 and small amounts of NO at 298°K is proposed.

$$Cl_2 + h\nu \ (366 \ nm) \rightarrow 2Cl \qquad\qquad Rate = I_a$$

$$Cl + O_2 + M \rightleftarrows ClOO + M \qquad\qquad 31, \ -31$$

$$ClOO + NO \rightarrow ClO + NO_2 \qquad\qquad 20a$$

$$\rightarrow ClNO + O_2 \qquad\qquad 20b$$

$$ClO + NO \rightarrow NO_2 + Cl \qquad\qquad 16$$

$$Cl + NO + M \rightarrow ClNO + M \qquad\qquad 32$$

$$Cl + ClNO \rightarrow Cl_2 + NO \qquad\qquad 33$$
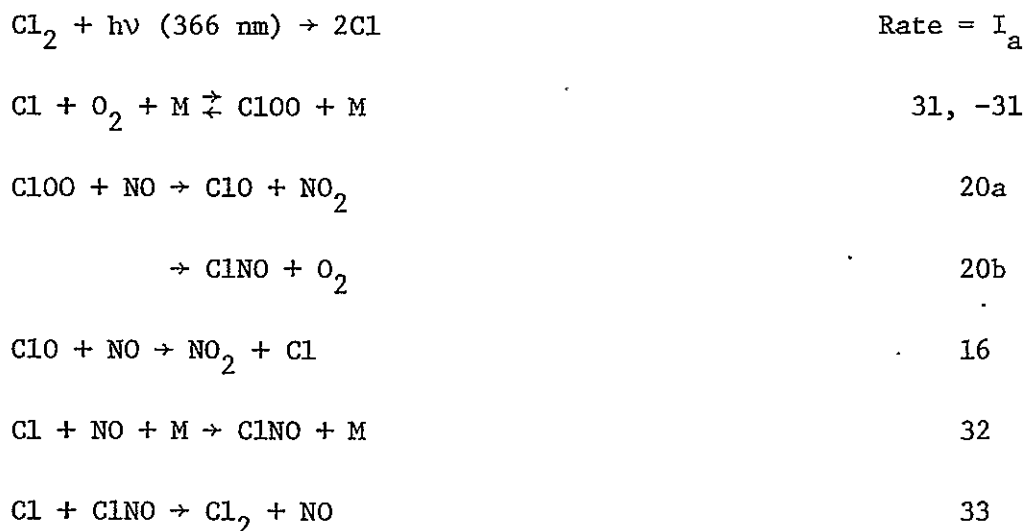
Reactions 31, −31, 16, 32, and 33 are well known, having been reported previously by Watson (41) and Hampson and Garvin (97). Reaction 20a is proposed to account for the observed NO removal, and reaction 20b is a possibility which must be considered. An analysis of the above mechanism leads to the following steady state expression for the radicals in the system.

$$[ClOO]_{ss} = K_{31,-31}[O_2][Cl]_{ss} \qquad\qquad XXIII$$

$$[ClO]_{ss} = \frac{K_{31,-31}k_{20a}[O_2][Cl]_{ss}}{k_{16}} \qquad \text{XXIV}$$

$$[Cl]_{ss} = \frac{I_a}{K_{31,-31}k_{20b}[O_2][NO] + k_{32}[NO][M]} \qquad \text{XXV}$$

The initial NO removal quantum yield under steady state conditions is expressed in equation XXVI.

$$-\Phi_i\{NO\} = \frac{2K_{31,-31}k_{20a}[O_2]}{K_{31,-31}k_{20b}[O_2] + k_{32}[M]} \qquad \text{XXVI}$$

where $[M] \simeq [O_2] + [N_2]$, and $K_{31,-31}$ is the equilibrium constant for reaction 31.

In deriving equation XXVI, Cl, ClOO, ClO, and ClNO were assumed to be in their steady states. The Cl, ClOO, and ClO radicals reach their steady state values almost instantaneously. The lifetime of ClNO can be calculated from equation XXVII.

$$\tau_{ClNO} = 1/k_{33}[Cl] \qquad \text{XXVII}$$

From equation XXV, the steady state value of Cl atoms is inversely proportional to [NO]. To calculate the longest possible lifetime of ClNO, the highest NO value was used. The result shows that the lifetime of ClNO can be as long as 2 sec. The minimum time interval over which the initial rates were measured was at least 30 sec, thus the assumption of the steady state for ClNO is a good approximation.

Equation XXVI predicts that $-\Phi_i\{NO\}$ should be independent of I_a, [NO], and $[O_2]$ when $[M] = [O_2]$. Due to the addition of N_2, the value of $-\Phi_i\{NO\}$ should decrease as [M] increases. These predictions

are completely consistent with the observed data (see Figures 25, 26,

and 27). Equation XXVI also predicts that the value of $-\Phi_i\{NO\}$

should approach zero as $[O_2]$ approaches zero. Although the $-\Phi_i\{NO\}$

in the absence of O_2 is low, it is not zero. As shown in Table 14,

$-\Phi_i\{NO\}$ ranges from 0.015 to 0.033. The residual NO removal process

may be attributed to hydrocarbon impurities in the N_2 and the small

amount of O_2 present in the N_2. The mechanism for this residual NO

removal process is as follows:

$$Cl + RH \rightarrow \dot{H}Cl + R \qquad\qquad 34$$

$$R + O_2 \rightarrow RO_2 \qquad\qquad 35$$

$$RO_2 + NO \rightarrow RO + NO_2 \qquad\qquad 36$$

$$RO + NO \rightarrow RONO \qquad\qquad 37$$

$$Cl + NO + M \rightarrow ClNO + M \qquad\qquad 32$$

$$Cl + ClNO \rightarrow Cl_2 + NO \qquad\qquad 33$$
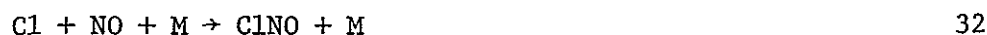
The expression for the residual NO removal quantum yield $-\Phi_0\{NO\}$ is:

$$-\Phi_0\{NO\} = \frac{4k_{34}[RH]}{k_{34}[RH] + 2k_{32}[NO][M]} \qquad\qquad XXVIII$$

If RH is CH_4, then at 300°K k_{34} is 1.1×10^{-13} cm^3sec^{-1} and k_{32} is

1.1×10^{-31} cm^6sec^{-1} as reported by Hampson and Garvin (97). This

reaction sequence could account for $-\Phi_0\{NO\} = 0.11$ when CH_4 present

in the N_2 is 2.5 ppm. This is the level of CH_4 detected in the

chromatographic analysis of N_2. This problem does not occur when O_2

is used in place of N_2 since the O_2 was made free of all hydrocarbons

as described in Section A.1. Equation XXVIII predicts that $-\Phi_i\{NO\}$

is [NO] dependent because the hydrocarbons are competing with NO

for Cl atoms. However in the absence of hydrocarbon impurities, that

is when the O_2 was used in place of the N_2, the NO removal quantum

yield would be independent of [NO] as predicted by equation XXVI.

When N_2 was used as a carrier gas, the measured quantum yields were

corrected by subtracting the residual quantum yield, $-\Phi_0\{NO\}$ as in

equation XXIX.

$$-\Phi_c\{NO\} = [-\Phi_i\{NO\}] - [-\Phi_0\{NO\}] \qquad\qquad XXIX$$

An alternative possibility for consuming NO in this system is

the sequence:

$$Cl + ClOO \rightarrow Cl_2 + O_2 \qquad\qquad 38a$$

$$\rightarrow 2ClO \qquad\qquad 38b$$

$$ClO + NO \rightarrow NO_2 + Cl \qquad\qquad 16$$

$$Cl + NO + M \rightarrow ClNO + M \qquad\qquad 32$$

$$Cl + ClNO \rightarrow Cl_2 + NO \qquad\qquad 33$$

This mechanism assumes that all ClOO radicals react with Cl atoms

through reaction 38 and reaction 16 is the only reaction responsible

for NO comsumption. If reactions 38a and 38b were important under

these conditions, then $\Phi_i\{NO\}$ would depend on I_a due to the radicals

recombining in reaction 38. The NO removal quantum yield would also

depend on [NO] because the ClOO radicals were competing with NO for

Cl atoms. These predictions are contrary to the observations. The

rate of NO consumption due to reaction 16 alone can be calculated from equation XXX.

$$\frac{-d[NO]}{dt} = 2k_{38b}K_{31,-31}[O_2][Cl]^2 \; cm^{-3}sec^{-1} \qquad\qquad XXX$$

where $k_{38b} \simeq 1.4 \times 10^{-12} \; cm^3sec^{-1}$ (97), $k_{31} = 5.6 \times 10^{-33} \; cm^6sec^{-1}$ (41), and $k_{-31} = 1.14 \times 10^{-14}$ or $1.15 \times 10^{-15} \; cm^3sec^{-1}$ (41). The results show that the rate of NO consumption due to reaction 16 alone is 50-100 times slower than the observed rate.

The competition between reaction 33 and the photodissociation of ClNO as in reaction 39 was also considered.

$$ClNO + h\nu \; (366 \; nm) \rightarrow Cl + NO \qquad\qquad 39$$

The ratio of the photodissociation rate and the rate of reaction 33 is given in equation XXXI.

$$\frac{R_{39}}{R_{33}} = \frac{\sigma \cdot I_a \cdot \ell}{k_{33}[Cl]} \qquad\qquad XXXI$$

where the absorption cross section for ClNO at 366 nm, $\sigma \simeq 4 \times 10^{-20} \; cm^3$ (41), the photolysis path, ℓ, = 10 cm, and $k_{33} = (3.0 \pm 0.5) \times 10^{-11} \; cm^3sec^{-1}$ at 298°K (41). The result shows that the photolysis rate of ClNO is at least three orders of magnitude less than the rate of ClNO with Cl atoms. Equation XXVI may be rearranged to:

$$[-\Phi_i\{NO\}]^{-1} = \frac{k_{20b}}{2k_{20a}} + \frac{k_{32}}{2k_{20a}K_{31,-31}} + \frac{k_{32}[N_2]}{2k_{20a}K_{31,-31}[O_2]} \qquad XXXII$$

A plot of $[-\Phi_i\{NO\}]^{-1}$ vs $[N_2]/[O_2]$ should be linear with a slope of

$k_{32}/2k_{20a}K_{31,-31}$ and an intercept of $k_{20b}/2k_{20a} + k_{32}/2k_{20a}K_{31,-31}$.

Figure 28 shows that the plot is reasonably linear and gives

$k_{20b}/k_{20a} = 11.0 \pm 2.1$ and $k_{32}/k_{20a}K_{31,-31} = 7.2 \pm 1.6$. In

evaluating k_{20b}/k_{20a} we have implicitly assumed that for reaction 32,

the efficiency of O_2 and N_2 are equal as third bodies. It was found

that $k_{20a}K_{31,-31} = (1.5 \pm 0.6) \times 10^{-32}$ cm^6sec^{-1} and $k_{20b}K_{31,-31} =$

$(1.6 \pm 1.0) \times 10^{-31}$ cm^6sec^{-1} at 298°K, using $k_{32} = (1.1 \pm 0.2) \times 10^{-31}$

cm^6sec^{-1} ($M = N_2$) (97).

The total third order rate coefficient for the combination of

Cl and NO with O_2 as the third body can be obtained by considering

two mechanisms. In the first mechanism, the termolecular process

may be divided into two steps: the combination of Cl and NO and

the subsequent stabilization by a third body, O_2. The presence of

the third body provides a means to remove the energy released and

stabilize the molecule formed from the combination of Cl and NO.

Cl + NO → ClNO*

ClNO* + M → ClNO + M
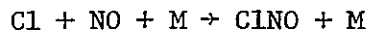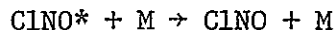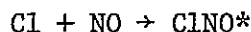
Cl + NO + M → ClNO + M   32

where $M = O_2$.

In the second mechanism, the net reaction 32 occurs via the

ClOO intermediate as the following:
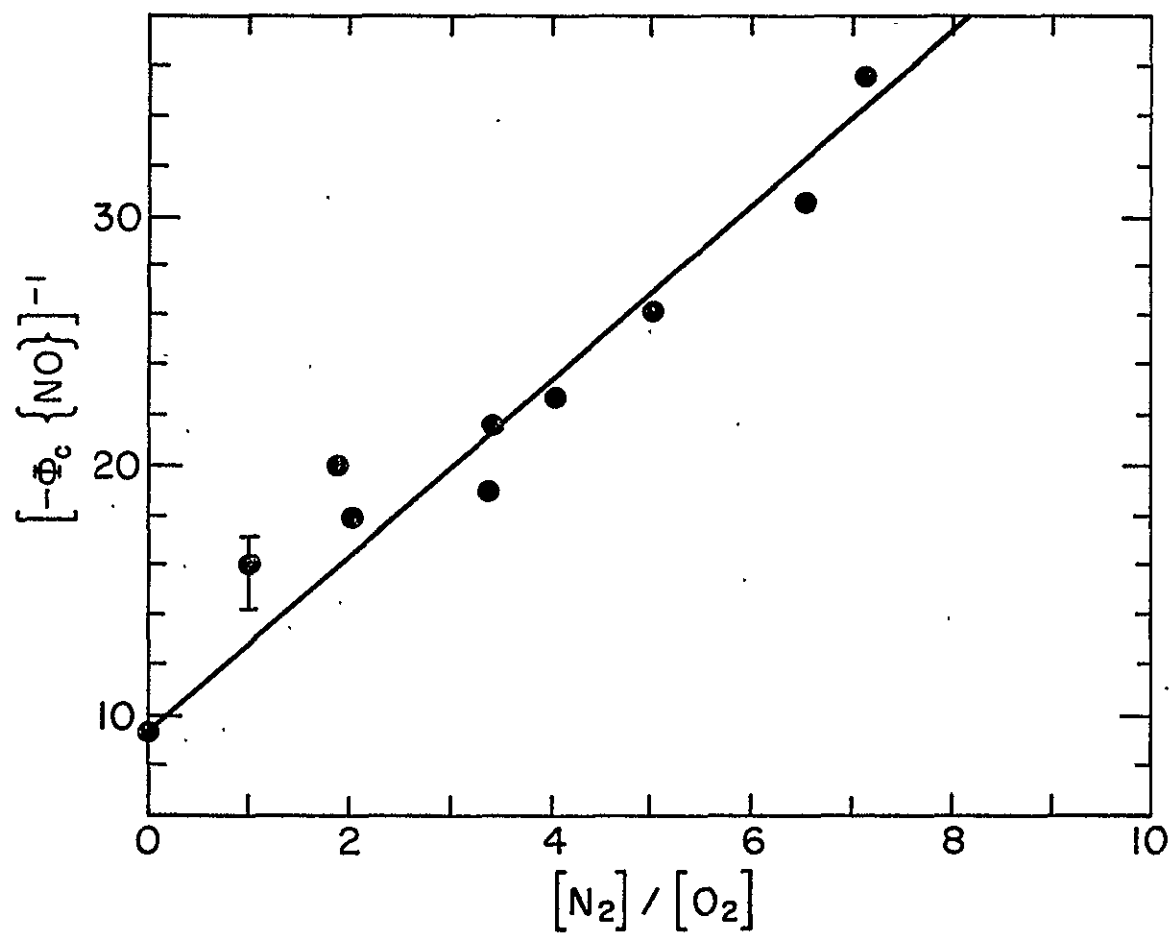
Figure 28. Plot of $[-\Phi_i\{NO\}]^{-1}$ vs. $[N_2]/[O_2]$. The point at $[N_2]/[O_2] = 0$ is the average $-\Phi_i^2\{NO\}$ of all the runs in the absence of N_2.

$$Cl + O_2 + M \rightarrow ClOO + M \hspace{3cm} 31, -31$$

$$ClOO + NO \rightarrow ClNO + O_2 \hspace{3cm} 20b$$

$$Cl + NO + M \rightarrow ClNO + M \hspace{3cm} 32$$

where $M = O_2$. The third order rate coefficient for the second

mechanism, $k_{20b}K_{31,-31}$, is $(1.6 \pm 1.0) \times 10^{-31}$ $cm^6 sec^{-1}$ from our

results. The total third order rate coefficient for the combination

of Cl and NO with O_2 as a third body is the sum of k_{32} from the

first mechanism and $k_{20b}K_{31,-31}$ which is $(2.7 \pm 1.0) \times 10^{-31}$ $cm^6 sec^{-1}$.

The value of k_{32} used for this calculation is $(1.1 \pm 0.2) \times 10^{-31}$

$cm^6 sec^{-1}$ for $M = N_2$ (97), assuming the efficiency of O_2 and N_2 are

the same. The value of the total third order rate coefficient is

a factor of 2.1 larger than the value $(1.3 \pm 0.3) \times 10^{-31}$ $cm^6 sec^{-1}$

determined by Clark et al. (98), using a low pressure flow discharge

system. However, within the stated error limits the two values

nearly overlap.

The ratio of $[ClNO]_{ss}/[NO]$ was calculated from equation XXXIII.

$$\frac{[ClNO]_{ss}}{[NO]} = \frac{k_{20b}K_{31,-31}[O_2] + k_{32}[M]}{k_{33}} \hspace{2cm} XXXIII$$

Using the values of $k_{20b}K_{31,-31} = 1.6 \times 10^{-31}$ $cm^6 sec^{-1}$, $k_{33} = 3 \times 10^{-11}$

$cm^3 sec^{-1}$ (41), and $k_{32} = 1.1 \times 10^{-31}$ $cm^6 sec^{-1}$ (97), the ratio of

$[ClNO]_{ss}/[NO]$ was calculated to be 0.15. Since the lifetime of ClNO

is approximately 2 sec, the NO profile should have a rapid drop by

15% of the initial [NO] within 2 sec. This is because NO is tied up

in ClNO due to reaction 32 for approximately 2 sec before ClNO reacts

further with Cl atoms to regenerate NO as in reaction 33. This drop

is not observed in the NO profiles (see Figure 24). The 15% drop in NO may be too small for us to have detected, or else the reported value for k_{33} may be in error by about a factor of two.

Figure 24 shows that the reaction rate decreases as the reaction proceeds. Presumably this inhibition is due to the reaction of NO_2 produced in reaction 20a with Cl atoms by way of the known reaction

$$Cl + NO_2 + M \rightarrow ClONO + M \qquad 22a$$

$$\rightarrow ClNO_2 + M \qquad 22b$$

which has a third order rate coefficient of 7.2×10^{-31} $cm^6 sec^{-1}$ reported by Watson (41). Analysis of the fall in the rate indicates that under our conditions, reaction 22 is too slow to influence the initial rate measurements.

D. Atmospheric Implications

In order to approximate the importance of reactions 20a and 20b in the stratosphere, the rates of reactions 20a and 20b were compared with the rates of reactions 10 and 21 in the 15 km region where the maximum effect is expected.

$$Cl + O_3 \rightarrow ClO + O_2 \qquad 10$$

$$HO_2 + NO \rightarrow HO + NO_2 \qquad 21$$

The ratios of the reaction rates are expressed in equations XXXIV and XXXV.

$$\frac{R_{20}}{R_{10}} = \frac{K_{31,-31}k_{20}[O_2][NO]}{k_{10}[O_3]}$$

XXXIV

$$\frac{R_{20}}{R_{21}} = \frac{K_{31,-31}k_{20}[Cl][O_2]}{k_{21}[HO_2]}$$

XXXV

In these computations our values of $k_{20a}K_{31,-31}$ and $k_{20b}K_{31,-31}$ at 298°K were employed in conjunction with the maximum values of $K_{31,-31}$ given by Watson (41). The rate coefficient data were also taken from Watson (41) and Hampson and Garvin (97). A Cl density of approximately 3×10^5 cm^{-3} was estimated at 15 km from the ClO densities measured by Hudson (99) and from the ratio of [Cl]/[ClO] given in equation XXXVI.

$$\frac{[Cl]}{[ClO]} = \frac{k_{17}[NO]}{k_{10}[O_2]}$$

XXXVI

The other pertinent concentrations were taken to be $[HO_2] = 2 \times 10^7$ cm^{-3}, $[NO] = 2 \times 10^9$ cm^{-3} and $[O_3] = 1 \times 10^{12}$ cm^{-3}.

The results show that at 15 km reactions 10 and 21 are about 400 and 100 times more important than reaction 20a. Reaction 20b is about 11 times more important than 20a, but under stratospheric conditions, the product ClNO is rapidly photodissociated to regenerate Cl and NO as in reaction 39. Therefore, it is concluded that reaction 20a and 20b are probably not important in the earth's atmosphere.

Chapter 4

THE Cl_2-NO_2-M SYSTEM: THE MECHANISM OF THE $Cl-NO_2$-M REACTION

AND THE KINETIC STUDY OF CHEMILUMINESCENCE IN THE $Cl-NO_2-O_3$ REACTION

A. Experimental

A.1. Materials and Their Purification

The NO_2 and Cl_2 were obtained from Matheson Gas Products. Cl_2

was purified by the distillation method described in Chapter 2 Section

A.1. NO_2 was purified by the method described by Stockburger ét al.

(100). Fifty to one hundred Torr of NO_2 with 600 Torr of O_2 was

repeatedly frozen at $-196°C$ and then warmed to room temperature until

the blue color of N_2O_3 disappeared. The mixture was then condensed

in a trap in $-196°C$, and the O_2 pumped out. Since the concentration

of NO_2 needed in our experiment was on the order of 50 mTorr, only

a few Torr of purified NO_2 diluted with 500-600 Torr of O_2 and N_2

was used. This dilute NO_2 mixture enabled us to measure the pressure

accurately. The dilute NO_2 mixture was kept in the dark at room

temperature.

Chlorine nitrite, ClONO, was prepared in the reaction cell by

mixing Cl_2O with ClNO at low temperature as reported by Molina and

Molina (49).

Chlorine monoxide, Cl_2O, was prepared from a procedure by

Schack and Lindahl (101). Freshly baked HgO (yellow form) was added

into a U-shaped Pyrex tube packed with glass beads. The beads served

to increase the reaction surface. Excess Cl_2 was condensed into this

U-tube and allowed to react overnight at -78°C. The product was separated from unreacted Cl_2 by distillation from -117°C to -196°C. The Cl_2O, a red solid, remained in the -117°C trap. Its gas phase UV spectrum taken on a Cary 14 spectrophotometer was in agreement with the Cl_2O spectrum reported by Lin (70).

The purity of the Cl_2O was determined by the following procedure. The Cl_2O was photolyzed at 366 nm using a medium pressure Hg lamp (Hanovia 404101).

$$2Cl_2O + h\nu \rightarrow 2Cl_2 + O_2$$
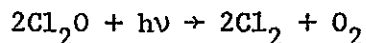
After photolysis, the UV spectrum of the only condensable product, Cl_2, was obtained. The concentration of the Cl_2 produced was calculated using the known absorption cross section at 400 nm. It was found that the Cl_2 concentration was 1.77% more than the stoichiometric ratio. Hence, the purity of Cl_2O was 98.23%, the main impurity being Cl_2.

ClNO was prepared by mixing Cl_2 with an excess of NO. The mixture was allowed to react in the dark for approximately two hours. The product was purified by distillation from -78°C to -117°C. ClNO, an orange solid, was collected at -117°C. Its gas phase infrared spectrum was obtained using a Beckman IR spectrophotometer. The product was identified as ClNO by comparing this absorption spectrum with the known spectrum (102).

N_2 and O_2 were purified by the method described in Chapter 3 Section A.1.

A.2. <u>Vacuum Line</u>

The mercury-free vacuum line described in Chapter 3 Section A.2 was used, with the addition of a section for Cl_2O preparation.

A.3. <u>Reaction Vessel and Photolysis Source</u>

The arrangements of the reaction vessel and the photolysis source are essentially the same as described previously in Chapter 3 Section A.3. A capillary tube was used which gave an evacuated leak rate of $(4.3 \pm 0.3) \times 10^{-4} \; sec^{-1}$. The total pressure drop in the reaction cell was approximately 2.6% per minute.

A.4. <u>The Analysis System</u>

The analysis system is the same as described in Chapter 3 Section A.4.

A.5. <u>Procedure</u>

In the reaction cell, mixtures of Cl_2 and NO_2 were irradiated at 366 nm. N_2 or O_2 was added to serve as a carrier gas. The experimental procedure was essentially the same as that used to determine NO by the chemiluminescent reaction with O_3 described in Chapter 3 Section A.6. Through a sampling capillary tube attached to the reaction cell, the cell contents could be leaked into a chemiluminescence chamber where they were mixed with ozonized oxygen. The resulting chemiluminescence was viewed with a photomultiplier

(EMI 9785B) through a Corning filter (CS 2-62). In one experiment a Corning filter (CS 2-64) was also used. The results were identical.

The chemiluminescence intensity was monitored continuously during irradiation and also after the radiation was terminated.

A.6. Actinometry

The absorbed light intensity, I_a, was determined by photolysis of optically equivalent amounts of NO_2 in the presence of N_2. NO is known to be a product of the photolysis as reported by Jones and Bayes (103). The NO produced was determined by the chemiluminescent reaction with O_3. The overall NO formation quantum yield for this system is 2.0.

B. Results

Mixtures of Cl_2 and NO_2 using N_2 or O_2 as a carrier gas were photolyzed at 366 nm in the reaction cell. Chemiluminescence was observed when the photolysis mixture was leaked into the chemilum-inescence chamber and mixed with ozonized oxygen. A typical emission profile is shown in Figure 29. The initial emission intensity grows rapidly and soon reaches a steady state value. If the radiation is terminated, the emission intensity decays exponentially. If the radiation is not terminated, the emission intensity eventually declines as the NO_2 is consumed.

The chemiluminescence is observed only when the photolysis is performed in the presence of both Cl_2 and NO_2, and only when the ozonizer is on. The results were independent of the carrier gas
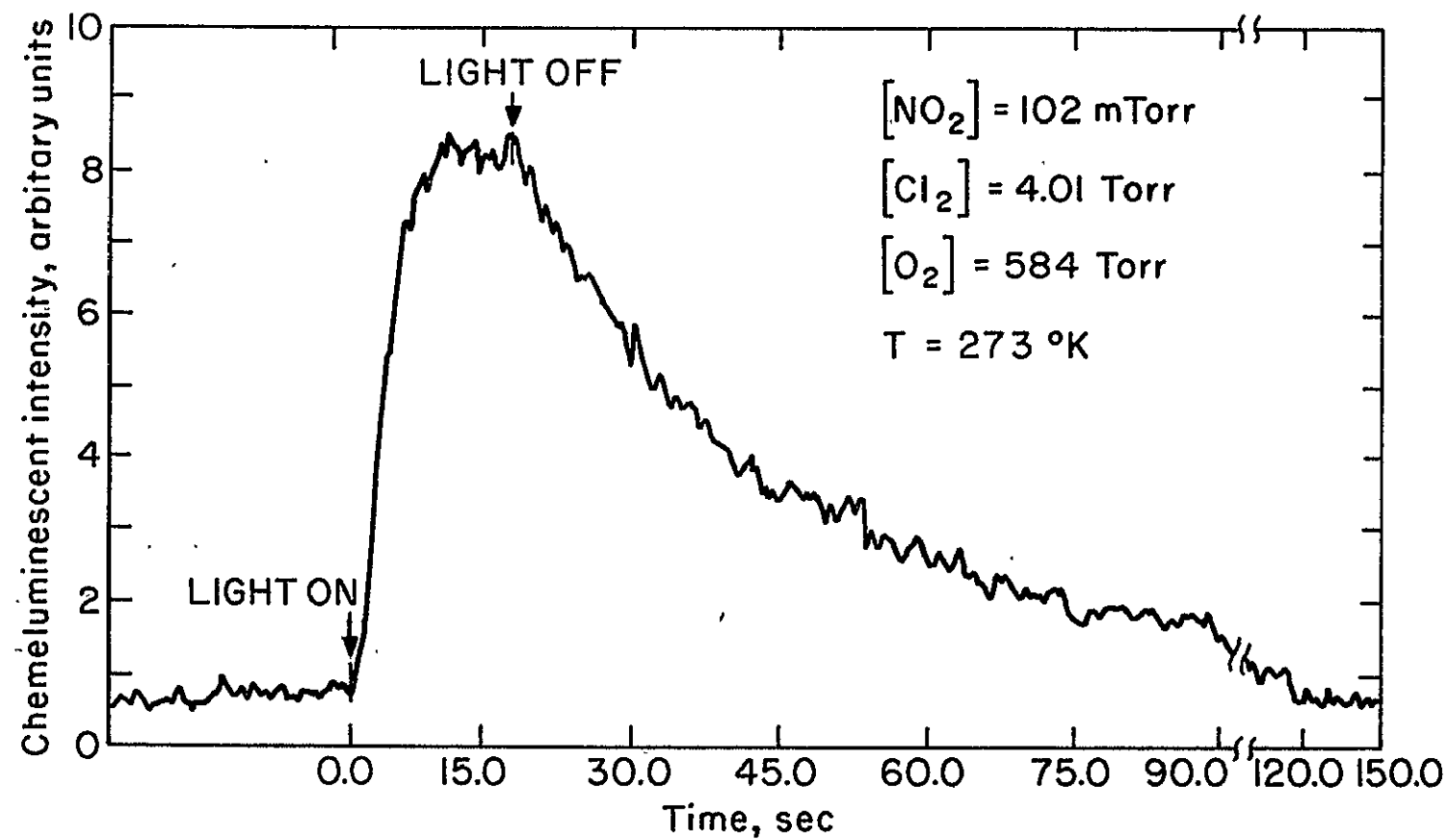
Figure 29. Light Emission Profile During and After Irradiation

used. From the known values of the absorption cross sections for Cl_2 and NO_2 (42,97), chlorine was always present at concentrations three to ten times more than that required to compete with the NO_2 photolysis. Therefore, the contribution to the total emission signal from the formation of NO due to NO_2 photolysis was negligible.

Values of $[Cl_2]$, $[NO_2]$, $[M]$, and I_a were varied over a wide range at each temperature. The results of the kinetic study are presented in Tables 15, 16, and 17 for I_a, $[NO_2]$, and $[M]$ variation at 273°K respectively. The results of the kinetic study at 238 and 219°K are presented in Tables 18 and 19 respectively. Emission could also be observed at 296°K, but the intensity was too low for any meaningful kinetic study.

The initial rates of the chemiluminescent emission were obtained from the initial slope of the emission profile. They were corrected for the electronic time constant of the measurement system which was 0.73 sec. This leads to a typical correction of 20-30%. Since the initial rates were obtained within approximately fifteen seconds of the irradiation, the correction due to the evacuation rate is negligible.

Since the absolute calibration for the emission intensity could not be obtained, the relative values are reported. Relative initial emission quantum yields for all temperatures $\Phi_i^{rel}\{I\}$, were obtained by normalizing to a value of 2.0 when NO_2 approached infinity. The reason for this normalization will be discussed in a later section.

I_a was varied by changing the Cl_2 pressure and also by using more than one filter to cut down the photolysis light intensity. The

Table 15

The Effect of I_a Variation on $\Phi_i^{rel}\{I\}$ and k_{42} at

$273 \pm 2°K$ in the Photolysis of Cl_2-NO_2-M Mixtures

[NO$_2$], mTorr	[Cl$_2$], Torr	[O$_2$], Torr	[N$_2$],[a] Torr	$10^{-13} I_a$, cm^{-3}sec^{-1}	$\Phi_i^{rel}\{I\}$	$10^2 k_{42}$, sec^{-1}
69.7	1.05	----	543.0	0.53[b]	0.44	----
67.3	3.84	603.2	----	2.09[b]	0.44	2.45
59.1	4.14	583.6	----	2.25[b]	0.51	3.22
67.0	1.05	----	543.0	2.92	0.44	3.29
54.5	8.52	470.0	----	4.63[b]	0.38	2.92
58.5	2.22	586.9	----	6.17	0.48	3.22
68.0	2.61	574.6	----	7.26	0.50	3.77
57.0	3.42	----	539.2	9.51	0.42	4.25
63.7	3.77	328.6	280.0	10.5	0.59	3.16
57.8	3.89	144.2	428.0	10.8	0.52	3.88
66.0	3.97	553.1	----	11.0	0.64	3.43
61.1	4.05	----	543.6	11.3	0.58	2.83
55.8	4.32	587.1	----	12.0	0.54	3.65
59.2	4.78	579.3	----	13.3	0.54	4.00
60.4	6.96	585.9	----	19.4	0.52	3.38
59.1	7.39	586.6	----	20.5	0.50	2.24
61.1	7.97	584.8	----	22.2	0.55	3.76

Table 15. (continued)

[a]The amounts of O_2 present in the reaction ranged from 0-5 Torr because NO_2 was stored in O_2.

[b]Two Corning CS 7-37 filters (rather than one) were used to isolate 366 nm photolysis beam.

Table 16

The Effect of [NO] Variation on $\Phi_i^{rel}\{I\}$ and k_{42}

at $273 \pm 2°K$ in the Photolysis of Cl_2-NO_2-M Mixtures

$[NO_2]$, mTorr	$[Cl_2]$, Torr	$[O_2]$, Torr	$[N_2]$,[a] Torr	10^{-13} I_a, $cm^{-3}sec^{-1}$	$\Phi_i^{rel}\{I\}$	10^2 k_{42}, sec^{-1}
32.6	1.67	---	537.7	4.67	0.28	2.94
32.6	2.26	---	537.1	6.28	0.28	3.03
33.1	2.29	---	542.1	6.37	0.30	2.42
43.7	2.73	---	543.0	7.58	0.36	3.96
47.3	4.05	495.4	---	11.3	0.42	2.44
48.2	3.28	---	535.8	9.12	0.36	4.03
50.4	1.91	---	536.6	5.30	0.39	2.98
52.6	4.24	547.6	---	11.8	0.47	2.40
55.9	4.32	587.1	---	12.0	0.54	3.65
61.1	4.05	---	543.6	11.3	0.58	2.83
65.9	3.97	553.1	---	11.0	0.64	3.43
69.3	4.40	---	539.3	12.2	0.50	4.59
70.5	4.12	---	432.4	11.5	0.58	3.89
81.5	3.73	549.4	---	10.4	0.71	4.63
99.2	3.89	527.3	---	10.8	0.89	2.69
101.8	4.01	583.9	---	11.1	0.90	3.80

Table 16. (continued)

$[NO_2]$, mTorr	$[Cl_2]$, Torr	$[O_2]$, Torr	$[N_2]$,[a] Torr	$10^{-13} I_a$, $cm^{-3}sec^{-1}$	$\Phi_i^{rel}\{I\}$	$10^2 k_{42}$, sec^{-1}
106.0	4.40	---	533.6	2.29^b	0.80	3.96
120.0	3.70	566.8	---	10.3	0.75	3.69
122.3	2.37	---	535.3	6.59	1.03	3.29
140.6	3.97	464.4	---	11.0	1.00	----
152.9	4.40	---	537.7	12.2	0.83	4.63
159.0	2.41	---	536.6	6.70	0.96	3.37

[a]The amounts of O_2 present in the reaction ranged from 0-5 Torr because NO_2 was stored in O_2.

[b]Two Corning CS 7-37 filters (rather than one) were used to isolate the 366 nm photolysis beam.

Table 17

The Effect of [M] Variation in $\Phi_i^{rel}\{I\}$ and k_{42}

at $273 \pm 2°K$ in the Photolysis of Cl_2-NO_2-M Mixtures

$[NO_2]$, mTorr	$[Cl_2]$, Torr	$[O_2]$, Torr	$[N_2]$,[a] Torr	$10^{-13}\ I_a$, $cm^{-3}sec^{-1}$	$\Phi_i^{rel}\{I\}$	$10^2\ k_{42}$, sec^{-1}
75.4	1.48	----	297.1	4.11	0.54	2.98
77.5	1.67	----	329.9	4.64	0.52	2.97
73.4	1.37	----	547.2	3.81	0.55	3.53
61.1	4.05	----	543.6	11.3	0.58	2.83
57.8	3.89	144.2	428.0	10.8	0.52	3.88
72.4	3.89	147.4	420.0	10.8	0.57	3.17
63.7	3.77	328.6	280.0	10.5	0.59	3.16
59.2	4.78	579.3	----	13.3	0.54	4.00
59.1	4.14	583.6	----	2.25[b]	0.51	3.22

[a]The amounts of O_2 present in the reaction mixtures ranged from 0-5 Torr because NO_2 was stored in O_2.

[b]Two Corning CS 7-37 filters (rather than one) were used to isolate the 366 nm photolysis beam.

Table 18

Photolysis of Cl_2-NO_2-M Mixtures at $238 \pm 1°K$

[NO_2], mTorr	[Cl_2], Torr	[N_2],[a] Torr	$10^{-13} I_a$, $cm^{-3} sec^{-1}$	$\Phi_i^{rel}\{I\}$	$10^3 k_{42}$, sec^{-1}
30.6	1.98	525.0	3.35	1.77	7.47
46.6	3.93	525.5	6.65	1.81	7.60
49.2	4.47	534.6	7.55	1.69	9.27
55.9	3.77	537.5	6.37	2.06	7.60
101.9	2.72	523.3	4.60	1.85	9.33
142.3	5.76	519.0	0.27[b]	1.93	9.09
326.4	6.15	524.3	0.29[b]	1.95	11.8
389.1	16.7	480.0	0.79[b]	1.95	8.85
532.8	6.11	518.5	0.29[b]	1.85	7.08
567.8	16.8	470.0	0.79[b]	1.55	9.33

[a] The amounts of O_2 present in the reaction mixtures ranged from 0-5 Torr because NO_2 was stored in O_2.

[b] Three Corning CS 7-37 filters (rather than one) were used.

Table 19

Photolysis of Cl_2-NO_2-M Mixtures at $219 \pm 1^\circ K$

$[NO_2]$, mTorr	$[Cl_2]$, Torr	$[N_2]$,[a] Torr	$10^{-13} I_a$, $cm^{-3}sec^{-1}$	$\Phi_i^{rel}\{I\}$	$10^3 k_{42}$, sec^{-1}
49.2	3.81	518.3	3.14	2.28	5.76
52.4	3.93	524.0	3.24	2.37	6.23
55.3	3.54	522.8	2.92	1.98	5.03
56.0	3.77	529.8	3.11	2.12	6.31
81.9	2.14	524.5	1.76	1.89	-----
96.1	1.83	513.6	1.51	2.37	6.15

[a]The amounts of O_2 present in the reaction mixtures ranged from 0-5 Torr because NO_2 was stored in O_2.

effect of varying I_a, $[NO_2]$, and total pressure, $[M]$, on $\Phi_i^{rel}\{I\}$ is shown in Figures 30, 31, and 32. It is apparent that $\Phi_i^{rel}\{I\}$ is independent of I_a and total pressure, $[M]$. However, at 273°K $\Phi_i^{rel}\{I\}$ increases with increasing $[NO_2]$ but is independent of $[NO_2]$ at lower temperatures.

Figure 29 shows that the intensity of the chemiluminescent emission decays when the radiation is terminated. Typical first order plots of the dark decay are shown in Figure 33. The plots are linear indicating that the dark decay of the chemiluminescent reaction follows first order kinetics. Presumably the decay is due to the reaction between the intermediate formed during the photolysis and the surface of the reaction vessel.

$$\text{Intermediate} \xrightarrow{\text{wall}} \text{Products} \qquad\qquad 42$$

Values of the first order decay, k_{42}, were obtained from the slope of the plots. They were corrected by subtracting off the evacuation rate. This leads to a correction of less than 10%. Since the dark decay is slow in comparison with the electronic time constant of the measurement system, the correction is insignificant. The corrected values of k_{42} are also tabulated in Tables 15-19. The average values of k_{42} at each temperature are given in Table 20. An Arrhenius plot of k_{42} is shown in Figure 34. The Arrhenius expression for k_{42} is

$$k_{42} = 46.1 \exp[-(2000 \pm 300)/T] \text{ sec}^{-1}$$

The low values of the preexponential factor and the low activation energy in k_{42} suggest that the decay of the species responsible for
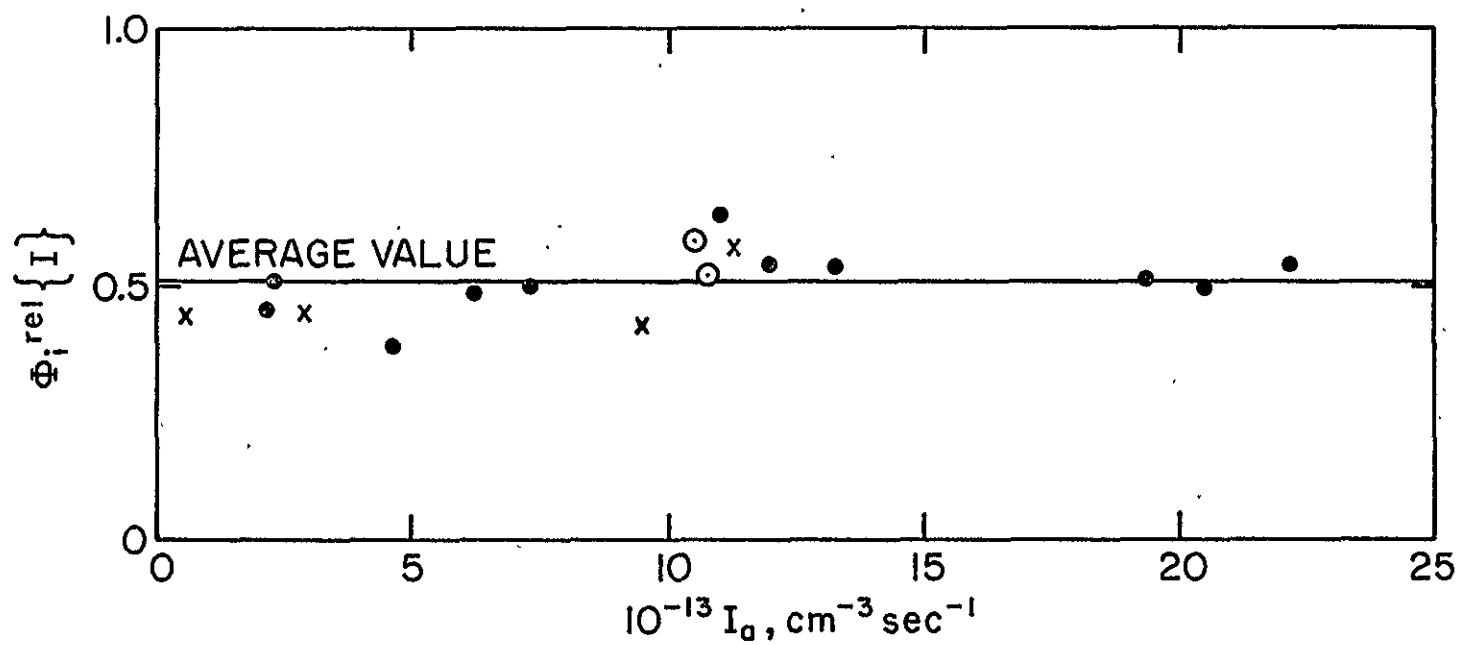
Figure 30. Plot of $\Phi_i^{rel}\{I\}$ vs. I_a in the Photolysis of Cl_2-NO_2-M Mixtures at $273 \pm 2°K$. x, values where M = N_2; ●, values where M = O_2; ☉, values where M = N_2 + O_2.
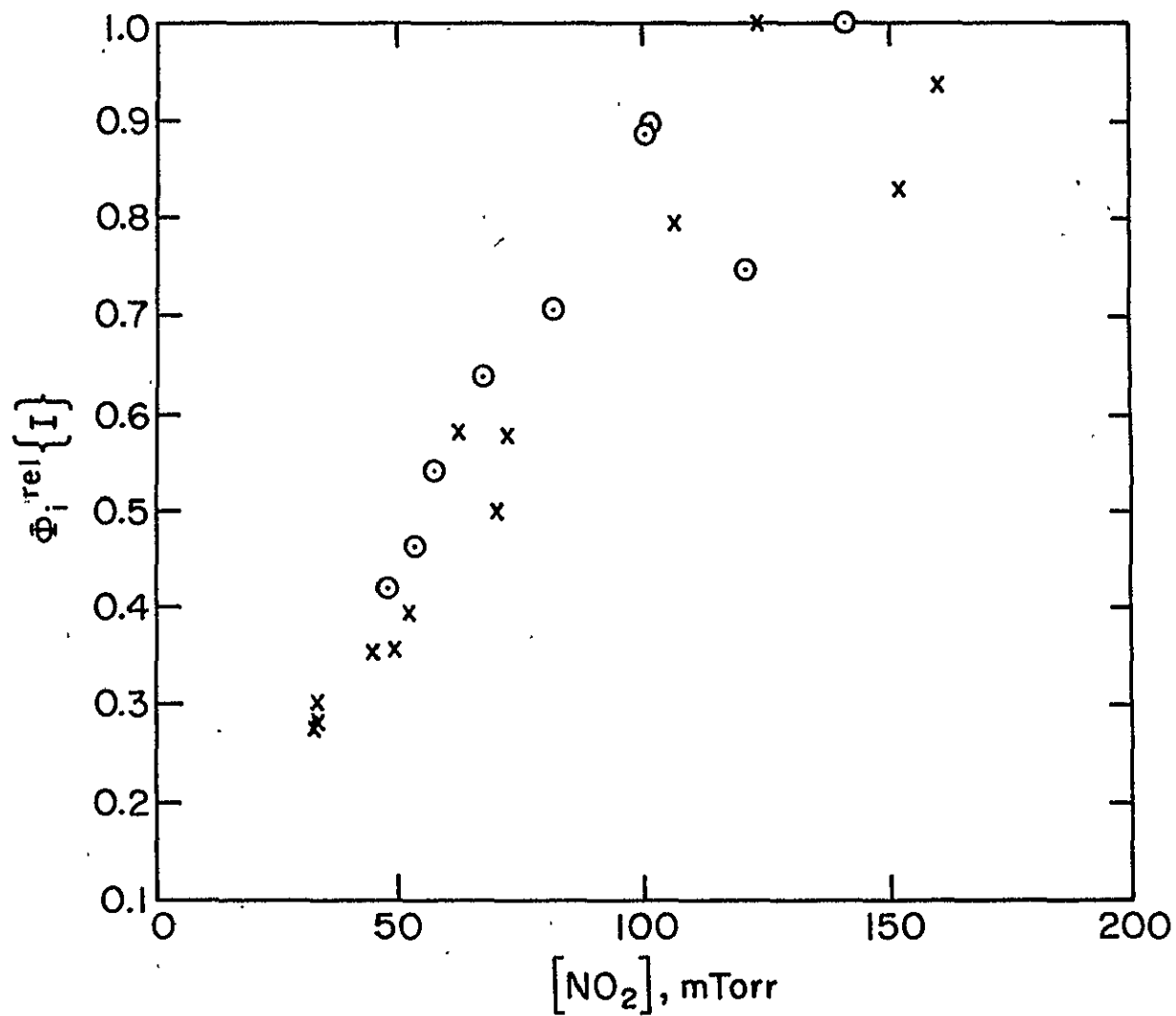
Figure 31. Plot of $\Phi_i^{rel}\{I\}$ vs. $[NO_2]$ at $273 \pm 2°K$. x, values where $M = N_2$; $\odot$, values where $M = O_2$.
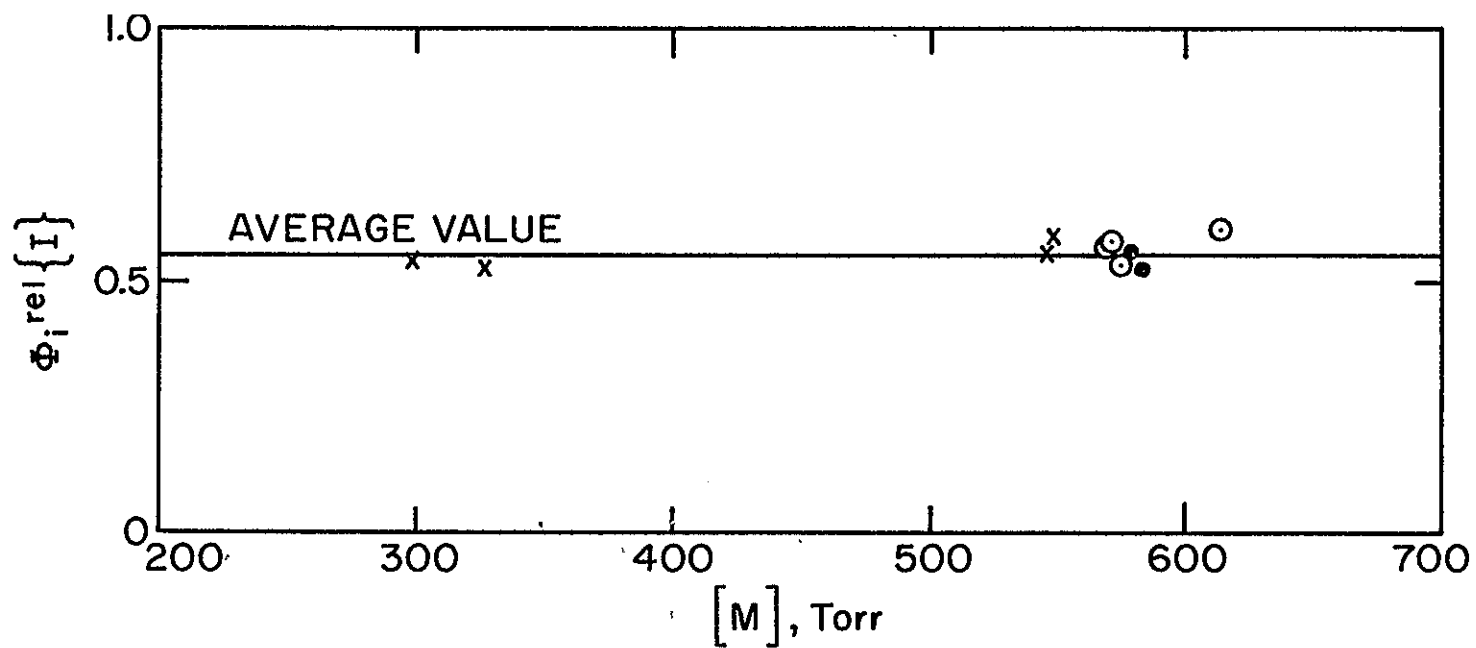
Figure 32. Plot of $\Phi_i^{rel}\{I\}$ vs. [M] in the Photolysis of Cl_2–NO_2–M Mixtures at $273 \pm 2°K$. x, values where M = N_2; ●, values where M = O_2; ⊙, values where M = $N_2 + O_2$.

Figure 33. First Order Plots for the Dark Decay of the
Chemiluminescence
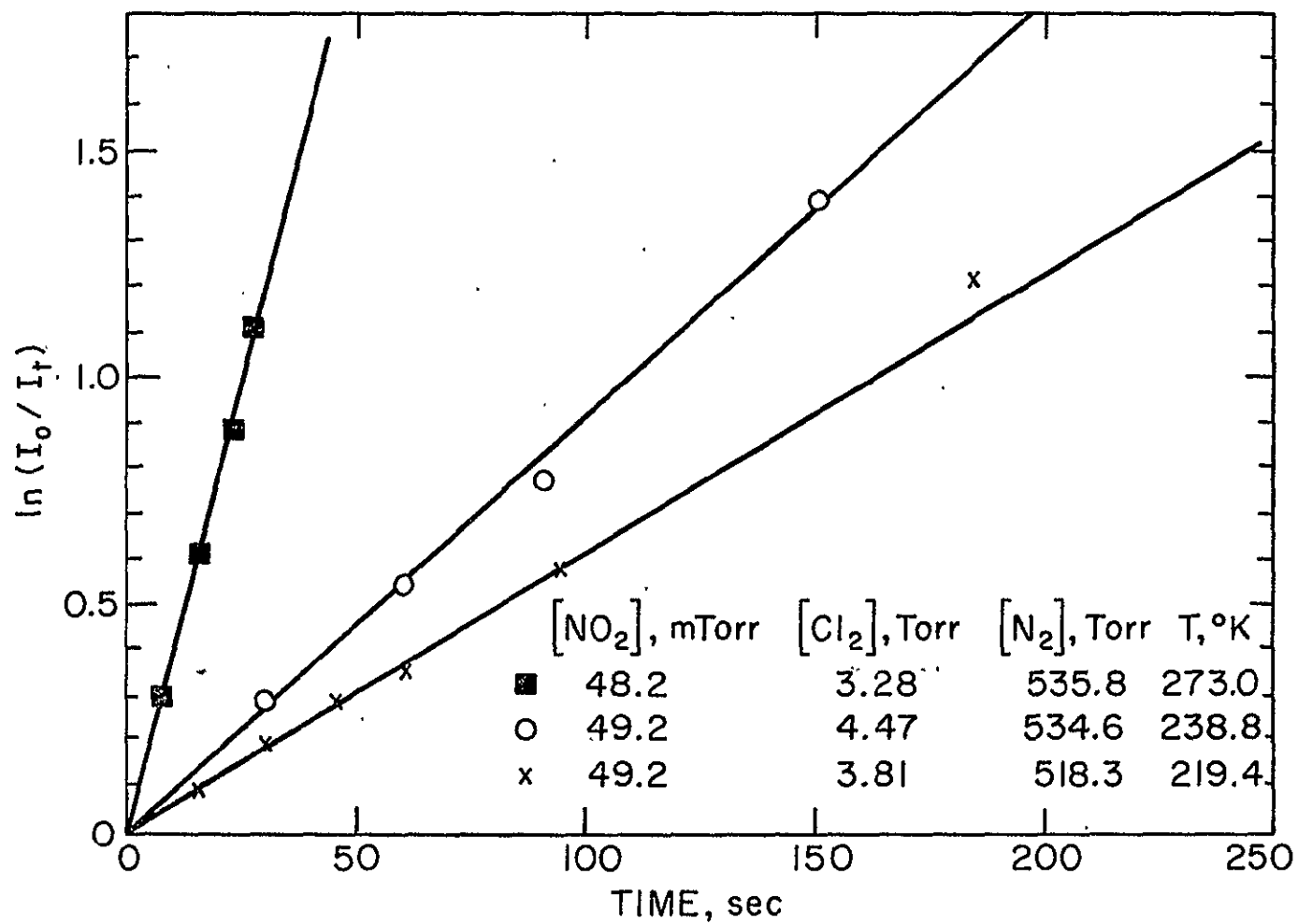
Table 20

Summary of the Average Values of the

Rate Coefficient for Reaction 42

k_{42}, sec^{-1}	T, °K
$(3.4 \pm 0.6) \times 10^{-2}$	273
$(8.74 \pm 1.38) \times 10^{-3}$	239
$(5.90 \pm 5.3) \times 10^{-3}$	219
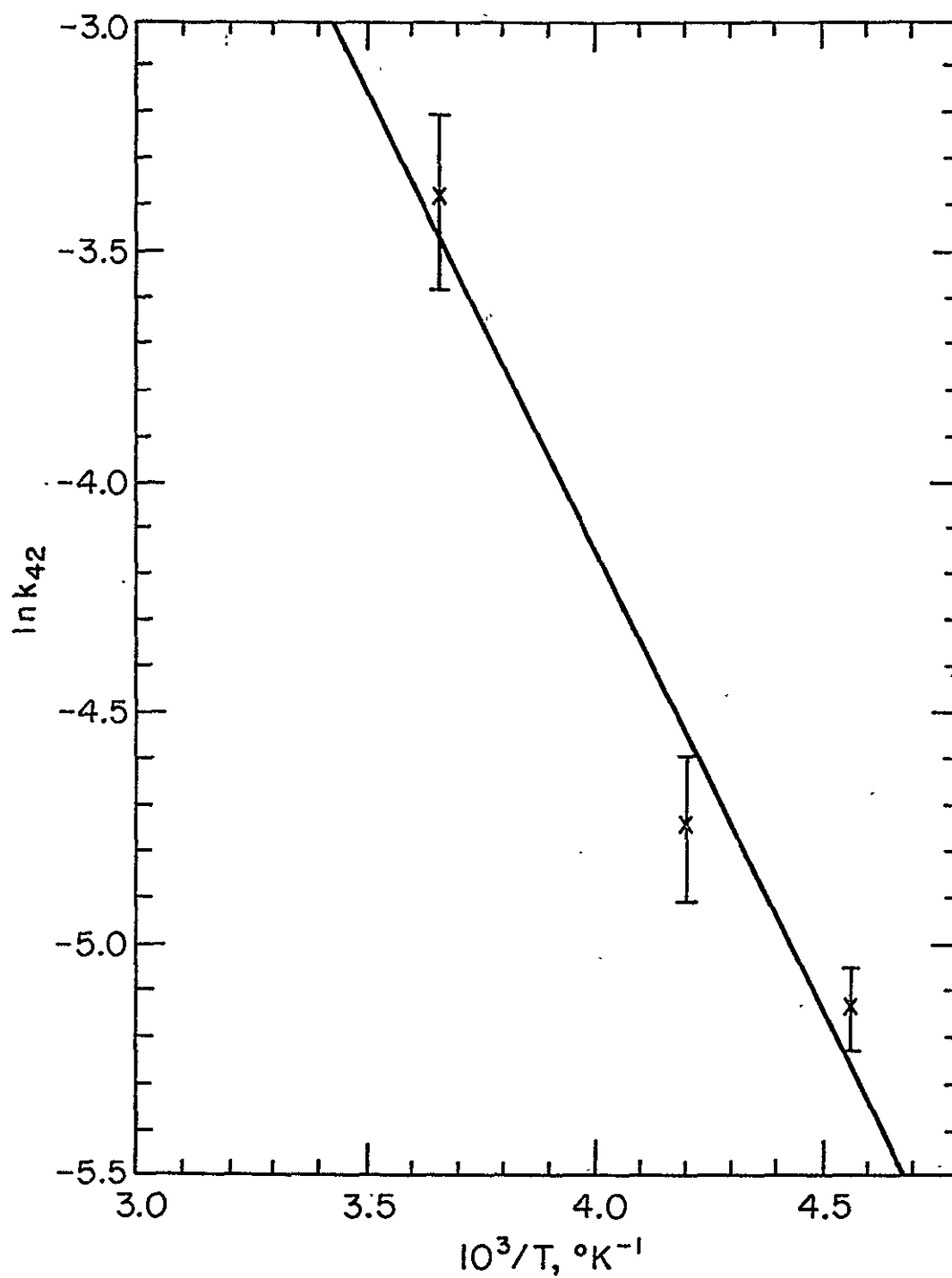
Figure 34. Arrhenius Plot of k_{42} in the Photolysis of Cl_2-NO_2-M Mixtures

the chemiluminescence is probably heterogeneous. Further evidence that the surface can influence the chemiluminescence intensity comes from attempts to prepare ClONO in the reaction cell. This will be discussed later in the Discussion section.

C. Discussion

C.1. Chemiluminescent Kinetics

All of the observations can be explained by assuming the formation of an unstable compound when Cl_2 is photolyzed in the presence of NO_2. In the chemiluminescence chamber the intermediate reacts with O_3 to produce the observed chemiluminescence. The proposed mechanism of the photolysis is the following:

$$Cl_2 + h\nu \ (366 \ nm) \rightarrow 2Cl$$

$$Cl + NO_2 + M \rightarrow ClONO + M \quad\quad\quad 22a$$

$$\rightarrow ClNO_2 + M \quad\quad\quad 22b$$

$$ClONO + NO_2 + M \rightarrow N_2O_4Cl + M \quad\quad\quad 40$$

$$ClONO \xrightarrow{\text{wall}} ClNO_2 \quad\quad\quad 41$$

$$N_2O_4Cl \xrightarrow{\text{wall}} ClNO_2 + NO_2 \quad\quad\quad 42$$
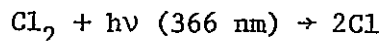
In the chemiluminescence chamber, N_2O_4Cl reacts with O_3 to produce the observed red emission.

$$N_2O_4Cl + O_3 \rightarrow Products + h\nu \ (red) \quad\quad\quad 43$$
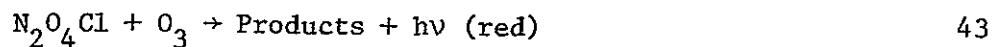
The reaction between Cl atoms and NO_2 is well·known. Clyne and White (63) using a discharge flow system, have obtained a rate coefficient of 7.2 x 10^{-31} $cm^6 sec^{-1}$ (M = N_2, at 298°K) at low pressure. Glavas et al. (104) using a competitive steady state photolysis experiment, have found a value of 2.5 x 10^{-31} $cm^6 sec^{-1}$ at 294°K and at pressure about 1 atm N_2. It is commonly assumed that the product of this reaction is nitryl chloride, $ClNO_2$ (63,64). Niki et al. (65) using a Fourier transform spectrometer method have shown that $ClNO_2$ and ClONO are the products of the photolysis mixtures. The principle product ($\geq$80%) is chlorine nitrite, ClONO, even though the formation of the ClONO isomer is less thermo-dynamically favored than $ClNO_2$ formation.

In order to account for the kinetic observation, at least a significant part of the time the product of reaction 22 is assumed to be ClONO. The formation of the intermediate responsible for the chemiluminescent reaction with O_3 is proposed to be by reaction 40, because the relative emission quantum yield is $[NO_2]$ dependent at 273°K. The intermediate $N_2 O_4 Cl$ will be referred to as I in the future.

Since $\Phi_i\{I\}$ is $[NO_2]$ dependent, it is necessary to have the competing reaction 41 for ClONO removal which is known to isomerize readily via a heterogeneous process to $ClNO_2$, (65,105). The dark decay of the chemiluminescence with a very low preexponential factor and a low activation energy requires the introduction of reaction 42.

The products of reaction 42 are very reasonable because of the proposed stoichiometry of reaction 22.

During the initial stage of photolysis in which reaction 42 is negligible, the proposed mechanism leads to the following steady state kinetic expression

$$\Phi_i\{I\} = \frac{2k_{40}(k_{22a}/k_{22})[NO_2]}{k_{41} + k_{40}[NO_2][M]}$$

XXXVII

Equation XXXI can be rearranged to yield

$$[\Phi_i\{I\}]^{-1} = \frac{k_{22}}{2k_{22a}} + \frac{k_{41}k_{22}}{2k_{40}k_{22a}[NO_2][M]}$$

XXXVIII

.Equation XXXVIII predicts that a plot of $[\Phi_i\{I\}]^{-1}$ or $[\Phi_i^{rel}\{I\}]^{-1}$ vs $[NO_2]^{-1}$ should be linear with slope/intercept = $k_{41}/k_{40}[M]$. Because the emission sensitivity for the reaction of N_2O_4Cl with O_3 is not known, absolute values of $\Phi_i\{I\}$ cannot be obtained. The relative quantum yields were normalized to the maximum possible value of $2k_{22a}/k_{22} = 2.0$ when $[NO_2] \rightarrow \infty$ as predicted by equation XXXVIII. In Figure 35, values of $[\Phi_i^{rel}\{I\}]^{-1}$ are plotted vs $[NO_2]^{-1}$ for three different temperatures. The lines are drawn with an intercept of $k_{22}/2k_{22a} = 0.50$.

At 273°K and low $[NO_2]$, the plot deviates slightly from that predicted by equation XXXVIII. However, the deviation is not sufficiently large to invalidate equation XXXVIII since the data at low $[NO_2]$ is the least accurate. Nevertheless, it is possible that the proposed mechanism is not complete or possibly ClONO is not
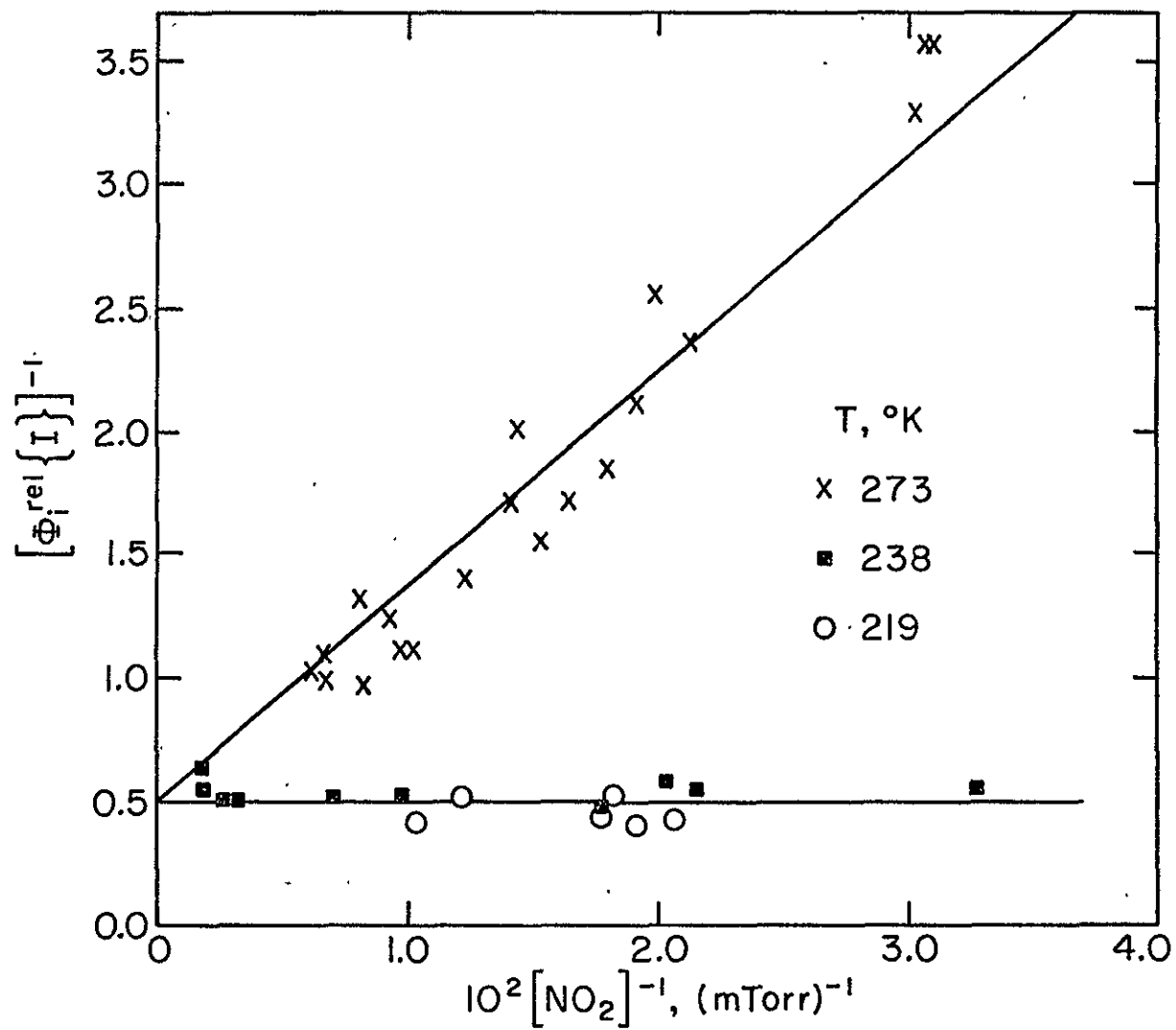
Figure 35. Plot of $[\Phi_i^{rel}\{I\}]^{-1}$ vs. $[NO_2]^{-1}$

completely in the steady state at low $[NO_2]$. At 239°K and 219°K the plot is of zero slope and of intercept 0.50. This result is consistent with the mechanism if $k_{41} \ll k_{40}[NO_2][M]$ at 239 and 219°K which is very reasonable and expected since ClONO isomerization to $ClNO_2$ has a significant activation energy (49,105). From the ratio of slope to intercept at 273°K, $k_{41}/k_{40}[M] = (6.2 \pm 0.9) \times 10^{15}$ cm^{-3} is obtained. Since reaction 41 must be slower than diffusion controlled to account for the lack of pressure dependence, k_{41} must be less than 0.6 sec^{-1}. Thus k_{40} is less than 1×10^{-16} $cm^3 sec^{-1}$.

An alternative mechanism which is kinetically indistinguishable from the proposed mechanism is

$$NO_2 + NO_2 \rightleftharpoons N_2O_4 \qquad\qquad\qquad 44,-44$$

$$N_2O_4 + Cl \rightarrow N_2O_4Cl \qquad\qquad\qquad 45$$

$$Cl + NO_2 + M \rightarrow ClONO + M \qquad\qquad 22a$$

$$\rightarrow ClNO_2 + M \qquad\qquad 22b$$

Using the literature values of k_{22} and $K_{44,-44}$ (97) the relative rate for Cl atom removal via reaction 45 and 22 is 0.02 for $NO_2 = $ 60 mTorr; thus reaction 45 is unimportant compared to reaction 22. Computation using the known value of the emission efficiency for the $NO-O_3$ reaction (93) and the relative emission efficiency for N_2O_4Cl and NO obtained in the present work shows that the emission for reaction 43 would have to be second order in NO_2 at all temperatures to account for the observed emission. Thus the mechanism involving N_2O_4 must be rejected.

C.2. The Mechanism of the Chemiluminescent Reaction

The observed chemiluminescence is probably due to the direct

production of electronically excited nitrogen dioxide, NO_2^*, or

to the production of NO in the reaction of N_2O_4Cl with O_3 (reaction

43) which then reacts with O_3 via the well-known NO-O_3 chemilum-

inescent reactions (93).

$$N_2O_4Cl + O_3 \rightarrow NO_2^* + \text{Other Products} \qquad \qquad 43a$$

$$\rightarrow NO + \text{Other Products} \qquad \qquad 43b$$

$$NO + O_3 \rightarrow NO_2^* + O_2 \qquad \qquad 5a$$

$$\rightarrow NO_2 \text{ (electronically ground state)} + O_2 \qquad 5b$$

$$NO_2^* \rightarrow NO_2 + h\nu \qquad \qquad 5c$$
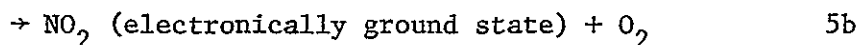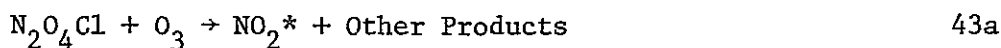
The NO-producing mechanism and the direct production of electronically

excited NO_2 in reaction 43a are kinetically indistinguishable. There

are many possible channels based upon stoichiometry for reaction 43

such as:

$$N_2O_4Cl + O_3 \rightarrow NO + ClNO_2 + 2O_2 \qquad \Delta H = -7.4 \text{ Kcal/mole} \quad 43c$$

$$\rightarrow NO + ClO_2 + NO_2 + O_2 \qquad \Delta H = 18.7 \text{ Kcal/mole} \quad 43d$$

$$\rightarrow 2NO_2 + ClO + O_2 \qquad \Delta H = 4.2 \text{ Kcal/mole} \quad 43e$$

$$\rightarrow NO + NO_3 + ClO + O_2 \qquad \Delta H = 26.9 \text{ Kcal/mole} \quad 43f$$
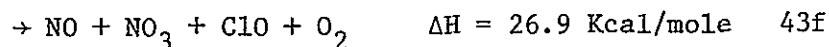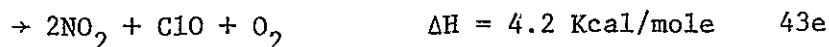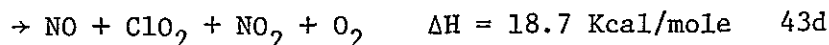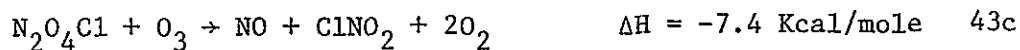
Only channel 43c appears likely to be exothermic. The heat of

formation for N_2O_4Cl is estimated to be ≥ 2 Kcal/mole by analogy with

the heat of formation for similar compounds N_2O_5 and N_2O_4. The values

for the heat of formation for ClONO and $ClNO_2$ were calculated from

the overall heat of formation for reactions 22a and 22b as reported by Niki et al. (65). For other species, the values used for the heat of formation were the values reported by Calvert and Pitts (96).

It is worth noting that if reaction 22a, 40 and 43 are combined together in the following manner

$$Cl + NO_2 + M \rightarrow ClONO + M \qquad\qquad 22a$$

$$ClONO + NO_2 + M \rightarrow N_2O_4Cl + M \qquad\qquad 40$$

$$\underline{N_2O_4Cl + O_3 \rightarrow Products \qquad\qquad\qquad\qquad} 43$$

$$Cl + 2NO_2 + O_3 \rightarrow Products \qquad\qquad \text{net reaction}$$
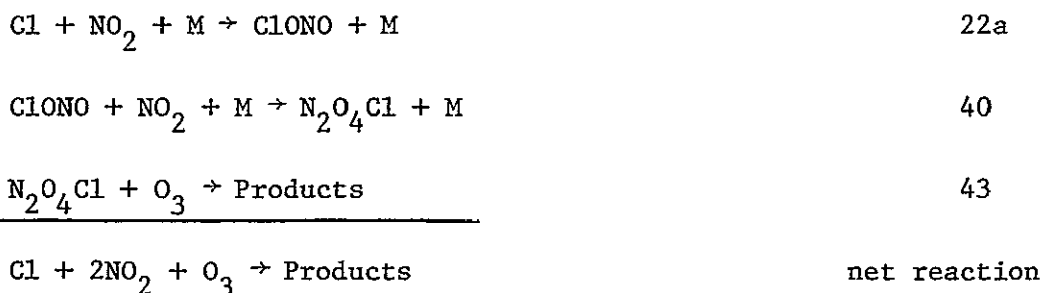
The heat of formation for the net reaction is exothermic for all of the possible channels for reaction 43. The values are -50.25, -24.20, -38.70, and -16.51 Kcal/mole for the products by reactions 43c, 43d, 43e, and 43f respectively.

Other species present in the system cannot be responsible for the emission because 1) there would be a conflict with the kinetic observations, 2) there would be an energy deficiency, or 3) the species are known not to chemiluminesce with O_3.

The reactants Cl_2 and NO_2 do not chemiluminesce with O_3 either with or without illumination at 366 nm. However NO_2 gives a weak signal due to NO formation from NO_2 photolysis. Other species such as $ClNO_2$ were considered.

$$ClNO_2 + O_3 \rightarrow ClO_2 + NO + O_2 \qquad \Delta H = 5.6 \text{ Kcal/mole} \qquad 46a$$

$$\rightarrow NO_2 + ClO + O_2 \qquad \Delta H = -8.8 \text{ Kcal/mole} \qquad 46b$$
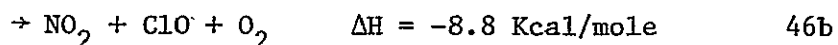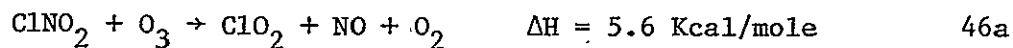
Even though some channels may be exothermic, the reactions are inconsistent with the observed kinetics. The observed results require that the emission be $[NO_2]$ dependent at 273°K.

The possibility that ClONO might be responsible for the chemiluminescent reaction with ozone was also considered. ClONO was prepared directly in the reaction cell by mixing Cl_2O and ClNO at 226°K. N_2 was added to the mixture after the reaction was carried out. The pressurized mixture was leaked out of the reaction cell to the chemiluminescence chamber and mixed with ozonized oxygen. The emission was completely suppressed. Two possible conclusions can be drawn from this experimental result. Either ClONO did not undergo a chemiluminescent reaction with ozone, or the surface of the reaction cell and the capillary were contaminated by Cl_2O or ClNO thus inhibiting the chemiluminescent reaction. The evidence that the surface can influence the chemiluminescent intensity became obvious later when there was no emission observed from the photolysis mixture of Cl_2-NO_2-M and ozonized oxygen. This experiment was performed immediately after the ClONO-O_3 experiment and under conditions in which a strong chemiluminescent emission had previously been observed. After the reaction cell was cleaned with a solution of $K_2Cr_2O_7$ and H_2SO_4 and reconditioned with several Cl_2-NO_2-M mixtures, the emission intensity recovered to its original value and became reproducible.

If the chemiluminescent reaction is due to the ClONO-O_3 reaction, the kinetics requires that the emission intensity is independent of $[NO_2]$ at any temperature. This prediction is contrary

to the observations, even though the reaction between ClONO and O_3 as in reaction 47 is exothermic.

$$ClONO + O_3 \rightarrow NO + ClO_2 + O_2 \qquad \Delta H = -4.45 \text{ Kcal/mole} \qquad 47$$

D. Atmospheric Implications

In the stratosphere, N_2O_4Cl may be formed by the following reactions:

$$ClO + NO + M \rightarrow ClONO + M \qquad 19$$

$$ClONO + NO_2 + M \rightarrow N_2O_4Cl + M \qquad 40$$

Reaction 19 was suggested by Molina and Molina (49). However, $k_{40}[M]$ is not likely to be larger than $1 \times 10^{-16} \text{ cm}^3\text{sec}^{-1}$ according to our estimation. Therefore, reaction 40 could not compete with the photodissociation of ClONO in the upper atmosphere.

Chapter 5

SUMMARY

The reactions of ozone with chlorine, oxides of chorine and

oxides of nitrogen are important in the chemistry of the stratosphere.

A general review of these reactions is given in Chapter 1 of this

thesis. Of all the interesting reactions in the stratosphere, the

research reported in this thesis dealt only with the following three

systems.

1. The Cl_2-O_3 system in which the reaction of ClO with O_3 and

the reaction of OClO with O_3 were studied.

2. The Cl_2-O_2-NO system in which the reaction between ClOO

and NO was investigated.

3. The Cl_2-NO_2-M system in which the mechanism of the $Cl-NO_2$

reaction was studied as well as the kinetics of the chemiluminescence

of the $Cl-NO_2-O_3$ reaction.

The experimental procedures, results and discussions for each

system are given in Chapters 2, 3, and 4 respectively.

The major conclusions drawn from the study of the Cl_2-O_3 system

are the following. The photolysis of Cl_2-O_3 mixtures at 366 nm

and in the temperature range 254-297°K led to the removal of O_3 and

Cl_2. The final products of the photolysis are O_2 and Cl_2O_7 with

OClO being an intermediate (76). The upper limit for the rate

coefficient of the reaction between ClO and O_3 is 1×10^{-18} cm^3sec^{-1}.

The recommended Arrhenius expression for the rate coefficient of the

reaction between OClO with O_3 is

$$k_{26} = 2.3 \times 10^{-12} \exp[-(4730 \pm 630)/T] \ cm^3 sec^{-1}$$

The low values of the rate coefficients for both reactions, ClO with O_3 and OClO with O_3, indicate that they are not important in atmospheric chemistry.

The conclusions drawn from the study of the Cl_2-O_2-NO system are the following. The photolysis of Cl_2-O_2-NO mixtures at 366 nm and at 298°K led to the formation of ClOO radicals which in turn reacted with NO via two channels.

$$ClOO + NO \rightarrow NO_2 + ClO \qquad\qquad 20a$$

$$\rightarrow ClNO + O_2 \qquad\qquad 20b$$

The ratio of k_{20b}/k_{20a} was found to be 11.0 ± 2.2. From the rate coefficients obtained in this study, it can be concluded that reactions 20a and 20b are probably not important in the stratosphere.

From the study of the Cl_2-NO_2-M system, the following conclusions can be drawn. An observed red emission when the photolysis mixtures of Cl_2-NO_2-M were mixed with a stream of ozonized oxygen, was caused by the reaction between an unstable intermediate N_2O_4Cl and O_3. One of

$$N_2O_4Cl + O_3 \rightarrow Products + h\nu \ (red) \qquad\qquad 43$$
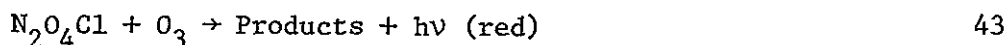
the products in reaction 43 was either electronically excited nitrogen dioxide (NO_2^*) or NO, which in turn could react further with O_3 to yield NO_2^*. The formation of N_2O_4Cl required that the major product of the Cl-NO_2-M reaction was ClONO rather than $ClNO_2$.

$$Cl + NO_2 + M \rightarrow ClONO + M \qquad\qquad 22a$$

$$\rightarrow ClNO_2 + M \qquad\qquad 22b$$

In the presence of NO_2, ClONO reacted further with NO_2 as in reaction 40 to form N_2O_4Cl

$$ClONO + NO_2 + M \rightarrow N_2O_4Cl + M \qquad\qquad 40$$

The upper limit for the second order rate coefficient of reaction 40 is 1×10^{-16} $cm^3 \cdot sec^{-1}$. Therefore, reaction 40 is too slow to compete with the atmospheric photolysis of ClONO. Thus, reaction 40 is not important in atmospheric chemistry.

Appendix I

PHASE/AMPLITUDE ADJUSTOR

The schematic circuit of the phase/amplitude adjustor is shown in Figure 36. The phase adjustor consisted of two capacitors and a variable resistor, R_1, connected in series. The phase of the signal from the two phototubes could be adjusted between 0° to 90° by the variable resistor R_1. The amplitude adjustor consisted of two fixed resistors and a variable resistor R_2 as shown in Figure 36. The amplitude of the signal from the two phototubes could be adjusted by this variable resistor.
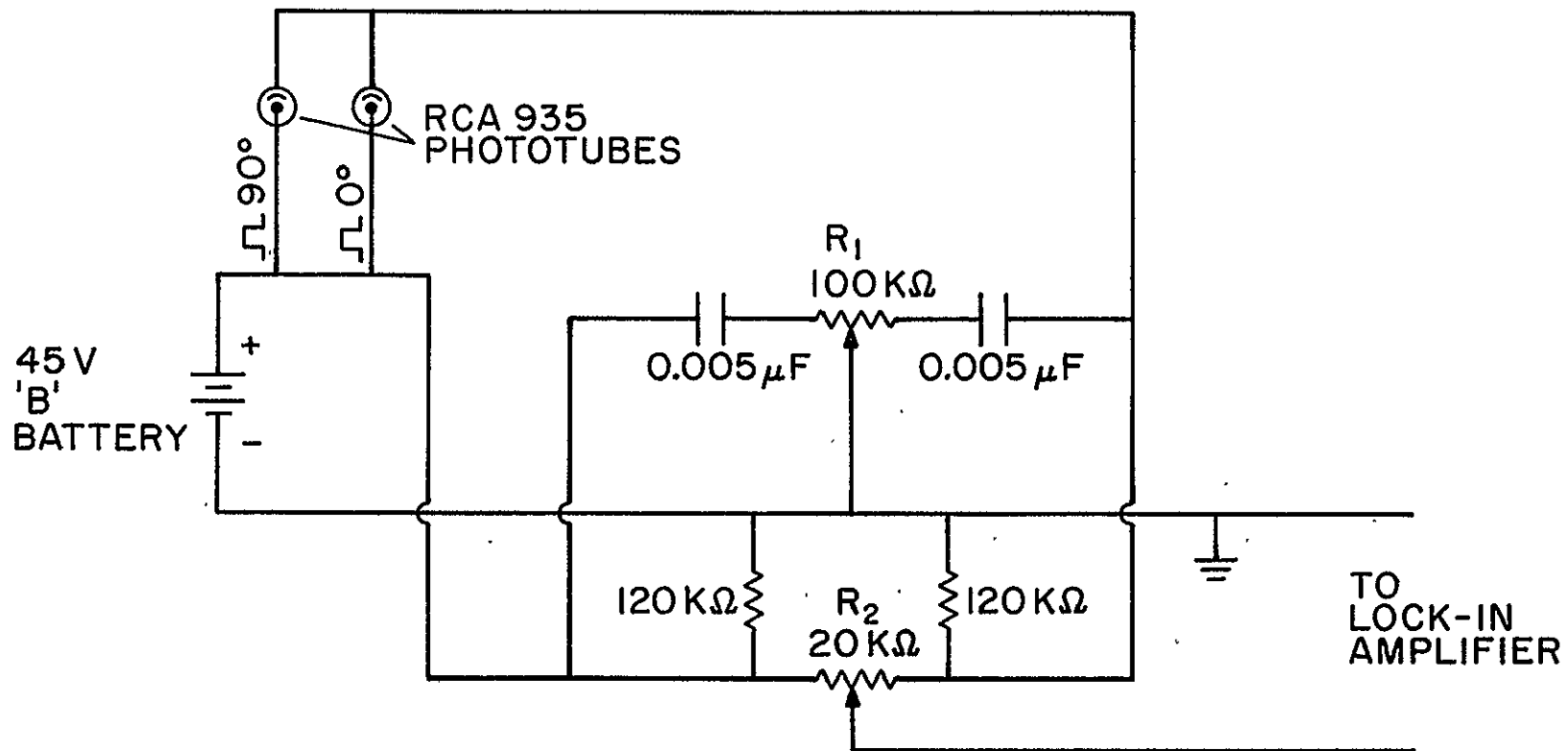
Figure 36. Circuit of the Phase/Amplitude Adjustor

Appendix II

METHOD OF SIMULATION OF THE ABSORPTION PROFILE OF OClO AND

THE EVALUATION OF THE RATE COEFFICIENTS FOR THE

EQUILIBRIUM REACTION 29

The three rate equations used to simulate the absorption of OClO are the following:

$$\frac{d[ClO]}{dt} = 2.0\ I_a + k_{-29}[M][Cl_2O_3] - k_{29}[M][ClO][OClO] -$$
$$[OClO]^2(k_{23c} + 2.0\ k_{23b}) \qquad \cdot \qquad \text{XXXIX}$$

$$\frac{d[Cl_2O_3]}{dt} = k_{29}[M][ClO][OClO] - k_{-29}[M][Cl_2O_3] \qquad \text{XXXX}$$

$$\frac{d[OClO]}{dt} = k_{23c}[ClO]^2 + k_{-29}[M][Cl_2O_3] -$$
$$k_{29}[M][ClO][OClO] - k_{26}[OClO][O_3] \qquad \text{XXXXI}$$

To derive these three equations, Cl atoms were assumed to reach the steady state value. The steady state value of Cl is given in equation I, Chapter 2. The integrated forms for equations XXXIX – XXXXI are the following:

$$[ClO]_t = [2.0\ I_a + k_{-29}[M][Cl_2O_3]_0 - k_{29}[M][ClO]_0[OClO]_0 -$$
$$\cdot \ [OClO]_0^2(k_{23c} + 2.0\ k_{23b})]\ \Delta t + [ClO]_0 \qquad \text{XXXXII}$$

$$[Cl_2O_3]_t = [k_{29}[M][ClO]_0[OClO]_0 - k_{29}[M][Cl_2O_3]_0]\ \Delta t +$$
$$[Cl_2O_3]_0 \qquad \text{XXXXIII}$$

$$[OClO]_t = [k_{23c}[ClO]_0^2 + k_{-29}[M][Cl_2O_3]_0 - k_{29}[M][ClO]_0[OClO]_0 -$$

$$k_{26}[OClO]_0[O_3]] \Delta t + [OClO]_0 \qquad\qquad\qquad XXXXIV$$

where $[x]_0$ = concentration of x at the time $t-\Delta t$, and

$[x]_t$ = concentration of x at any time t.

The above integrated equations are applicable when the time interval, Δt, is sufficiently small. Using equations XXXXII – XXXXIV, the concentrations of OClO, Cl_2O_3 and OClO at any time could be calculated.

The rate coefficients for reaction 29 and –29 were calculated using an adaptive pattern search routine (91). The routine varied the values of $k_{29}[M]$, $k_{-29}[M]$, k_{23c} and k_{26} within a specified range. For each set of rate coefficients, the error was calculated by comparing the simulated OClO profile with the experimental profile. The error at any particular time interval is defined by equation XXXXV.

$$(Error)_i = \frac{[OClO]_{calculated} - [OClO]_{experimental}}{[OClO]_{experimental}} \qquad XXXXV$$

To calculate the total square error and the average error for the whole simulated OClO profile, the following equations were used:

$$\text{Total square error} = \sum_{i=1}^{n} (Error)_i^2 \qquad XXXXVI$$

$$\text{Mean square error} = \frac{\text{Total square error}}{n} \qquad XXXXVII$$

$$\text{Average error} = (\text{Mean square error})^{1/2} \qquad XXXXVIII$$

where n = the number of intervals. The set of rate coefficients which gave the minimum average error was selected.

References

1. J. Heicklen, "Atmospheric Chemistry," Academic Press, New York, 1976.

2. K. Smith, P. Bener, M. Caldwell, F. Daniels, Jr., A. Giese, T. Goldsmith, W. Klein, J. Lee, F. Urbach, A. Zucker, and D. Holtz, "Biological Impacts of Increases Intensities of Solar Ultraviolet Radiation", National Academy of Sciences, Washington, D.C., 1973.

3. F. Urbach, D. Berger, and R. E. Davies, Proceedings of the Third Conference on Climatic Impact Assessment Program, DOT-TSC-OST-74-15, pp. 523-535, U.S. Dept. of Transportation, Washington, D.C., 1974.

4. R. E. Dickinson, Can. J. Chem., 52, 1616 (1974).

5. G. Eaton, J. Geophys. Res., 68, 521 (1963).

6. J. Cronin, Science, 172, 847 (1971).

7. R. A. Duce, J. Geophys. Res., 74, 4597 (1969).

8. P. Buat-Menard and R. Chesselet, C. R. Acad. Sci. Paris, 272, 1330 (1971).

9. M. J. Molina and F. S. Rowland, Nature, 249, 810 (1974).

10. M. J. Molina and F. S. Rowland, Geophys. Res. Lett., 1, 309 (1974).

11. M. J. Molina and F. S. Rowland, J. Phys. Chem., 79, 667 (1975).

12. F. S. Rowland and M. J. Molina, Rev. Geophys. Space Phys., 13, 1 (1975).

13. S. C. Wofsy, M. B. McElroy, and N. D. Sze, Science, 187, 535 (1975).

14. R. J. Cicerone, R. S. Stolarski, and S. Walters, Science, 185, 1165 (1974).

15. M. Nicolet and E. Vergison, Aeron. Acta, A-91 (1971).

16. P. J. Crutzen, J. Geophys. Res., 76, 7311 (1971).

17. M. B. McElroy and J. C. McConnell, J. Atmos. Sci., 28, 1095 (1971).

18. H. S. Johnston, Proc. Nat. Acad. Sci., U.S.A., 69, 2369 (1972).

19. M. Nicolet and W. Peetermans, _Ann. Geophys._, 28, 751 (1972).

20. P. Warneck, _J. Geophys. Res._, 77, 6589 (1972).

21. G. Brasseur and M. Nicolet, _Planet. Space Sci._, 21, 939 (1973).

22. M. Nicolet, _Planet. Space Sci._, 23, 637 (1975).

23. P. J. Crutzen, _Quart. J. Roy. Meterol. Soc._, 96, 320 (1970).

24. H. S. Johnston, _Science_, 173, 517 (1971).

25. P. J. Crutzen, _Can. J. Chem._, 52, 1569 (1974).

26. M. Nicolet, _Rev. Geophys. Space Phys._, 13, 593 (1975).

27. S. Chapman, _Quart. J. Roy. Meteorel. Soc._, 3, 103 (1930).

28. J. W. Birks, B. Shoemaker, T. J. Leck, and D. M. Hinton, _J. Chem. Phys._, 65, 5181 (1976).

29. D. H. Stedman and H. Niki, _J. Phys. Chem._, 77, 2604 (1973).

30. J. A. Ghormley, R. L. Ellsworth, and C. J. Hochanadel, _J. Phys. Chem._, 77, 1341 (1973).

31. P. P. Bemand, M. A. A. Clyne, and R. T. Watson, _J. Chem. Soc., Faraday Trans. II_, 70, 564 (1974).

32. K. H. Becker, U. Schurath, and H. Seitz, _Int. J. Chem. Kinet._, 6, 725 (1974).

33. A. B. Harker and H. S. Johnston, _J. Phys. Chem._, 77, 1153 (1973).

34. D. D. Davis, J. T. Herron, and R. H. Huie, _J. Chem. Phys._, 58, 530 (1973).

35. T. G. Slanger, B. J. Wood, and G. Black, _Int. J. Chem. Kinet._, 5, 615 (1973).

36. D. Marsh and J. Heicklen, _J. Phys. Chem._, 69, 4410 (1965).

37. R. K. M. Jayanty, R. Simonaitis, and J. Heicklen, _J. Photochem._, 4, 381 (1975).

38. R. Milstein and F. S. Rowland, _J. Phys. Chem._, 79, 669 (1975).

39. R. S. Stolarski and R. J. Cicerone, _Can. J. Chem._, 52, 1610 (1974).

40. S. C. Wofsy and M. B. McElroy, <u>Can. J. Chem.</u>, <u>52</u>, 1582 (1974).

41. R. T. Watson, <u>J. Phys. Chem. Ref. Data</u>, <u>6</u>, 871 (1977).

42. P. P. Bemand, M. A. A. Clyne, and R. T. Watson, <u>J. Chem. Soc.</u>, <u>Faraday Trans. I</u>, <u>69</u>, 1356 (1973).

43. M. A. A. Clyne and R. T. Watson, <u>J. Chem. Soc., Faraday Trans. I</u>, <u>70</u>, 2250 (1974).

44. M. T. Leu and W. B. DeMore, <u>J. Phys. Chem.</u>, <u>82</u>, 2049 (1978).

45. M. T. Leu, C. L. Lin, and W. B. DeMore, <u>J. Phys. Chem.</u>, <u>81</u>, 190 (1977).

46. J. W. Birks, B. Shoemaker, T. J. Leck, R. A. Borders, and L. J. Hart, <u>J. Chem. Phys.</u>, <u>66</u>, 4591 (1977).

47. F. S. Rowland, J. E. Spencer, and M. J. Molina, <u>J. Phys. Chem.</u>, <u>80</u>, 2711 (1976).

48. J. P. Jesson, P. Meakin, and L. C. Glasgow, 172nd American Chemical Society National Meeting, San Francisco, CA, 1976.

49. L. T. Molina and M. J. Molina, <u>Geophys. Res. Lett.</u>, <u>4</u>, 83 (1977).

50. F. Weigert, <u>Ann. Phy. (Leipzig)</u>, <u>24</u>, 243 (1907).

51. K. F. Bonhoeffer, <u>Z. Phys.</u>, <u>12</u>, 94 (1923).

52. M. Bodenstein, P. Harteck, and E. Padelt, <u>Z. Anorg. Allg. Chem.</u>, <u>147</u>, 233 (1925).

53. M. Bodenstein and H. J. Schumacher, <u>Z. Phys. Chem., Abt. B</u>, <u>5</u>, 233 (1929).

54. A. J. Allmand and J. W. T. Spinks, <u>Nature (London)</u>, <u>124</u>, 651 (1929).

55. A. J. Allmand and J. W. T. Spinks, <u>J. Chem. Soc.</u>, 1652 (1931).

56. A. J. Allmand and J. W. T. Spinks, <u>J. Chem. Soc.</u>, 599 (1932).

57. L. J. Heidt, G. B. Kistiakowsky, and G. S. Forbes, <u>J. Am. Chem. Soc.</u>, <u>55</u>, 223 (1933).

58. G. K. Rollefson and A. G. Byrns, <u>J. Am. Chem. Soc.</u>, <u>56</u>, 364 (1934); <u>56</u>, 1250 (1934); <u>56</u>, 2245 (1934).

59. R. G. W. Norrish and G. H. J. Neville, <u>J. Chem. Soc.</u>, 1864 (1934).

60. R. W. Davidson and D. G. Williams, J. Phys. Chem., 77, 2515 (1973).

61. M. A. A. Clyne, D. J. McKenny, and R. T. Watson, J. Chem. Soc., Faraday Trans. I, 71, 322 (1975).

62. C. L. Lin, S. Jaffe, and W. B. DeMore, paper presented at the 169th American Chemical Society National Meeting, Philadelphia, 1975; W. B. DeMore, private communication.

63. M. A. A. Clyne and I. F. White, as reported by R. T. Watson (ref. 41).

64. A. R. Ravishankara, G. Smith, and D. D. Davis, 13th Informal Conference on Photochemistry, Paper R1, Clearwater Beach, FL, 1978.

65. H. Niki, P. D. Maker, C. M. Savage, and L. P. Breitenbach, Chem. Phys. Lett., 59, 78 (1978).

66. F. E. King and J. R. Partington, J. Chem. Soc., 928 (1926).

67. R. Renaud and L. C. Lietch, Can. J. Chem., 32, 549 (1954).

68. R. K. M. Jayanty, unpublished work (1976).

69. C. F. Goodeve and B. A. M. Windsor, Trans. Faraday Soc., 32, 1518 (1936).

70. C. L. Lin, J. Chem. Eng. Data, 21, 411 (1976).

71. C. F. Goodeve and F. D. Richardson, Trans. Faraday Soc., 33, 453 (1937).

72. P. Riguad, B. Leroy, G. Le Bras, G. Poulet, J. L. Jourdain, and J. Combourieu, Chem. Phys. Lett., 46, 161 (1977).

73. M. H. Jones and E. W. R. Steacie, J. Chem. Phys., 21, 1018 (1953).

74. G. R. Hoey and K. O. Kutschke, Can. J. Chem., 33, 496 (1955).

75. F. Wenger and K. O. Kutschke, Can. J. Chem., 37, 1546 (1959).

76. W. W. Stuper, R. K. M. Jayanty, R. Simonaitis, and J. Heicklen J. Photochem., 10, 163 (1979).

77. M. S. Zahniser, F. Kaufman, and J. G. Anderson, Chem. Phys. Lett., 37, 226 (1976).

78. M. J. Kurylo and W. Braun, Chem. Phys. Lett., 37, 232 (1976).

79. M. T. Leu and W. B. DeMore, Chem. Phys. Lett., 41, 121 (1976).

80. R. T. Watson, G. Machado, S. Fischer, and D. D. Davis, J. Chem. Phys., 65, 2126 (1976).

81. M. A. A. Clyne and W. S. Nip, J. Chem. Soc. Faraday Trans. II, 72, 838 (1976).

82. M. S. Zahniser and F. Kaufman, J. Chem. Phys., 66, 3673 (1977).

83. N. Cohen and J. Heicklen, Compr. Chem. Kinet., 6, 1 (1972).

84. N. Basco and S. K. Dogra, Proc. Roy. Soc. London, Ser. A, 323, 29 (1971).

85. N. Basco and S. K. Dogra, Proc. Roy. Soc. London, Ser. A, 323, 401 (1971).

86. H. S. Johnston, E. D. Morris, Jr., and J. Van den Bogaerde, J. Am. Chem. Soc., 91, 7712 (1969).

87. C. H. Wu and H. S. Johnston, Bull. Soc. Chim. Belg., 81, 135 (1972).

88. M. A. A. Clyne and J. A. Coxon, Proc. Roy. Soc. London, Ser. A, 303, 207 (1968).

89. M. A. A. Clyne and I. F. White, Trans. Faraday Soc., 67, 2068 (1971).

90. M. A. A. Clyne and R. T. Watson, J. Chem. Soc., Faraday Trans. I, 73, 1169 (1977).

91. E. S. Buffa and W. H. Taubert, "Production-Inventory Systems, Planning and Control," R. D. Irwin, Homewood, IL, 1972.

92. D. H. Stedman, E. E. Daby, F. Stuhl, and H. Niki, J. Air Pollut. Control Assoc., 22, 260 (1972).

93. P. N. Clough and B. A. Thrush, Trans. Faraday Soc., 63, 915 (1967).

94. A. Fontijn, A. J. Sabadell, and R. J. Ronco, Anal. Chem., 42, 575 (1970).

95. M. A. A. Clyne, B. A. Thrush, and R. P. Wayne, Trans. Faraday Soc., 60, 359 (1964).

96. J. G. Calvert and J. N. Pitts, "Photochemistry," John Wiley, New York, 1967.

97. R. F. Hampson, Jr. and D. Garvin, "Reaction Rate and Photochemical Data for Atmospheric Chemistry," 1977, National Bureau of Standards Special Publication 513, Washington, D.C., 1977.

98. T. C. Clark, M. A. A. Clyne, and D. H. Stedman, Trans. Faraday Soc., 62, 3354 (1966).

99. R. D. Hudson, Ed., "Chlorofluoromethanes and the Stratosphere," NASA Reference Publication 1010, Washington, D.C., 1977.

100. L. Stockburger, III, B. K. T. Sie, and J. Heicklen, Sci. Total Environ., 5, 201 (1976).

101. C. J. Schack and C. B. Lindahl, Inorg. Nucl. Chem. Lett., 3, 387 (1967).

102. C. T. Ratcliffe and J. M. Shreeve, in "Inorganic Synthesis," Vol. XI, W. L. Jolly, Ed., McGraw-Hill, New York, 1968, p. 194.

103. I. T. N. Jones and K. D. Bayes, J. Chem. Phys., 59, 4836 (1973).

104. S. Glavas, R. Simonaitis, and J. Heicklen, to be published (1979).

105. B. Janowski, "Chlornitrit (ONOCl), ein metastabiles Zwischenprodukt bei der Reaktion des Dichlormonoxids mit Nitrosylchlorid," Ph.D. dissertation, Kiel University, West Germany, 1975.

VITA

Wanee Wongdontri Stuper was born ████████ ██ ████████
████████████████ Her early education up to the high school
level was in Bangkok, Thailand. She was awarded a four-year
scholarship for undergraduate study from the Australian Government.
She received the Bachelor of Science degree in chemistry from the
University of Newcastle, N.S.W. Australia, in March 1974. In
September 1974, she entered the graduate school of The Pennsylvania
State University. She is a member of Sigma Xi, the American
Chemical Society, the Royal Australian Chemical Institute, the
Air Polution Control Association, and Sigma Delta Epsilon.

Stuper, Wanee Wongdontri, The Photolysis of Chlorine in the Presence of Ozone, Nitric Oxide and Nitrogen Dioxide, Electrical Engineering, University Park, Pennsylvania, 16802, 1979.
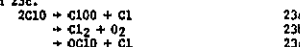
PSU-IRL-SCI-462

Classification Numbers

1.9.2 Chemical Aeronomy

The following three systems were investigated. the Cl_2-O_3 system, the Cl_2-O_3-NO system and the Cl_2-NO_2-M system. In the first system, the reaction between ClO and O_3, the reaction between OClO and O_3, and the mechanism of the Cl_2-O_3 system were studied. In the second system, the reaction between ClOO and NO was investigated. In the last system, the reaction between Cl and NO_2 was investigated as well as the kinetics of the chemiluminescence of the $Cl-NO_2-O_3$ reaction.
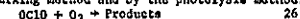
In the first system, Cl_2 was photolyzed at 366 nm in the presence of O_3 within the temperature range 254-297°K. O_3 was removed with quantum yields of 5.8 ± 0.5, 4.0 ± 0.3, 2.9 ± 0.3 and 1.9 ± 0.2 at 297, 283, 273, and 252°K respectively, invariant to changes in the initial O_3 or Cl_2 concentration, the extent of conversion or the absorbed intensity, I_a. The addition of nitrogen had no effect on $-\phi(O_3)$. The Cl_2 removal quantum yields were 0.11 ± 0.02 at 297°K for Cl_2 conversions of about 30%, much higher than expected from mass balance considerations based on the initial quantum yield of 0.089 ± 0.013 for OClO formation at 297°K. The final chlorine-containing product was Cl_2O_7. It was produced at least in part through the formation of OClO as an intermediate which was also observed with an initial quantum yield of $\phi_i(OClO) = 2.5 \times 10^3 \exp[-(3025 \pm 625)/T]$ independent of $[O_3]$ or I_a. The addition of nitrogen and oxygen had no effect on the values of $\phi_i(OClO)$ and $-\phi(Cl_2)$.

The results showed that OClO was formed by ClO radical combination as in reaction 23c.

$$2ClO \rightarrow ClOO + Cl \qquad 23a$$
$$\rightarrow Cl_2 + O_2 \qquad 23b$$
$$\rightarrow OClO + Cl \qquad 23c$$

The relative importance of the channels for reaction 23 at 296°K are the following·
$k_{23a}/k_{23} - 0.63$; $k_{23b}/k_{23} - 0.34$; $k_{23c}/k_{23} - 0.032$ Also, $k_{23c}/k_{23b} = 2.5 \times 10^3 \exp[-(3025 \pm 625)/T]$.

The rate coefficient for the reaction of OClO with O_3 was studied by a direct mixing method and by the photolysis method.

$$OClO + O_3 \rightarrow Products \qquad 26$$

The temperature dependence of k_{26} was studied in the temperature range 264-297°K. However, at temperatures below 297°K, the equilibrium reaction 29 complicated the kinetics

Stuper, Wanee Wongdontri, The Photolysis of Chlorine in the Presence of Ozone,
    Nitric Oxide and Nitrogen Dioxide, Electrical Engineering, University
    Park, Pennsylvania, 16802, 1979.

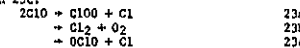The following three systems were investigated. the Cl_2-O_3 system, the
Cl_2-O_3-NO system and the Cl_2-NO_2-H system. In the first system, the reaction between
ClO and O_3, the reaction between OClO and O_3, and the mechanism of the Cl_2-O_3
system were studied. In the second system, the reaction between ClOO and NO was
investigated. In the last system, the reaction between Cl and NO_2 was investigated
as well as the kinetics of the chemiluminescence of the Cl-NO_2-O_3 reaction.
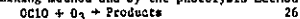   In the first system, Cl_2 was photolyzed at 366 nm in the presence of O_3
within the temperature range 254-297°K. O_3 was removed with quantum yields of
5.8 ± 0.5, 4.0 ± 0.3, 2.9 ± 0.3 and 1.9 ± 0.2 at 297, 283, 273, and 252°K respec-
tively, invariant to changes in the initial O_3 or Cl_2 concentration, the extent
of conversion or the absorbed intensity, I_a. The addition of nitrogen had no effect
on $-\phi\{O_3\}$. The Cl_2 removal quantum yields were 0.11 ± 0.02 at 297°K for Cl_2
conversions of about 30%, much higher than expected from mass balance considerations
based on the initial quantum yield of 0.089 ± 0.013 for OClO formation at 297°K.
The final chlorine-containing product was Cl_2O_7. It was produced at least in part
through the formation of OClO as an intermediate which was also observed with an
initial quantum yield of $\phi_i\{OClO\}$ = 2.5 x 10^3 exp{-(3025 ± 625)/T} independent of
$[O_3]$ or I_a. The addition of nitrogen and oxygen had no effect on the values of
$\phi_i\{OClO\}$ and $-\phi\{Cl_2\}$.
    The results showed that OClO was formed by ClO radical combination as in
reaction 23c.

    2ClO → ClOO + Cl   23a
        → Cl_2 + O_2 23b
        → OClO + Cl   23c

The relative importance of the channels for reaction 23 at 296°K are the following.
k_{23a}/k_{23} - 0.63; k_{23b}/k_{23} - 0.34; k_{23c}/k_{23} - 0.032. Also, k_{23c}/k_{23b} = 2.5 x 10^3
exp{-(3025 ± 625)/T}.
    The rate coefficient for the reaction of OClO with O_3 was studied by a
direct mixing method and by the photolysis method.

    OClO + O_3 → Products   26

The temperature dependence of k_{26} was studied in the temperature range 264-297°K.
However, at temperatures below 297°K, the equilibrium reaction 29 complicated the
kinetics.